POLITECNICO DI MILANO

School of Industrial and Information Engineering

Department of Energy Engineering

Experimental analysis and modeling of oil effects on a microchannel evaporator

Advisor: Luca Molinaroli

Co-advisor: Lorenzo Cremaschi

Tesi di laurea di:

Stefano Dell'Orto 800739

ANNO ACCADEMICO 2013-2014

“Santità non è farsi lapidare in terra di Paganìa

o baciare un lebbroso sulla bocca,

ma fare la volonta di Dio con prontezza,

si tratti di restare al nostro posto, o di salire più in alto”

(Paul Claudel)

Dedicata alla mia famiglia e ai miei amici

Thanks to Andrea, Ardi, Sarath,Jeremy, Pratik, Pedro,

Thiam, Weiwei, Ellyn and Arkasama who worked with me at OSU

1 Sommario 11
2 Abstract 13
3 Introduction 15
4 Literature review 19
4.1 Previous works on microchannel 19
4.2 History of refrigerants 20
4.3 Refrigerants used in the present study 21
4.4 Lubricant used in the present study 23
4.4.1 Oil influence on flow boiling 23
4.4.2 Refrigerant and oil mixture flow characteristics study 25
4.4.3 Effects of oil on refrigeration units 27
4.5 Previous works on modelling system and heat exchanger 32
5 Experimental Apparatus 39
5.1 Air conditioning loop 39
5.2 Microchannel heat exchanger 40
5.3 Air sampling Device 41
5.4 Refrigerant loop 42
5.5 Oil loop 46
5.6 Uncertainty of the transducers 46
5.6.1 Specification of the transducers air side 47
5.6.2 Specification of refrigerant side transducers 48
5.7 Test procedure 50
5.8 Water test 53
5.9 Data reduction 54
5.9.1 Heat transfer Calculation 55
5.9.2 HTPF and PDPF calculation 56
5.9.3 Oil retention volume calculation 57
6 Experimental results 61

6.1 R410A Evaporator A 61
6.1.1 Oil retention volume 61
6.1.2 Heat transfer factor 63
6.1.3 Pressure drop factor 63
6.2 R410A Evaporator B 64
6.2.1 Oil retention volume 64
6.2.2 Heat transfer factor 65
6.2.3 Pressure drop factor 66
6.3 R134a and R1234yf 67
6.3.1 Oil Retention Volume 68
6.3.2 Heat Transfer Factor 69
6.3.3 Pressure Drop Factor 70
6.4 More observations 71
6.5 Effect of superheating 73
7 Model Development 77
7.1 Assessment of previous work 77
7.2 Development of the model 77
7.3 Wet surface conditions 80
7.4 Air side heat transfer coefficient and pressure drop 81
7.5 Refrigerant side correlations 82
7.5.1 Heat transfer coefficient 82
7.5.2 Pressure drop correlations 84
7.6 Pressure drop in the headers 85
7.7 Calculation of refrigerant-oil mixture properties 86
7.7.1 Bubble Point Temperature Calculation 88
7.7.2 Enthalpy variation 89
7.7.3 Liquid mixture density 90
7.7.4 Miscibility 90
7.7.5 Liquid mixture viscosity 90
7.7.6 Liquid mixture thermal conductivity 91

7.7.7 Liquid mixture surface tension....91
7.7.8 Liquid mixture specific heat....92
7.8 Void fraction and oil retention....92
8 Model results for pure refrigerant....95
8.1 Validation of the correlations used....95
8.2 Validation of the heat exchanger....98
8.3 More results....102
9 Model results with oil....107
9.1.1 Oil retention volume....107
9.1.2 Heat transfer factor....108
9.1.3 Pressure drop factor....109
9.2 Results for R410A....110
9.2.1 Oil retention volume....110
9.2.2 Heat transfer factor....114
9.2.3 Pressure drop factor....116
9.3 Results for R134a....118
9.3.1 Oil retention volume....118
9.3.2 Heat transfer coefficient....119
9.3.3 Pressure drop factor....121
10 Conclusion....123
10.1 Conclusion from the experimental work....123
10.2 Conclusion from the modeling work....124
10.3 Future works....125
11 Nomenclature....127
12 References....131

Figure 4.1 % variation of the capacity of the evaporator at different oil mass fraction measured predicted by Lottin [33] 34
Figure 5.1 Air conditioning loop inside the psychrometric chamber 39
Figure 5.2 Picture of the air sampling device 42
Figure 5.3 Picture of the subcooler, the pump and the refrigerant mass flow meter 43
Figure 5.4 Schematics of the thermodynamic cycle 45
Figure 5.5 Schematic of the device used for the water test 54
Figure 5.6 time occurring between observation time at sightglass 1 and sightglass 2 58
Figure 5.7 Mass of oil retained in the suction line 59
Figure 6.1 Normalized oil retention volume for evaporator A and R410A 62
Figure 6.2 Heat transfer coefficient for evaporator A and R410A 63
Figure 6.3 Pressure drop factor for evaporator A and R410A 64
Figure 6.4 Normalized oil retention volume for evaporator B and R410A 65
Figure 6.5 Heat transfer coefficient for evaporator B and R410A 66
Figure 6.6 Pressure drop factor for evaporator B and R410A 67
Figure 6.7 Normalized Oil Retention Volume for experiments using R134a and R1234yf 68
Figure 6.8 Heat transfer factor for experiments using R134a and R1234yf 69
Figure 6.9 Pressure Drop Factor for experiments using R134a and R1234yf 70
Figure 6.10 Effect of superheating on normalized oil retention volume 73
Figure 6.11 Effect of superheating on heat transfer factor 74
Figure 6.12 Effect of superheating on pressure drop factor 75
Figure 7.1 Graphic explanation of the model 79
Figure 7.2 Schematic of an inlet header. The picture is taken by a patent from Johnson Control 86
Figure 8.1 Comparison between experimental data from literature and the model 96
Figure 8.2 Comparison of the modelling results with experimental data from literature. 97
Figure 8.3 Comparison between the predicted capacity and the experimental ones 98
Figure 8.4 Comparison between the predicted pressure drop and the experimental one 99
Figure 8.5 Comparison of the predicted temperature of the air at the outlet and the experimental one 100
Figure 8.6 Infrared picture of the coil 101
Figure 8.7 Comparison of the predicted surface temperature with the experimental one 102

Figure 8.8 Predicted temperatures of the system 103
Figure 8.9 Heat transfer coefficient along the coil 104
Figure 9.1 Comparison of the predicted oil retention volume with the experimental one 108
Figure 9.2 Comparison of the predicted heat transfer factor with the experimental one 109
Figure 9.3Comparison of the predicted pressure drop factor with the experimental one 110
Figure 9.4 Comparison of the predicted oil retention volume with the experimental one 111
Figure 9.5 Normalized oil retention segment by segment 113
Figure 9.6 Comparison of the predicted heat transfer coefficient with the experimental one 114
Figure 9.7 Effect of the oil on heat transfer coefficient..... 115
Figure 9.8 Predicted temperatures of the heat exchanger 116
Figure 9.9 Comparison between the predicted pressure drop factor and the experimental one 117
Figure 9.10 Comparison between the predicted and experimental normalized oil retention volume..... 118
Figure 9.11 Comparison between the predicted and the experimental heat transfer factor 120
Figure 9.12 Predicted temperatures in case of oil injected in the coil 121
Figure 9.13 Comparison between the predicted and the experimental pressure drop factor 122

Table 1 Dimensions of the evaporators.....40
Table 2 Air side temperature transducer specifications 47
Table 3 Relative Humidity air side transducer specifications.....47
Table 4 Air mass flow meter specification.....47
Table 5 Refrigerant side temperature transducers specifications 48
Table 6 Refrigerant side pressure transducers specifications.....48
Table 7 Refrigerant side pressure transducer specifications 48
Table 8 Microchannel pressure drop differential pressure transducers specifications 49
Table 9 Refrigerant mass flow meter transducer specifications.....49
Table 10 Oil mass flow meter transducer specifications.....49
Table 11 Weighing scale specifications 49
Table 12 Test matrix 53
Table 13 Uncertainty of the calculated parameters.....60
Table 14 Empirical constants used to calculate the bubble point temperature of refrigerant-oil mixture 89
Table 15 Pressure drop section by section.....104
Table 16 Results of the simulation with oil 111
Table 17 Increase of pressure drop section by section 117
Table 18 Results of the simulations at different oil mass fraction 119

1 Sommario

Il presente lavoro studia gli effetti della presenza di olio lubrificante all'interno di un evaporatore a microcanale per la climatizzazione di ambienti. Il lavoro presentato ha una doppia finalità: il primo obiettivo è realizzare una serie di esperimenti per verificare gli effetti della presenza dell'olio, il secondo è realizzare un modello semiempirico dello scambiatore che possa aiutare a comprendere più approfonditamente il fenomeno.

Una certa quantità di letteratura è disponibile a riguardo degli effetti dell'olio all'interno degli scambiatori e della modellazione di scambiatori di calore in caso di refrigerante puro. Al contrario ben poco materiale è stato prodotto a riguardo della simulazione dell'intero scambiatore in presenza di olio nel caso di un microcanale. Il presente lavoro è unico per le condizioni di lavoro utilizzate. L'utilizzo di un sistema specifico e non un intero sistema di climatizzazione ha permesso di evitare gli effetti della maldistribuzione per misurare contemporaneamente l'olio trattenuto nel sistema e il suo effetto sulla potenza termica scambiata e sulle perdite di carico. Si è lavorato con due differenti evaporatori a microcanale, tre temperature di saturazione (1°C, 4.5°C e 10°C), tre tipi di refrigerante (R410A, R134a e R1234yf) e quattro diverse concentrazioni di olio (0.5%, 1%, 3% e 5%). L'olio è stato Polioliestere (POE) per tutti gli esperimenti.

Per valutare gli effetti dell'olio sono stati presi in considerazioni tre parametri. Il primo è il volume di olio trattenuto nel sistema normalizzato rispetto al volume dello scambiatore. Il secondo è il rapporto tra potenza termica scambiata in presenza e in assenza di olio. L'ultimo è il rapporto tra perdite di carico con e senza olio.

La quantità di olio trattenuta nel sistema aumenta quando cresce la frazione massica di olio circolante nel sistema e al diminuire del flusso di massa all'interno dello scambiatore. Con uno degli scambiatori si è osservato un interessante fenomeno di riempimento dell'header di uscita, la presenza di una quantità anche minima di olio determina l'accumulo una consistente quantità di olio.

La presenza di olio determina una riduzione della potenza termica scambiata. L'olio fa sì che la miscela si comporti come un fluido zeotropico, di conseguenza una parte del refrigerante non evapora causando una diminuzione dell'effetto utile. La potenza scambiata si riduce mediamente al 92% per una frazione di olio del 5% con un effetto proporzionale alla presenza di olio nel sistema.

L’olio presenta una viscosità decisamente superiore a quella del refrigerante. Inoltre non evaporando rende il flusso bifase nella parte finale dello scambiatore. Tutto questo fa aumentare le perdite di carico. Le perdite di carico aumentano con la quantità di olio in circolo nel sistema. Le perdite di carico aumentano solitamente attorno al 30% quando la frazione di olio circolante è pari al 5%.

Il modello si basa sul metodo di segmentazione. Lo scambiatore viene suddiviso in segmenti, 100 nel presente lavoro, la capacità termica di ciascuno di questi viene calcolata con il metodo ε-NTU. Per ogni segmento poi vengono calcolate le perdite di carico. La pressione e l’entalpia all’uscita da un segmento vengono usate come input per il successivo finche l’intero scambiatore viene risolto.

Il modello è stato validato prima in caso di puro refrigerante. I risultati predetti sono stati confrontati con quelli sperimentali. Il modello è stato in grado di predire la potenza termica nella totalità degli esperimenti con un errore inferiore al 5% ed un errore medio dell’1.4% Il 90% delle previsioni delle perdite di carico è stato predetto con un errore inferiore al 30% e l’errore medio è del 14%.

Essendo la tensione di vapore dell’olio pressoché nulla alle temperature considerate il vapore è considerato refrigerante puro. Sono state poi implementate le funzioni per calcolare le proprietà della miscela liquida in presenza di olio. Le proprietà di miscela sono state utilizzate per calcolare il coefficiente di scambio termico e le perdite di carico. L’olio trattenuto nello scambiatore è calcolato a partire dalla frazione di vuoto calcolata nelle varie parti dello scambiatore. La quantità di olio presente viene sensibilmente sottostimata, i valori predetti sono circa un quarto di quelli misurati. Il modello, in particolare quando viene usato R410A, coglie la riduzione di potenza termica scambiata. Invece il modello generalmente sottostima l’aumento di perdite di carico legato alla presenza di olio.

Parole chiave: evaporatore, microcanale, modellazione, accumulo di olio, perdite di carico, potenza scambiata

2 Abstract

The present work is focused on the effect of the presence of lubricant oil in a microchannel evaporator for air conditioning purpose. This work is composed of two different sections. The first one is aimed to perform experiments to measure the effect of oil in the heat exchanger. The second one is to develop a semi empirical model of the coil so that it can be used to have a deeper comprehension of the effect of the oil.

A certain amount of literature is available about the effect of oil during flow boiling and some works developed model for heat exchanger for pure refrigerant. On the other hand, little literature is available about modeling a microchannel evaporator when oil is present in the system. The unique feature of this work is the fact that measured at the same time the oil retention and the increase of pressure drop and the decrease of capacity caused by the presence of oil. In the present work two different heat exchangers were used, three saturation temperatures (1°C, 4.5°C and 10°C), three different type of refrigerants (R410A, R134a and R1234yf) and four oil mass fractions (0.5%, 1%, 3% and 5%). The oil was POE for all the experiments.

In order to evaluate the effect of oil three parameters were used. The first one is the normalized oil retention volume (ORV_N), to normalize it the volume of the coil was used. The second one is the heat transfer factor (HTF), the ratio between the capacity with and without oil. The third one is the pressure drop factor (PDF), ratio between the oil case and the case for pure refrigerant.

The amount of oil retained increased as the oil mass fraction increased and the mass flux decreased in the heat exchanger. One of the heat exchanger showed an interesting filling mechanism in the outlet header. Even a very small oil mass fraction caused a large amount of oil to be retained in the coil.

The presence of oil decreased the capacity of the coil. The oil made the mixture behave like a zeotropic fluid, as a consequence a part of refrigerant was still liquid at microchannel outlet. This caused a decrease in latent load and decreased the capacity of the coil. The capacity decreased about 8% when the oil mas fraction was 5%.

Lubricant has a viscosity far larger than pure refrigerant. Furthermore the fact that is always liquid in the temperature range makes the flow always two phase in the heat exchanger. These facts caused the pressure drop to increase.

The pressure drop showed to increase as the oil mass fraction increased. Pressure drop rose about 30% when the oil mass fraction was 5%.

The model is based on the segmentation method. The heat exchanger is divided in smaller parts, 100 I the present work, the capacity of each segment is calculated using the ε-NTU method. For each segment pressure drop are calculated. Enthalpy and pressure at the outlet of a segment are given as input in the downstream segment until the whole coil is solved.

The model was validated in case of pure refrigerant. The predicted results were compared with the experimental results. The model was able to predict the capacity for all the tests with an error smaller than 5%, the mean absolute error was 1.4%. The 90% of the predicted values for pressure drop had an error smaller than 30%, the mean absolute error being 14%.

Since the oil is not boiling in the working conditions of the tests, the vapor is considered as pure refrigerant. Correlations are used to calculate the properties of the oil-refrigerant mixture. Mixture properties are used to calculate the heat transfer coefficient and the pressure drop. The oil retained in the system is calculated using the void fraction for each segment. The amount of oil retained is under predicted, the values from the model are about one quarter of the experimental ones. The model, especially when R410A was used, provide a good agreement for the reduction of capacity caused by the presence of the oil. On the other hand, the model still under predict the increase in pressure drop caused by the oil.

Keywords: evaporator, microchannel, modeling, oil retention, pressure drop, capacity

3 Introduction

In the refrigeration and air-conditioning vapor compression systems, oil is necessary for a correct working of the compressor. Its main role is indeed to ensure the existence of a thin film allowing the lubrication of the mechanical moving elements to protect them against wear. The lubricant simultaneously ensures several secondary roles among which serving as a seal element between the high and low pressure side inside the compressor, limiting the noise, or helping the evacuation of chemical impurities or deposits that may be present in the system. Lastly, in many situations, the oil is also used as a heat transfer medium for cooling the compressor. However, the presence of a lubricant is also accompanied by several drawbacks, among which the most important are the reduction in heat transfer coefficients and the increase of the pressure drop in the two-phase heat exchangers (condenser and evaporator). The presence of oil also induces changes in the flow configurations, modifies the thermodynamic equilibrium and thermodynamic properties of the refrigerant (liquid–vapor equilibrium, enthalpy, viscosity, surface tension, etc.). The question of the impact of oil in refrigeration is hence still of uttermost importance. It was also raised in the context of the development of new environment friendly refrigerants (or rediscovery of ‘‘old’’ refrigerants) over the last two decades.

Because of its complexity and delicateness the compressor is often considered the heart of the vapor compression cycle and lubricant oil is always used to protect it. Actually all the favorable actions of oil listed before show that oil is definitely useful in refrigeration units. The problem arises that when the refrigerant leaves the compressor at high velocity since it carries away some droplets of oil which is entrained in it. The oil separator used on the discharge line is not always 100% efficient or may have lost its efficiency over time, thus a fractional amount of the oil is carried along with the vapor refrigerant to the discharge line after the separator. The interval required and the ability for the oil to be carried back to the compressor from the system is a complex function of interdependent parameters like the geometry of the system and its components, fluid viscosities, refrigerant vapor velocity, fluid densities, surface tension of fluids with each other and with the metal they contact, load on the heat exchangers, and the temperature and pressure at which the particular

component is operating. The oil return is very significant for the reliability of the compressor, actually if a consistent part of oil is retained in the other parts of the system the oil available at the compressor will decrease and this could cause problems for the lack of lubrication. In order to improve the oil return, the design of the layout of the pipelines, condenser, evaporator, suction line, and other system components should be such that the lubricant is effectively removed from them without clogging or being trapped. Decreasing oil retention in the system is also good because oil retention increases the pressure drop and causes heat transfer degradation in the heat exchangers. As a result, proper oil management is necessary in order to improve compressor reliability, increase overall efficiency of the system, and minimize system cost by avoiding redundancy and waste of energy.

To have a deep understanding of the oil retention a thermodynamic properties of the mixture are necessary. Also the oil-refrigerant mixture composition is different in different sections of the refrigeration cycle, as the solubility of the refrigerant in oil depends on the pressure and temperature at that particular section. The refrigerant and oil can form a fairly homogeneous mixture in the liquid state, or the oil can exist as a separate film inside the refrigeration system components such as liquid lines, suction lines, heat exchangers, or the small tubes and headers of a microchannel heat exchanger. The amount of oil retained in these components is affected by the system condition at that moment. Previous researches [1] [2]pointed out that the oil retention increases with the oil concentration in the mixture and decreases with mass flux.

The goal of this work is to experiment the effects of lubricant on the heat transfer rate and pressure drop in a microchannel heat exchanger evaporator. Many of the experiments performed on heat exchangers to date are based on pure refrigerants or neglect the presence of the lubricant, this is a simplify way to consider the problem. Now that the efficiency is considered always more important new and more rigorous test are required. It is necessary to consider that the thermodynamic and transport properties of the resulting oil-refrigerant mixture are different from those of pure refrigerant. Predicting the thermodynamic performance of a microchannel heat exchanger is possible only when the contributions of the individual refrigerant and oil in the mixture are known. So rules are necessary to obtain the properties of the mixture, the literature provides plenty of these. Many researchers [3] [4] [5]studied the effects of oil retention in refrigeration units using many pairs of refrigerant and oil. On the contrary this work focuses on microchannel heat exchangers, a particular kind of heat exchangers which provide excellent performances with low pressure drop and good capacity. This research project tries to fill in these

gaps in the oil retention studies by providing experimental results of oil retention and its effects on the microchannel heat exchanger. The refrigerants used for the test are two of the most common HFC available, R410A and R134a. In a series of test also R1234ys has been used, it is a new HFC that will probably replace R134a in most of the refrigeration unit because of its very low GWP. The lubricant used for the tests is a synthetic polyol ester (POE). This kind of lubricant is used since HFC started to be used and aroused the issue of lack of miscibility between Mineral Oil an HFC. The oil used in the experimental tests is an ISO VG 32 POE.

The second part of the research is focused on the modelling of a microchannel heat exchanger considering the effects of oil retentions. To achieve this goal is necessary to develop a physics-based and semi-empirical model of the oil retention. The theoretical equations will be implemented in a heat exchanger numerical solver based on a previous work carried out at Oklahoma State University. The solver will help in the design predicting the Oil Retention Volume and the effects of oil retention on the pressure drop and the heat capacity. The model will be based on the Control Volume Method and so all the thermodynamic properties will be available in each point of the evaporator. The model does mass and energy balance for every segment and at the same times moves in the refrigerant flow direction along the heat exchanger.

This work is part of a longer one focused on the effects of oil retention in heat exchangers. The work was carried out in a research project between Oklahoma State University and ASHRAE. Previous works on a microchannel condenser were used as reference for this work. Deokar [6],[7].

4 Literature review

4.1 Previous works on microchannel

For this work a microchannel heat exchanger has been considered. This kind of heat exchanger is becoming always more common. Actually it provides several relevant advantages compared to other solutions. A good overview on this promising technology was provided by a report about the innovation for energy efficient system by Garimella [8]. The microchannel solution was compared to previous kind of heat exchangers. One of the previous solutions was the fin and tube one. Usually the heat transfer coefficient on the refrigerant side is far larger than the one on the air side. So to increase the capacity of the heat exchanger the area on the air side is increased. The first way used to achieve this goal was to add some plate connected to the tube. The air-side heat transfer coefficient in round tube/plate fin heat exchangers is still inherently low. Only increasing the air side surface, results in large heat exchangers. To reduce the size of the heat exchangers automobile air-conditioner manufacturers have developed microchannel tube, multilouver fin heat exchangers. They replaced conventional evaporators and condensers. The heat transfer coefficients in these microchannel tubes are significantly higher than those in conventional tubes. In addition, interrupted multilouver fins reduce air-side boundary-layer resistances, which results in larger heat transfer coefficients. Microchannel heat exchangers also has smaller frontal obstruction to air flow compared to round-tubes, and larger surface area per unit volume. Smaller frontal obstruction reduces the drag and fan power, while the large surface area/volume ratio results in compactness. Compact geometries would, in turn, result in low refrigerant charge. Considering the concern for the impact of refrigerants on global warming, the choice of microchannel heat exchangers seems to be even more favorable. Studies on the application of microchannel heat exchangers in residential air-conditioning in Jiang and Garimella [9] have demonstrated a remarkable size reductions achieved by using microchannel heat exchangers.

In their work Jiang and Garimella showed that the material required for the heat exchanger for a heat pump using microchannel is only 36% of the round tube system. A microchannel heat exchanger requires a more careful design too. Actually problem due to maldistribution could be more severe, especially in the evaporator. Jiang and Garimella's work proved that adopting a

microchannel solution, the refrigerant inventory decreases. Their heat pump required 2 kg of refrigerant in the round tube system and 1.7 kg in the microchannel configuration. Very significant in their study was also the reduction of the total frontal area of the two heat exchangers, the microchannel system had an area of only 32% of the flat and tube solution. Last but not least the favorable features of the microchannel provided a slight increase in the COP both in the heating and the cooling mode.

4.2 History of refrigerants

At the beginning of the history of the refrigeration the choice for the refrigerants was only guided by the effectiveness. The problem was that most of the solutions found revealed to be either toxic or flammable. Many accidents occurred because of leak or failure in refrigeration units. The most common refrigerants used were ammonia (NH_3), chloromethane (CH_3Cl), propane (C_3H_8) and sulphur dioxide (SO_2). However each of them was either highly toxic, flammable or explosive.

In 1928 a team of the Frigidaire division of General Motors synthesized dichlorofluoromethane, R12, the first CFC. In the 1930 this discovery was announced publicly and it was trademarked as Freon. In a public demonstration a member of the team inhaled an amount of Freon and after that exhaled it on a flame. It was the evidence that this new refrigerant was neither toxic nor flammable. In this way the CFC family became to dominate the scene of refrigeration and the HVAC industries. During the 1950s the hydrochlorofluorocarbons (HCFCs) widened the portfolio of refrigerant alternatives. The fortune of CFCs changed during the 1970s. In 1973 prof. James Lovelock found traces of refrigerant gases in the upper part of the atmosphere. One year later Sherwood Rowland and Mario Molina first stated that the presence of refrigerants in the high stratosphere could damage the ozone layer. The discovery of the “ozone hole” over the Antarctic proved all the concern to be real. As a consequence in 1987 The Montreal protocol went into effect. It is an international treaty that established phase-out dates for the use and production of ozone-depleting substances. According to this protocol, CFCs were to be replaced with HCFCs and HFCs, and then HCFCs were to be phased out. Developed countries were to phase out CFCs in 1993 and achieve a 50% reduction in HCFCs by 1998.

During the 1990s the HFCs were developed as a substitute for CFCs and HCFCs. The HFCs are ozone-friendly and energy efficient, have low toxicity and

flammability, but have high global warming potential (GWP). The R134a and R410A refrigerants used for this work are part of the HFCs developed in this period, another their advantage is that they did not require major modifications to the system components. The working conditions are similar to the ones of the previous refrigerants.

Global warming arose as the new threat from refrigerants, which acted as greenhouse gases. Global warming potential (GWP) is a relative measure of how much heat a greenhouse gas traps in the atmosphere. It compares the amount of heat trapped by a certain mass of the gas in question to the amount of heat trapped by a similar mass of carbon dioxide. A GWP is calculated over a specific time interval, commonly 20, 100 or 500 years. GWP is expressed as a factor of carbon dioxide (whose GWP is standardized to 1). In the 1997 the Kyoto Protocol of the United Nations Framework Convention on Climate Change went into effect. This protocol targeted phasing out the refrigerants responsible for global warming, like HFCs, in developed countries. The R134a and R410A refrigerants used for this work are part of the HFCs developed in this period.

In the European Union strict law were established to limit the use of refrigerant with high GWP. In 2006, the EU adopted the Mobile Air Conditioning (MAC) Directive that would reduce the climate impact of air conditioning in cars sold in the EU. The MAC Directive requires an automotive refrigerant with a GWP of less than 150 for use in new model vehicle platforms. This requirement went into force on January 2013. This new challenge lead to the synthetizing of the R1234yf as a replace for R134a for mobile air conditioning. Actually the GWP of R134a is 1430 which is far more than the limit set for mobile air condition, on the other hand R1234yf has a GWP of only 4.

4.3 Refrigerants used in the present study

As it was stated in the introduction the oil is present in the system only for its advantages provided at the compressor. Unfortunately it is not possible to prevent the oil escaping from the compressor, oil droplets are carried by the high velocity vapor at the discharge line and it is impossible to obtain a 100% efficiency separation. At the same time, it is not possible to have always an oil separator device or it is ineffective for some pair of oil and refrigerant. For this reason two different issue arises: the first is the oil return to the compressor and the second are the effects of the oil on the other parts of the system, these

are the core of this work. So it is necessary to know the properties of the oil and the refrigerant separately and how they behave in a mixture.

In this work two of the most common HFCs refrigerants, R134a and R410A, are used. Although the thermodynamic features of these two refrigerants are similar to the CFCs they replaced, they provide poor miscibility with previous used Mineral Oil (MO). So it is necessary to use more expensive and hygroscopic POE. If lubricant is exposed to the open air it absorbs the water present in the atmosphere. Moreover POEs also cause irritation if they come in contact with the skin. The miscibility is a very important properties both for the oil return and the overall performance.

The first refrigerant used the tests is R-410A, it is a near-azeotropic mixture of 50 wt. % HFC-32 and 50 wt. % of HFC-125. A composition tolerance of +0.5% −1.5% for R-32 and +1.5% −0.5% for R-125 is allowed by ASHRAE. R-410A belongs to the safety group A1: very low toxicity and flammability. The ozone depletion potential (ODP) is zero, but it has a very high global warming potential (GWP, 100 years) of 2100. When it is used for retrofits of unity previously using R-22 it has higher working pressures. The critical temperature is rather low (72.8° C) and so it behaves as a high boiling behavior, the critical pressure is 4,86 MPa. The letter “A” in the R-410A identifies the percentage of R-32 and R-125 in it. Bivens and Yokozeki [10] present data for change in the composition of the HFC mixture inside an R-410A storage tank when the liquid level drops from 85% to 2% while the refrigerants extracted isothermally: at 25°C. The composition changed by a maximum of 0.4%, and at 40°C it hanged by a maximum of 0.5% in both R-32 and R-125 proportions. They also showed that refilling the tank with fresh R-410A changed the composition further, but within an acceptable limit. So it is possible to make the assumption that the composition of the refrigerant in the system is always more or less the same even in case of frequent charge and discharge.

R-134a is the second refrigerant used; it also belongs to the group of A1. The ODP is zero as well, but the GWP calculated for 100 years is 1430. The critical temperature for R-134a is 100.95°C, which is quite high, the critical pressure is 4,06 MPa . The letter “a” in the R-134a stands for the type of isomer, its molecular formula is 1,1,1,2-tetrafluoroethane.

The fact that the two refrigerants have different critical properties makes them suitable for different purpose. A high critical temperature usually provides good performances. This because efficiency losses are lower as it is possible to see on a T-s chart. On the other hand, refrigerants with high critical

temperature usually work at lower pressure and so at low density. To provide the same mass flow rate the compressor would be bigger and the volumetric cooling capacity decreases, so the size of the heat exchanger increases. Thus refrigerants with low critical temperature (i.e. R-410A) are suitable to obtain compact and cheap units whereas refrigerants with high critical temperature serve well in bigger units where the efficiency becomes always more important.

As stated before, concerns about global warming are increasing the relevance of GWP in the choice of refrigerants. Actually the strict regulations adopted the Mobile Air Conditioning brought to the synthesizing of the hydrofluoroolefin (HFO) R-1234yf (CH_2=$CFCF_3$). Its critical temperature is 94.7°C and its critical pressure is 3.382 MPa. This features make it a suitable replace for R-134a with a GWP 350 times smaller. This result is achieved thanks to a very short lifetime in the atmosphere. The refrigerant is claimed to be a replacement of R134a since it has a very similar saturation curve on P-T chart. At the same time R-1234yf units are proved to grant the same COP of equivalent units using R-134a The two refrigerants are both miscible with POE and R-1234yf is compatible with motor and sealing materials. The main concern about this refrigerant is its flammability. Studies from the DuPont laboratories [11] showed that the energy necessary to start a combustion is about 1 J. It is a very high value compared to the one of other flammable refrigerants, 4000 times the one for Propane. The burning velocity showed to be negligible, only 1,5 cm/s. Although it is flammable, its use in mobile conditioning seems to be secure.

4.4 Lubricant used in the present study

The choice of the lubricant is mainly driven by its interaction with the refrigerant. First of all it must not react with the refrigerant. Another important characteristic is the miscibility, as stated before. This issue forces the use of POE when HFCs or HFOs are used. The lubricant (oil) used in the system mentioned in this work is Emkarate RL 32- 3MAF, which is an ISO VG 32 synthetic polyol ester (POE) lubricant with additives less than 1%. POE - ISO VG 32 has a midpoint viscosity of 0.032 Pa s at 40°C (ASTM 2007). This work uses the terms “lubricant” and “oil” interchangeably.

4.4.1 Oil influence on flow boiling

Due to its large viscosity and mass transfer resistance effect, the lubricant tends to decrease the heat transfer and increase the pressure drop of

refrigerant, especially at high lubricant fraction However, the opposite phenomena on heat exchanger capacity have been observed in some cases [12] at low oil concentrations, generally lower than 2%. This shows that the lubricant influence on refrigerant heat transfer and pressure drop is a complex subject, and no consistent agreement has been reached to date.

The work from Shen and Groll [13] provides one of the best review available. The first effect that their study pointed out was the impact on flow pattern. Actually the increased mixture viscosity and surface tension promotes the early formation of annular flow. This factor is likely to benefit the flow boiling at low and intermediate qualities. The oil also enhances the formation of foam. The presence of bubbles increases the volume occupied by the fluid, and as a result the increased fluid volume is more effective to wet the heat transfer surface. In this region, nucleate boiling is a main component of heat transfer, which can be enhanced by the lubricant as well. As observed by Manwell and Bergels [14] On the other hand, the increased mixture viscosity and the oil mass transfer resistance effect cause a decrease in the convective evaporation. This impairs the flow boiling at high quality. Several studies [15] [16] claimed that the optimum oil concentration for heat transfer was determined by the trade-off between the reduced convective heat transfer and the increased wetted surface. The optimum concentration regarding heat transfer was found to be around 1%. In any case, an increase of the oil viscosity results in a decrease of the capacity of the heat exchanger.

The lubricant influence on the flow boiling heat transfer is specific to the quality. Since the oil concentration increases with the vapor quality, the mixture viscosity, and local oil accumulation effect become very significant at high quality. Some studies reported an oil “hold-up” phenomenon at high quality. The oil “hold-up” means that a large amount of lubricant is trapped in a special region, usually at high vapor quality. This effect increased the local bubble temperature, viscosity, and mass transfer resistance significantly. An increase in the mass flux mixes the refrigerant and oil more uniformly and it can reduce the detrimental effects from the oil mass transfer resistance and the local oil accumulation effects, which is a positive factor.

Many works [12] [17] used heat transfer correlation developed for pure refrigerant using the mixture properties. This procedure was effective in predicting the heat transfer degradation caused by the presence of oil, but was not able to predict the unusual phenomena of the increase of the local heat transfer when the amount of oil was small. This happened because no model

was able to account the tendency of the oil presence to increase the wetted surface with using the refrigerant-oil mixture properties.

Most of the studies reviewed in the second part of the work from Shen and Groll [18] reported that the oil presence increases the pressure drop during the evaporation. Schlager et al. [19] cited two possible explanations for the increase in pressure drop. The first explanation is that the relatively thick oil film reduces the flow area. The second explanation is that the use of a miscible oil resulted in an earlier formation of annular flow, which increases the pressure drop, compared to the stratified flow. As it was expected, in all the studies the pressure drop penalty ratio increased with the oil mass fraction. The effect of oil was found to increase as the diameter of the ducts decreased. At the same time, the lubricant influenced the two-phase pressure drop drastically at high vapor quality, where the local oil mass concentrations were the largest. The increased pressure drop was mainly due to the increased mixture viscosity at high quality and to the foaming behavior of the refrigerant-oil mixture at low quality.

The increase of viscosity at the end of the evaporator could cause the flow pattern to change from turbulent to laminar. This should be considered since most of the pure refrigerant pressure drop correlations are based on the assumption of turbulent flow. This almost always happens in microchannel heat exchanger since the diameter of the tube is very small.

4.4.2 Refrigerant and oil mixture flow characteristics study

One of the most significant conditions for the flow is the pattern it assumes. Several studies were done in diabatic and adiabatic conditions considering the effect of oil or using pure refrigerant.

Kattan et al [20] proposed an improved two phase flow pattern for evaporation in horizontal tube. The adiabatic model proposed by Steiner [21] was improved and the result was a new map. Their map was developed based on flow pattern data for five different refrigerants covering a wide range of mass velocities and vapor qualities. Their map is valid for both adiabatic and diabatic (evaporating) flows. It could accurately identify 674 of the 702 data points. Their map was presented in coordinates mass velocity versus vapor quality. They also provided an equation for the prediction of the onset of dryout at the top of the tube

during evaporation inside horizontal tubes. The dryout is a function of heat flux and flow parameters.

This work was tested subsequently by Zurcher[12]. They used the oil-refrigerant mixture viscosity in place of the pure refrigerant and the flow map. Without further modifications, they predicted the R-134a/oil and R-407C/oil data quite accurately. In this case the viscosity of the liquid mixture changed as a function of the vapor quality. The local value of the viscosity was calculated as a function of the local bubble point.

The model proposed in Kattan [20] was further improved by Wojtan [22] investigating the flow boiling in horizontal tubes. In this work a more detailed description of the stratified-wavy region was developed. An analytical form for the transition from annular to dryout and from dryout to mist flow was developed too. Their work was based both on observation and on heat transfer measurement to identify the dryout region. Their model can be easily used for advanced methods of boiling heat transfer coefficient since it does not require any iterative calculations.

There are also works focused was on the presence of oil. The flow pattern is very important for the oil return. Fukuta *et al*. [23]studied the flow characteristics of oil films in suction lines of refrigeration cycles. Air with 20 and 56 VG MO oil was used as working fluids in their experiments. The main focus of this work was the oil return in presence of upward flow. Their results showed that oil could always flow upward even in case of low gas velocity. They proposed the refrigerant gas core Reynolds number to be the main parameter upon which flow pattern depends. By experimental results, they correlated the oil film thickness, pressure gradient, and oil film average velocity to the Reynolds number of the core region. They also developed a correlation between the Re of the gas core and the liquid film Re.

Hwang *et al*. [24]investigated the flow characteristics of refrigerant-oil mixtures in vertical upward suction line. Their work can be significant especially for the modelling of the last part of the heat exchanger in which superheated vapor is present. The Reynolds number ranged between 3000 and 22000. This paper described a test method to estimate the mean oil film thickness and to observe the flow pattern in vertical upward flow in a R134a suction line. Three kinds of oils (a mineral oil and two Alkylbenzenes) have been tested with R-134a in the facility. A vertical tube extended vertical upward the evaporator represented the test section. Sight tubes were installed at the evaporator outlet to check the flow pattern, a camcorder was used to record the results. At the same

time, the mean oil film thickness in the test section was calculated by integrating the oil flow rate difference between injected and returned quantities over time. Within the range of refrigerant mass flow rate and oil flow rate investigated in this study, only two flow patterns were observed: churn flow and annular flow.

At very low mass flow rate the flow pattern was churn for all oils and volume flow rate. In churn flow, the oil film on the wall flowed downward, accumulated and eventually formed a "bridge". The bridge essentially was a plug that was pushed upward by the refrigerant vapor. The plug disintegrated into oil film waves and droplets. The flow pattern just above the test section showed droplets moving upward after they were broken from the liquid film. At low mass flow rate oil film thickness on the wall was relatively thicker than in other cases due to the unstable flow of oil.

For higher refrigerant mass flow rate cases, the flow pattern was annular flow for all oil types. In the annular flow pattern, the oil film on the wall flowed upward at a certain range of velocities in wavy form. At high mass flow rates the amount of oil stored is similar regardless of oil viscosity and oil type. On the other hand, for low refrigerant mass flow rate the oil stored was influenced by the oil viscosity and oil type. In the case of Alkylbenzenes, the observation time delay of the low viscosity oil was less than that of the high viscosity oil. The miscibility of the oil was important too. The results indicate that the oil that has a poor miscibility and higher viscosity creates a thicker oil film in the tube and delays oil return.

4.4.3 Effects of oil on refrigeration units

When the oil comes out from the compressor and it is not separated, it affects the other components decreasing the performance of the system. Many experiments have been carried out aimed to find all the relevant characteristics of the interaction between the oil and the refrigerants.

One of the main consequence of the oil retention is its effect on oil return. If the oil is retained in the other components of the circuit there will be less lubricant available at the compressor. The property that has always been considered as the most important for the oil return is the miscibility. Experiments to prove the importance of miscibility in oil return have been performed in the work of Sundaresan et al[3]. He aimed to prove the common believed relationship between miscibility and oil return. The goal of their work was to understand if it was possible to replace completely miscible POE with

poorly miscible MO without compromising performances and reliability of the system. The facility they used for their test consisted of a heat pump unity. It used a scroll compressor fitted with sightglass and a sight tube with a scale graded in millimeters. In this way it was always possible to check the level of the oil available at the compressor. For the experiments three pair of lubricant and refrigerant were used: R-407C/MO which are poorly miscible, R-407C/POE and R-22/MO which are completely miscible. All the pairs were compared using the same test conditions, during tests the unit worked both as a heat pump and as a cooling unit. The most drastic change in the oil level occurs during the start of the system so a more severe cyclic test was performed consisting of five on and off periods for a duration of three hours. Lastly the most severe test performed consisted in injecting the oil only in the discharge line, so the system could rely only on the oil returning from the refrigerant loop (pump out conditions).

During the steady state the R-407C/MO showed a lower level in the oil tank due to a higher oil retention caused by poor miscibility. The steady state conditions also took more time to establish. During the pump out test the two miscible pairs were able to recover oil after a certain amount of time whereas the R-407C/MO pair did not show sign of recovery for all the duration of the test

The predominant oil return mechanism is the shear force which pushes the oil film along the tube wall. In case of poor miscibility this mechanism showed to be little effective. The miscibility and thus the presence of liquid refrigerant in the oil rich phase reduces drastically the viscosity. The two phase flow was observed also in the liquid line, the agitation and the lower oil viscosity due to the high temperature were not enough to prevent the formation of an oil layer. The following variables were identified as major relevant parameters for the oil retention: velocity, viscosity, pressure, temperature and surface tension. A model able to correlate successfully these properties is expected to be effective in predicting the oil retention.

In a later study by Schnur [4] the effects of miscibility and viscosity were correlated both with the performance of the system using the COP and with the reliability of the system and the oil return. Schnur thought that since oil-refrigerant pair changed compared to the previous experiments, the influence of viscosity on the performance should be studied again. The refrigerant used in this work was R-134a, the three lubricants were two POE and a MO. The POE 1 lubricant and the MO lubricant were used to analyze miscibility effects on system performance. Actually they had the same viscosity grade of ISO 32, and

similar viscosity dependence on temperature, whereas the POE 2 lubricant had a lower viscosity of ISO 22. The comparison with POE 1 was used to investigate viscosity effects on system performance. The facility test consisted of a 10.5 kW vapor compression system operating with R-134a. The system had a reciprocating compressor, a tube and fin evaporator and the condenser is a counter flow heat exchanger using water on the secondary side. The mass fraction of oil circulating in the refrigerating system was assumed as constant at the value of 0.3%. It was measured by removing liquid samples from the high pressure line while the system was operating. The first test used MO and POE 1, the two lubricants were used in the unit and compared having the same parameters. The POE 1 showed a COP always larger than MO, with a difference between 2% and 5%. The difference was larger when the temperature of the air at the evaporator was high and the temperature of the water at the condenser was low. The difference they reported in the COP was significantly bigger than the uncertainty of the measurement (0.8%). The capacity of the heat exchangers also increased when the miscible oil was used. When the temperature of the water at the condenser was high a difference of 2% was measured in the capacity. The different became negligible at low water temperature, and this increase of capacity was consistent since the uncertainty was estimated to be around 0.3%. Miscible mixture of oil and refrigerant showed higher heat transfer coefficient, as a consequence difference in temperature decreased and so the pressure at the end of the evaporator was higher. This leaded to a higher density at the compressor suction line and a higher mass flow rate circulating in the system with the difference being between 0.5% and 2% (uncertainty 0.34%). The miscibility of the oil also affected the compressor power consumption. The experiment proved that the power consumption was bigger using the MO. The larger variations were around 5% and were observed at low temperature of the water at the condenser. The estimated uncertainty for the power consumption was 0.5%

The second comparison considered POE 1 and POE 2, that had the same miscibility but different grade of viscosity. The COP increased up to 3% decreasing the viscosity, the largest variations occurred at very low temperature of the air at the evaporator. The variations became negligible when the temperature at the evaporator was high and the temperature at the condenser was low. The difference was more significant in the heat exchanger capacity. The variations were about 3,5% at all the temperature tested. The pressure at the end of the evaporator was 5kPa higher, this was the consequence of a larger heat transfer coefficient. The result proved the importance of the viscosity of the mixture in the heat exchanger. On the other

hand the increase of viscosity positively affected the compressor power consumption, with difference varying from 0.5% to 3.5%. Overall this result was offset by the increased capacity of the heat exchangers.

More specific study about the effects of oil on heat exchangers had been carried out. A brief summary of these papers that are focused on the microchannel heat exchangers is provided below. One of the main concern for microchannel is the maldistribution of refrigerants among the channels. DeAngelis and Hrnjak [25] experimentally studied the oil effect on small R744 system which had a microchannel evaporator. They found that decreasing viscosity is beneficial for capacity and COP, but Oil Circulating Rate (OCR) effect was not clear. Zou and Hrnjak [26] investigated oil effect on refrigerant distribution in vertical inlet headers. At 0.5% oil concentration, distribution was found to become worse. This might be due to the significant increase of viscosity that creates difficulty for the working fluid to reach the top tubes. On the other hand at 2.5% and 4.7% oil concentration, distribution became improved which was attributed to the large amount of foams making the flow regime more homogeneous. Li and Hrnjak [5] incorporated the lubricant effect into the microchannel evaporator model developed by Tuo et al.[27]. It has been found that high viscosity is detrimental for refrigerant distribution. At low OCR, as the fraction of oil increases, distribution becomes worse. After a certain value of OCR a further increase in OCR leads to a better distribution.

A more recent experiment performed was the one of Hrnjak et al[5]. They studied the effects of lubricant on the performance of two microchannel evaporators in a typical mobile air conditioning system using R-134a and PAG46 as lubricant. The OCR in the experiment varied from 0.1% to 8.2%. The facility included a variable speed compressor and a microchannel condenser which were realistic components used in a major brand vehicle. The microchannel evaporator has a single pass and single slab which is specially designed for the experimental purpose.The first result they provided was the effect of oil on pressure drop. The lubricant can significantly increase the viscosity of refrigerant-oil mixture in the liquid phase especially in the high quality region, actually most of the refrigerant was already evaporated and so the local oil fraction was very high. Thus the pressure drop increased. The increase of pressure drop was up to 300% when the OCR changed from 0% to 10%, the variation of pressure drop was more or less linear with OCR.

In conventional size tubes, the addition of lubricant increases the surface tension of the working fluid, thus suppresses nucleate boiling. On the contrary the lubricant can create foaming and increase surface wetting. So the lubricant

effect on heat transfer is complicated and sometimes contradictory. Neither data in the previous literature nor Hrnjak et al [5] experiments were able to determine the overall impact of the presence of oil on the heat transfer coefficient.

The specific enthalpy difference represents the cooling capacity per unit of unit mass flow rate of working fluid and it is determined in this study as system capacity divided by the total mass flow rate including pure refrigerant and lubricant. By using data extrapolation, it had been found that 10% OCR results in 19.5% total reduction of the specific enthalpy difference compared with the reference of pure refrigerant. The major reduction was due to the replacement of 10% pure refrigerant with 10% non-evaporative lubricant. Furthermore, certain amount of refrigerant was dissolved in the lubricant, the quantity of which was determined by the temperature, pressure and the solubility curve of the refrigerant-oil pair. Under the experimental condition in this study, the local oil concentration in the liquid mixture at the compressor inlet was 80% and the quality of the flow was 87.5% which means 2.5% liquid refrigerant was trapped in the oil. For this reason it was not contributing to the cooling capacity. While going through the expansion device, refrigerant evaporated to cool itself from condensing temperature to evaporation temperature. Since lubricant is non-evaporative within the temperature range of air conditioning application, certain amount of pure refrigerant needed to evaporate to remove the sensible heat of lubricant from condensing temperature to evaporation temperature. In such a way, 3.8% pure refrigerant was used without generating any cooling capacity. The remaining losses (3.2%) could not be quantified in that study among the other causes the heat of mixing should be accounted.

Another important fact was observed during their tests .Higher oil concentration caused higher bubble point temperature of the refrigerant-oil mixture. As a consequence the superheat was higher at a fixed pressure. So as OCR increased, in order to maintain the same superheat, a higher mass flow rate was required to achieve similar local oil concentration at the compressor inlet compared with lower OCR cases. The increased mass flow rate resulted in an improved distribution of the refrigerant within the channels. Eventually this can result in an improved capacity of the coil. During their experiment the decrease in specific enthalpy difference was found to be the predominant effect of the presence of oil and the capacity of the heat exchanger decreased.

In 2002 Lee et al [2] investigated the effects of oil on a refrigeration cycle using R744, the purpose of their study were to experimentally measure oil retention and pressure drop. They used the oil injection-extraction test method to

examine the oil distribution for various oil circulation rates. They found that the oil retained in the evaporator increased as the oil circulation rate increased and the refrigerant mass flow rate decreased. However the increase of oil retained became negligible if the refrigerant mass flow rate was above a certain value. Experiments also showed that higher inlet vapor quality in the evaporator resulted in higher oil retention since a greater portion of the evaporator is in the high quality and superheated region.

In 2005 Cremaschi et al [28] considered refrigerants R22, R410A, and R134a with miscible and non-miscible lubricants to investigate oil retention physics in the widest possible range of transport properties. The main part of this work is a parametric analysis in the suction line but they also studied the oil retention in the whole system. The first result they found was that the oil retention is proportional to the oil mass fraction in each component of the system. The most critical part of the system is where the refrigerant is vapor, (i.e. the suction line and the last part of the evaporator) because of the liquid high viscosity and the low inertia force from the vapor refrigerant core. To decrease the oil retention, it is possible to reduce the pipe diameter increasing the frictional factor increased and the pressure drop therefore, a compromise for the diameter of the duct should be found. The viscosity is a key parameter for the oil retention, the miscibility between refrigerant and oil helps in reducing the liquid viscosity. As showed in the previous experiments the presence of oil decreased the performance of the system. An increase up to 7% of oil mass fraction leaded to a decrease of 9% of the COP of 7% in the system capacity.

4.5 Previous works on modelling system and heat exchanger

One of the first remarkable work about modeling heat exchangers was the one from Jiang [29]. He used a segment-by-segment approach within each tube. This made the model able to account for two-dimensional non-uniformity of air distribution across the exchanger, to address the significant change of properties and heat transfer coefficients. It was able to consider the two-phase regime and heterogeneous refrigerant flow patterns through a tube too. The effectiveness-NTU method for cross-flow configuration was also used for combined heat and mass transfer problems under dehumidification, by defining equivalent thermal resistance and heat capacity. The air-to-refrigerant heat transfer and the refrigerant pressure drop are calculated for each individual segment. On the refrigerant side, each segment is provided with an

inlet enthalpy, an inlet pressure, and a mass flow rate. The predicted conditions at the outlet of the segment are passed as input for the adjacent section until the entire refrigerant circuitry is completed. On the air side, the inlet air temperature is provided for each segment.

In 2001 Youbi-Idrissi et al [30] proposed a method for the calculation of the enthalpy of an oil-refrigerant mixture. Their proposed correlation was validated in 2004 [31] and it showed a good agreement with the experimental results. They found that that an increase in the superheat decreased the amount of liquid refrigerant in the flow. As a consequence the penalization factor caused by the presence of the oil in the system decreased in case of high superheat.

The work by Schwentker [32] improved the previous model including the effects of the oil on heat exchangers and the development of a specific model for plate tube heat exchangers. He included correlations developed specifically for refrigerant-oil mixtures to calculate heat transfer coefficients and pressure drop, and he calculated oil retention in heat exchangers with the use of correlations for the void fraction. The model was validated comparing the predicted results with the experimental ones. The model predicted the capacity the data for the capacity of the microchannel heat exchanger with an average absolute error of 1.6% and the pressure drop with an average absolute error of 25.9%.

The work of Lottin et al [33] can be used as a reference since is an example of modelling a refrigerating system. The work is divided in two parts, the first is about the main features of the model, starting from the determination of the physical properties of the mixture to the performance of the whole system. The second part is focused on the heat exchangers. Even though they used plate heat exchanger this work provided useful reference and evaluation for the correlations to be used. The work was based on a unit using R-410A and POE. Because the refrigerants was a mixture it was necessary to find a function which provided the vapor-liquid equilibrium (VLE). The starting point was the interaction of R-32 and R125 with the oil. The second step was the calculation of the properties of the oil, actually the oil manufacturer did not provide plenty of information. They provided details for the assumption for the compressor and the expansion device. To verify the convergence the model goes on running until the first law of thermodynamics is respected. The data they presented showed clearly that the increase, from 0% to 0.5%, of the oil mass fraction in the system was without significant consequence: the evaporator and condenser heat capacity rose very slightly. The power at the compressor rose too and the COP was almost unaffected. This slight increase in the

exchanged heat was linked to variations of the refrigerant side heat transfer coefficient in the heat exchangers. On the other hand, the effects of oil became important when its mass fraction was higher than 0.5%. The heat flux transferred to the coolant at the condenser changed only slightly, but it was noted a rather significant fall of the heat exchanged at the evaporator It decreased by up to 13%, when the amount of oil reached 5% of oil mass fraction as shown in Figure 4.1. This fall was related to the remaining of a high quantity of liquid at the evaporator outlet The remaining liquid was a mixture of oil and diluted refrigerant that, while not evaporating, did not produce any more the required thermal effect. It was also possible to notice an appreciable increase in the power provided by the compressor. The ratio between the high and low pressures remained similar at different oil mass fraction. On the other hand, the mass flow rate increased. The increase of the power provided at the compressor was linked both to the high heat capacity of the lubricant and to the energetic cost induced by its heating in the compressor.

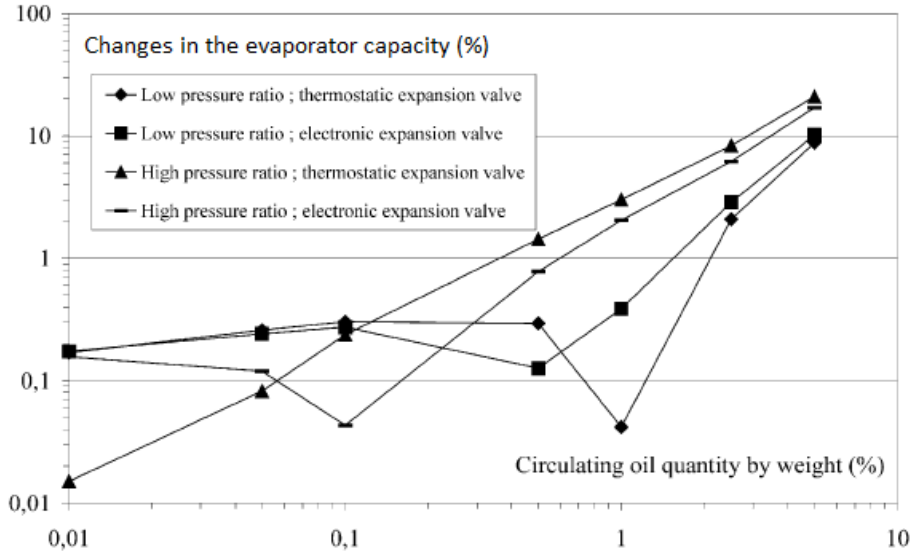

Figure 4.1 % variation of the capacity of the evaporator at different oil mass fraction measured predicted by Lottin [33]

In Figure 4.1 it is possible to see that the performance of the evaporator showed a negligible shift from the baseline without oil if the OCR was below 0.5%. The heat exchanged shows a severe drop when the oil mass flow rate increases further.

The second part of their work [34] was more focused on modelling the heat exchangers.A brief summary of the part concerning the evaporator is reported

below. The model had to account for three different phenomena caused by the presence of oil. There was a change in the resistance to heat transfer in the liquid phase, a modification of the thermodynamic equilibrium between the vapor and liquid phases of the oil-refrigerant mixture and an increase in the pressure drops since the viscosity of the oil was higher than that of refrigerant. The last one magnified in the evaporator because the low temperature caused a great increase in the oil viscosity. The predictions using several correlations for the heat transfer coefficient and the pressure drop were compared with the experimental results. For the refrigerant side in the evaporator the correlations of Yan and Lin , Gungor and Winterton and Bivens and Yokozeki were used. The aim was both to study the evolution of the heat transfer coefficient when the liquid evaporated and to investigate the change in the heat transfer coefficient when the oil mass fraction changed. Even if they presented two very different trends the equations from Bivens and Yokozeki and Gungor and Winterton were able to predict the correct mean value within the tube. Since the focus of the work was on the overall performance it was not possible to say which of the two was better and both were recommended for future calculations. The effect of the presence of oil on these correlations was investigated. All of them showed a maximum around 0.1% of OCR, thus because of the mixing rules which were linear for thermal conductivity and exponential for viscosity. The presence of liquid in the last part of the evaporator, caused by the presence of the oil, resulted in local improvement of the heat transfer coefficient. Above the value of 0.1% the heat transfer decreased in a very significant way. The bubble temperature increased because of the presence of oil decreasing the capacity of the heat exchanger. The correlation established by Yan and Lin was used for the calculation of the friction coefficient during the evaporation. This correlation was used only for quality lower than 0.85, otherwise the homogeneous model from Talik et al [35] was used. Since only one correlation was used the focus was on the effects of oil on pressure drop. The simulation showed that the effects of oil were negligible as long as the OCR was below the value of 0.5%. At higher oil mass fraction there was an increase between 4 and 6.5 times the baseline depending on the expansion valve control.

Another significant example of modelling is found in Cremaschi et al [1]. The focus of this work was on the modelling of oil retention in the suction line and in the evaporator. This paper stressed the importance of the void factor as one of the most importance parameters to be calculated. Many model to predict void fraction were developed, the most recommended are Premoli [36] and Turner and Wallis. The Premoli's empirical model is based on the slip ratio, the ratio between the velocities of vapor and liquid mixture. Below a certain

temperature, which is function of the pressure, the two fluids could be immiscible. Premoli's model is not good for immiscible mixture because it accounts for average properties. Case of immiscibility can arise when the temperature is above a certain limit for the R-410A/POE pair. In case of partial miscibility the liquid film viscosity and surface tension should be increased to account for local behavior. The heat transfer coefficient on the refrigerant side was calculated using the Lockhart-Martinelli parameter, a function correlated the two-phase heat transfer coefficient with the single-phase one. The latter used the liquid mixture properties.The results of simulations showed several interesting point. The first is that at the outlet of the evaporator there was still liquid refrigerant in the flow. This reduced the effectiveness of the system since the cooling capacity decreased for the loss of latent load. This was caused by the increasing of the T_{bub} because of the presence of oil. This results stressed the importance of considering the effect of oil on the temperature of the mixture. The work provided a sensitivity analysis on the number of segments used in the calculation. The difference between using 16 and 30 segments was negligible, so to increase the number of volume above a certain number is not only time consuming but quiet meaningless. The oil retention in each volume was calculated. It decreased along the tube when the quality was small but it increased suddenly in the last part of the evaporator. At the beginning of the evaporator the oil retention decreased since the predominant effect was the reduction of the liquid film. When the local concentration of oil increased the effect of oil on viscosity caused an increase in the oil retention and the highest value was calculated at the outlet of the evaporator. The model provided promising results, the prediction of oil retention showed an average deviation about 21% and the standard deviation was 15%. The cooling capacity of the system was computed within 12% relative error.

A remarkable work is the recent work of Jin and Hrnjak [37]. They modelled a plate and fin horizontal evaporator and a microchannel condenser investigating the capacity and predicting the oil retention. To calculate the heat transfer coefficient they used a correlation for pure refrigerant but account for the mixture properties, the same approach was used for the pressure drop. For the oil retention, they made the following two assumption:, the oil and the refrigerant are perfectly miscible and the bottom headers have liquid level filled up to the channel inlets. They tested several void fraction and pointed out that often they overestimate the void fraction since they were not developed for such a viscous fluid as it is the oil-refrigerant mixture at high quality. Compared with experiments, refrigerant and lubricant mass was predicted within 20% in the evaporator. In the microchannel condenser, lubricant mass

was consistently under-predicted while refrigerant mass was predicted within 15% error. Combining theoretical analysis and additional experiments, it was hypothesized that the lubricant was separated from the flow in the condenser header and started to accumulate in the bottom channels. Although the number of liquid channels was not predicted so far, it was the first time in open literature that such phenomenon was documented.

Li and Hrnjak [38] developed a model based on two channels to investigate the effect of viscosity and oil mass fraction on the distribution of the flow among the channels in a microchannel evaporator. They considered two parallel channels, the first one with an inlet quality of 20% and a second one with an inlet quality of 70%. The first one was called liquid channel and the second one vapor channel. The pressure drop was forced to be the same for the two channels and the total mass flow rate for each tube to require this condition was found. The difference in the flow caused by the different pressure drop affected the distribution among the channels. An increase of the viscosity of the oil affected more the vapor rich channel rather than the liquid rich one. When most of the liquid phase was composed by refrigerant the effect of the oil on the viscosity was little. On the other hand, the oil rich liquid in the vapor channel after the dryout was largely affected by the increased viscosity of the oil. The vapor rich tube had fewer liquid and the liquid rich tube had more liquid, as a consequence the distribution became worse. An increase of the oil mass fraction from 0.1% to 3% resulted in an increase of the flow in the liquid channel. The larger amount of oil in the last part of the channel increased the pressure drop in the vapor rich channel. As a consequence a larger mass flow rate passed through the liquid channel compared to the vapor one. As stated before, an increase of the mass flow rate in the liquid tube resulted in a worse distribution. When the oil mass fraction increased up to 10% the presence of oil affected in a significant way also the liquid tube. As a consequence the difference of flow rate between the liquid tube and the vapor tube was smaller and the maldistribution was reduced.

The last work presented was the one from Li and Hrnjak [39]. They presented the results for their model for a microchannel evaporator. The approach was similar to the one used in Jin and Hrnjak [37] but an empirical method based on infrared images was used to account for the maldistribution among the channels. The model was used to predict the effect of oil on pressure drop. A big part of the paper is used to compare the results with the thermodynamic approach to the approach considering all the flow as pure refrigerant or a slightly improved model which deducted the lubricant and considered a reduced flow of pure refrigerant. The thermodynamic approach always

provided the best prediction, the model using pure refrigerant over-predicted the capacity and the model with deducted lubricant under-predicted the pressure drop.

5 Experimental Apparatus

The development of the experimental apparatus was not the main point of this work, but since it is very important to understand the experimental part of this study a brief description of the system will be provided. The facility was designed and built by Ardiyansyah Yatim and Pratik Deokar current Ph.D. student at Oklahoma State University. Originally the goal of this system was to test the effects of oil retention on a microchannel condenser. After these tests the system was modified in order to work with an evaporator. A complete description of the condenser test facility was written by Deokar [6] and it has been used as a reference for this chapter

5.1 Air conditioning loop

A schematic cross-section of the Psycrometric Chamber and the position of the various components and instrumentation is shown in Figure 5.1. The position of the temperature, pressure and relative humidity transducers is reported too.

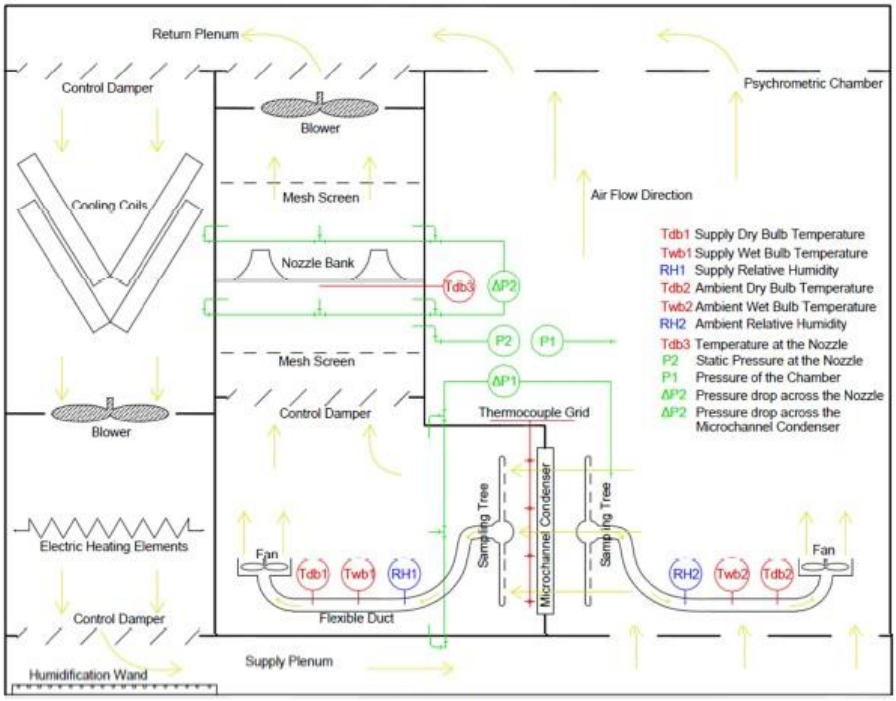

Figure 5.1 Air conditioning loop inside the psychrometric chamber

The microchannel heat exchanger was installed inside the psycrometric chamber. The psycrometric chamber helps to control the condition of the air flowing across the microchannel heat exchanger by using its cooling coils and electrical heaters. The design and the specification of the psycrometric chamber can be found in the paper by Cremaschi and Lee [40]. The chamber has temperature, differential pressure and relative humidity sensors for the air property measurement. The nozzle bank on the air supply duct on the downstream side of the microchannel heat exchanger helps in the calculation of the air flow rates. The flow was provided by a blower, thanks to a variable frequency drive it was possible to change the fan speed to have always the same air flow even changing configuration.

5.2 Microchannel heat exchanger

The microchannel heat exchanger is placed inside the psychrometric chamber, while the remaining components in the test setup are installed outside the chamber. The microchannel is placed in a duct so that the velocity of the air is the same on the entire slab. The oil, liquid, and vapor lines entered the chamber through its wall, travelled inside the air supply duct and at the end are connected to the heat exchanger. Two pressure lines were added during this work. In this way it was possible to use more accurate differential pressure transducers to measure the pressure drop in the microchannel. All the connecting lines inside the air supply duct are insulated to prevent their thermal interference with the air supply. A grid of 18 welded thermocouples was used on the air supply side and was placed 3 cm away from the microchannel heat exchanger slab. Inline thermocouples and absolute pressure transducers were placed at the inlet and at the outlet of the microchannel on refrigerant side. Two different heat exchangers were tested, the first one will be called evaporator A and the second evaporator B. Evaporator B was installed in the duct upstream Evaporator A, ball valve were placed in order to insulate the heat exchanger when it was not used. In front of the evaporators an air tunnel of about 40 cm was built in order to guide the flow and to have the same velocity profile on all the surface area. The psychrometric chamber supplies air with uniform temperature and relative humidity. The dimensions of the evaporators are provided in Table 1

Table 1 Dimensions of the evaporators

Parameter	Evaporator A	Evaporator B
Coil length	884 mm	501 mm
Coil height	438 mm	546 mm

Num of tubes	98	50
Tube thickness	0,35 mm	0,4 mm
Fin Height	7,44 mm	7,62 mm
Fin Pitch	0,787 fin/mm	0,630 fin/mm
Coil depth	25,4 mm	30,5 mm
Hydraulic Diameter	1,36 mm	0,87 mm
Overall free flow area	1234,8 mm2	1100 mm2
Number of pass	1	2
Material	Aluminium	Aluminium
Header diameter	31,75 mm	33 mm
Header to header length	924,5 mm	536,575 mm
Header to header height	508 mm	574,7 mm
Evaporator volume	1,526 dm^3	1,900 dm^3

5.3 Air sampling Device

The sampling devices on the two sides of the microchannel heat exchanger were built according to ANSI/ASHRAE Standard 41.1 (ASHRAE 1986). A picture of the air sampling device is shown in Figure 5.2. The two were similar in construction, each sampling tree was constructed of a horizontal 10 cm diameter PVC pipe and the center was connected to a flexible duct. Holes drilled into the branches face the air flow. The construction of the tree helps to mechanically collect small samples of air (collected through these holes) over a large region, mix them in the central horizontal PVC pipe, and then transport the mixture further through the flexible duct.

Figure 5.2 Picture of the air sampling device

The sampled air gets carried through a long PVC pipe to the dry bulb and wet bulb temperature-measuring RTDs. The long PVC pipe assists in having a fully developed flow before the air reaches the temperature sensors. In-line centrifugal blower helps to overcome the pressure drop in the flexible duct and the PVC pipe from the sampling tree to the dry and wet bulb RTDs. The blower then returns the sampled air back to the main airstream. The dew point of the air is calculated using either the dry bulb and the wet bulb temperature or the dry bulb temperature and the relative humidity.

5.4 Refrigerant loop

The refrigerant loop starts from the pump. The system uses a gear pump by Micropump [Model #GC-M25.JVS] it can supply fluid at a rate of 1.82 ml/rev at a maximum differential pressure of 862 kPa. The pump's rotational speed depends upon the frequency of the alternating voltage supplied to it by the Variable Frequency Drive (VFD). The VFD is manufactured by Baldor Electric Company [Model #VS1SP21-1B]. The VFD requires a 3 phase input of 230 V at 60 Hz, and is configured for the motor of the gear pump. The power input of the electric motor of the gear pump is about 750 W and can rotate at 3450 rpm; the motor is manufactured by Baldor (Reliance Super-E motors [Model #CEM3545]).

Changing the rotational speed of the refrigerant gear pump and thus its volumetric discharge is the easiest way to control the mass flow rates through the microchannel heat exchanger. The pump has an automatic control which disengages the pump in case cavitation is occurring. In Figure 5.3 it is possible to see the pump and the subcooler on the left and the refrigerant mass flow meter at the bottom.

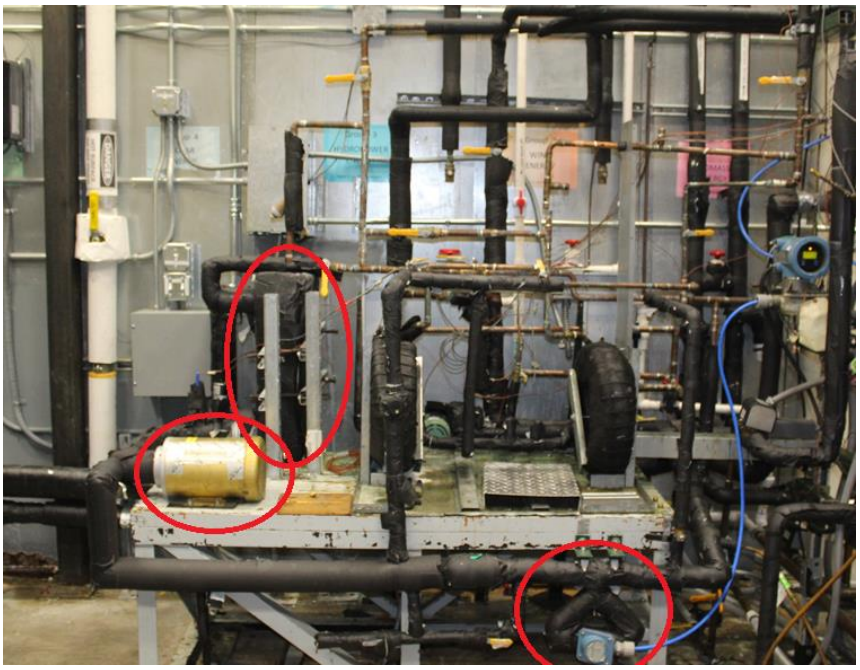

Figure 5.3 Picture of the subcooler, the pump and the refrigerant mass flow meter

The refrigerant passes through the filter-dryer placed right after the refrigerant gear pump to removes any moisture, dirt, acid, and sludge from the liquid refrigerant. The filter-dryer is manufacturer by Parker Hannifin Corp. Sporlan Division [C-083-S-HH 3/8]. After the filter the mass flow rate of the liquid refrigerant is measured accurately using the Coriolis mass flow meter. The Coriolis mass flow meter is manufactured by Micro Motion Inc. [CMF025], its specifications and uncertainty are discussed in details in section 5.8.

At this point to reach the correct inlet conditions a series of electrical heaters is used. The first one is a variable power electrical heater, the presence of a Variac change the voltage and so the heat to the system, it can provide up to 600W. Usually at the outlet of this heater the refrigerant has a large subcool and so it is possible to have a very reliable measurement of the pressure and of

the temperature. The two preheater placed downstream the first heater can provide a power of 300W each and they are used to reach refrigerant conditions close to saturation at microchannel inlet. Since it can happen to have a quality greater than zero the measurement of the enthalpy at microchannel inlet is not reliable and the vapor could affect the pressure measurement. So the enthalpy is calculated using the pressure and the temperature measured before the preheaters. There the refrigerant is always subcooled and the enthalpy calculated is reliable. After that the heat provided by the pre-heaters is added to obtain the enthalpy at microchannel inlet. All the liquid line is made with copper tube 3/8 size (10,9 mm).

After the evaporator the refrigerant passes through the two sightglasses used for the measurement of the oil retention. Since the refrigerant is in vapor phase and the pressure is rather low, this position is suitable to place the helical separator and coalescent separator. They are necessary to remove the entrained droplets of oil in the refrigerant vapor and so to prevent an uncontrolled recirculation of the oil in the loop. The helical separator is manufactured by Henry Technologies Inc. [Model #S-5188]. The coalescent separator is manufactured by Temprite [Model #925R] and can separates up to 0.05 microns particles. Both the separators were selected with no internal float valves, the presence of the float valves in the early separators caused problems like sticking of the internal valves and pulsating oil flow at its drain. These separators are also the main components of the oil extraction system, which extracts the oil during the actual tests. Since the conditions of the refrigerant are very favorable an efficiency of 100% is accounted for the couple of the separators. All the vapor line is made with copper tube size 5/8 (16,7 mm).

At the end of the vapor line the refrigerant reaches a plate heat exchanger (manufactured by Flat Plate, model 131006667). On the other side of the plate Dynalene HC40 flows at very low temperature. The aim of this heat exchanger is to obtain subcooled liquid at the suction line of the pump in order to prevent cavitation. The cold Dynalene HC40 is provided by a chiller, the chiller is manufactured by Cooling Technology model CPCW-12, has a maximum capacity of about 9kW and it can provide HC40 at a minimum temperature of -26 °C.

The schematic of the system is presented in Figure 5.4.

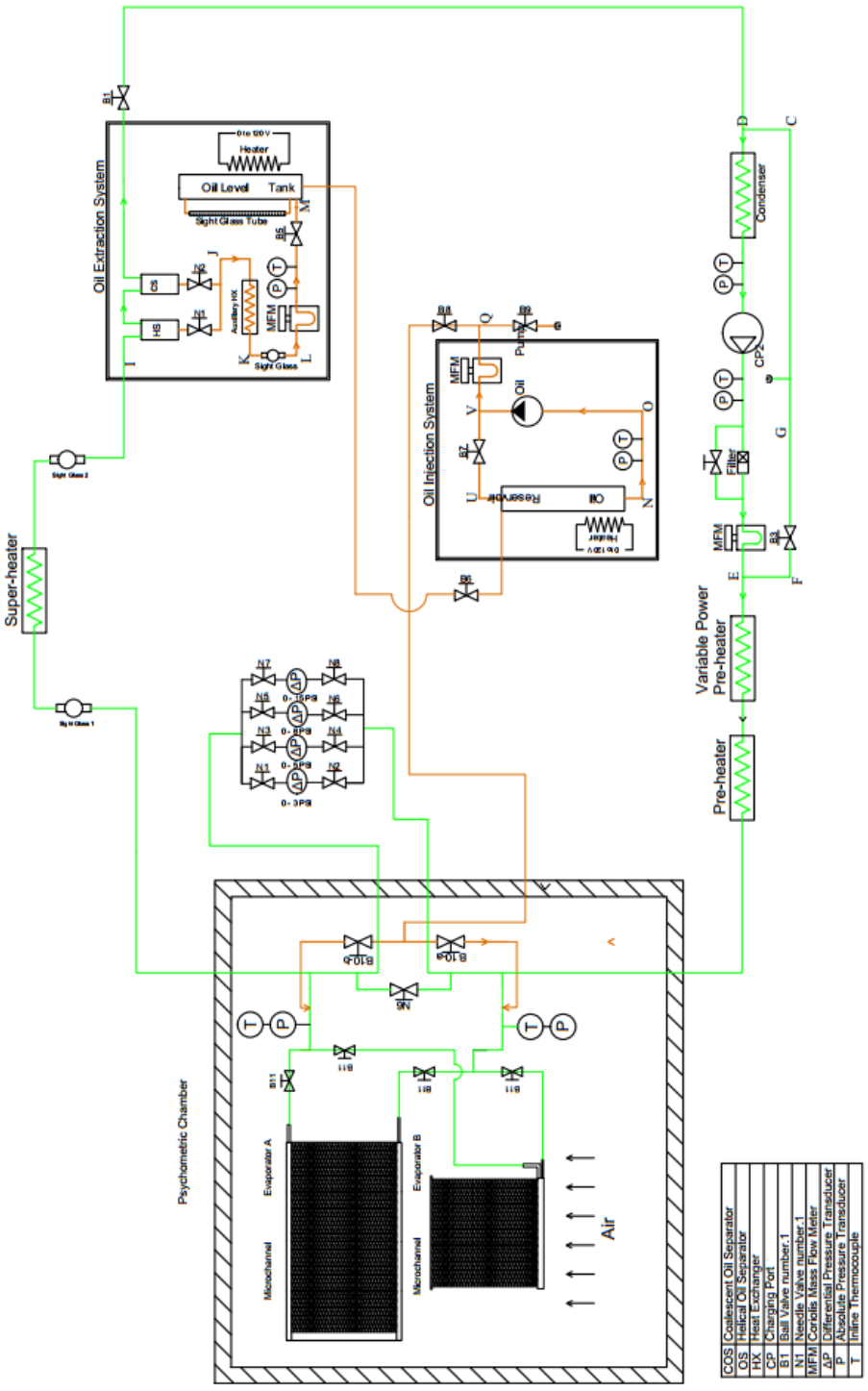

Figure 5.4 Schematics of the thermodynamic cycle

5.5 Oil loop

Before the injection the oil is stored in the reservoir tank, manufactured by Emerson Climate Technologies [Model #AOR-].Vapor refrigerant is used to pressurize the tank so that it is possible to inject oil in the system. The refrigerant vapor slowly dissolves in the liquid oil. If the refrigerant concentration is too high the pressure drop along the injection line could cause the refrigerant to flash and make the flow unstable. To prevent this problem an electrical heater is applied to the tank to boil out the refrigerant from the liquid oil and the tank is periodically vacuumed To inject the oil in the refrigerant loop a gear pump is used, similar to the refrigerant's one. The VFD is present also in this pump to provide the possibility to change the amount of oil injected in the system but it is not the main way used during the injection tests. Actually it is easier to use the needle valve controlled manually. A Coriolis mass flow meter and its screen helps in having exactly the correct amount of oil in the refrigerant.

The oil injection port consists of a small diameter copper tube connected perpendicularly to the refrigerant lines of the test section. The intersecting copper tube is nearly flush with the inside surface of the main refrigerant line at the injection ports. The injected oil is carried with the high velocity refrigerant at the intersection. Injection port-at the inlet is around 0,75m before the first pressure tap to ensure that a fully developed flow is achieved and the pressure measurement remains independent of the method of oil injection. The section between injection port and the microchannel heat exchanger's inlet has a total of 6 sharp elbows. This configuration helps to mix the refrigerant liquid and the oil before the mixture enters the heat exchanger.

5.6 Uncertainty of the transducers

Quantitative analysis of a system is possible only if the techniques and instruments used to obtain the measurements of system parameters are accurate enough so that the uncertainties and their propagation in further investigations are reduced to a tolerable limit. Errors in any experimental measurements are inevitable. Although these errors cannot be avoided or eliminated, they can be kept to a minimum value if care is taken and exact procedures are followed to get the readings. These experimental errors or uncertainties propagate when used in calculation, and if large, will skew the

results to make them impractical, and no conclusions can be drawn from the expensive and time-consuming experiments. The goal is to estimate reliably all the possible uncertainties so that the final results of the experiments are convincing. The methods of error analysis and uncertainty propagation outlined in Taylor are used in this study.

The experimental system in the project uses multiple sensors to measure the temperatures, pressures, mass flow rates, volume flow rates, and other properties of air, refrigerant, and oil. These sensors are discussed in brief in the following sections. Along with the description of the instruments/sensors and uncertainty in their measured outputs is reported.

5.6.1 Specification of the transducers air side

The following tables show the specifications of the instrumentation used to measure air side parameters.

Table 2 Air side temperature transducer specifications

Item	Resistance Temperature Detector
Use	Measure dry and wet bulb temperature
Type	Pt 100
Range	-100 to 400°C
Accuracy	±0.05°C after calibration
Manufacturer	Omega Engineering, Inc.

Table 3 Relative Humidity air side transducer specifications

Item	Relative Humidity Sensor
Use	Measure the relative humidity air side
Model	HX71-MA
Range	0-100%
Accuracy	±3.5% from RH =15% to RH = 85% at 23°C
Manufacturer	Omega Engineering, Inc.

Table 4 Air mass flow meter specification

Item	Air flow nozzles

Use	Measure the volumetric air flow
Model	Aluminium elliptical nozzle
Range	255 to 3400 m^3/h
Accuracy	±0.4% of flow rate
Manufacturer	Helander Metal Spinning Company

5.6.2 Specification of refrigerant side transducers

The following tables show the specifications of the instrumentation used to measure refrigerant side parameters.

Table 5 Refrigerant side temperature transducers specifications

Item	Inline thermocouple
Use	Measure the temperature refrigerant side
Type	T-type (copper - constantan)
Range	-40 to 54°C
Accuracy	±0.2°C after calibration.
Manufacturer	Omega Engineering, Inc.

Table 6 Refrigerant side pressure transducers specifications

Item	Absolute pressure transducer
Use	Measure the pressure refrigerant side
Model	206
Range	50 to 3450 kPa
Accuracy	±4.5 kPa
Manufacturer	Setra System, Inc.

Table 7 Refrigerant side pressure transducer specifications

Item	High precision gauges pressure transducer
Use	Measure the pressure at microchannel inlet
Model	DPGM409
Range	from 0 to 1200 kPa
Accuracy	±1 kPa
Manufacturer	Omega Engineering, Inc.

Table 8 Microchannel pressure drop differential pressure transducers specifications

Item	Differential pressure transducer
Use	Measure the pressure drop across the microchannel
Model	P55D
Range	Four different range from 0 to 86 kPa
Accuracy	±0.25% of full scale; lower than ±0.2 kPa
Manufacturer	Validyne Engineering

Table 9 Refrigerant mass flow meter transducer specifications

Item	Refrigerant mass flow meter
Use	Measure the refrigerant mass flow
Model	Coriolis mass flow meter 2700C12
Range	from 0 to 2180 kg/h
Accuracy	±0.10% of the flow rate
Manufacturer	Micro Motion Inc.

Table 10 Oil mass flow meter transducer specifications

Item	Oil mass flow meter
Use	Measure the oil mass flow
Model	Coriolis mass flow meter 2700C12
Range	from 0 to 108 kg/h
Accuracy	±0.10% of the flow rate
Manufacturer	Micro Motion Inc.

Table 11 Weighing scale specifications

Item	Weighig scale
Use	Measure the weight of the oil sample
Model	SAW-L
Range	from 0 to 22 kg

Accuracy	±2.2 g
Manufacturer	Arlyn scales

5.7 Test procedure

Before starting the oil injection is necessary to achieve the correct conditions for the test. To be sure that this conditions are stable enough and that is not happening a long lasting transient the injection starts after 20 minute of having the proper conditions. The period of injection is enough to reach steady state conditions for at least 10 minutes. The period of time before the injection is also used as a baseline with oil mass fraction equal to zero to which compare the results of the test.

To achieve the desired condition in the system it is possible to use several tools:

- As said before the best way to change the refrigerant mass flow rate is to use the VFD of the pump. It is actually possible to set the desired value of RPM and the VFD will provide it in a very fast and precise way.
- The first option to change the pressure and the temperature of the system is changing the temperature of the room. An increase of the room temperature cause an increase of the temperature at the outlet of the microchannel heat exchanger and thus an increase in the pressure of the system. To have a fair comparison among the same series of experiment the temperature of the room is always the same and the speed of the blower sending the air to the microchannel has changed only after the installation of the second evaporator to keep constant the air mass flow rate.
- Another way to change the condition of the system is to change the temperature of the Dynalene coming from the chiller. The chiller is provided with a control system to have the Dynalene at the correct temperature, an heater is placed to remove the excess of cooling provided by the chiller. The temperature of the Dynalene must always be low enough to prevent the pump from cavitating but can be changed. A decrease of the Dynalene temperature will result in a decrease of the temperature of the refrigerant in the liquid side of the circuit, the pressure will slightly decrease too.
- The electrical heaters are used to bring the refrigerant close to saturation conditions. They are actually able to affect the conditions of the system, the two pre-heaters can only be put inline whereas the Variac provide the possibility to change the heat entering in the system.

An increase of the heat from the electrical heaters results in a increase of the temperature at the inlet of the microchannel and of the pressure in the system

- The best way to decouple pressure and temperature in the system is to charge refrigerant. This results in an increase of the pressure of the system with a negligible effect on temperature

When setting the conditions a great attention was paid to the conditions of the refrigerant at preheater inlet. Since pressure and temperature transducer were not able to provide information about the quality the enthalpy at the inlet of the heat exchanger was calculated doing an heat balance. The pressure and the temperature were measured at preheater inlet where refrigerant was sub-cooled, this way it was possible to calculate the enthalpy. Accounting for the heat gain in the pipeline the enthalpy at microchannel inlet was calculated. Furthermore measuring the electrical power and accounting for the heat received by the ambient it was calculated the required subcool at preheater inlet in order not to have a too high quality at microchannel inlet. A double check of uniform distribution was to take picture of the evaporator with a thermocamera and watch at the temperature profile thorough all the channels. They always showed a very good profile so the refrigerant was assumed to have always a good distribution among the channels. On the air side an air tunnel of about 40 cm was built in front of the microchannel in order to guide the flow and to have the same velocity profile on all the surface area. The psycrometric chamber supplies air with uniform temperature and relative humidity.

After 20 minutes of stable conditions the injection starts. The valve connecting the oil loop to the system is opened and the oil is injected at the inlet of the microchannel. It is very important to keep always monitored the oil flow and the refrigerant too in order to achieve steady state conditions during the injection. The oil flow is controlled using a metering valve in the oil loop whereas the RPM of the refrigerant pump is changed to maintain constant the refrigerant flow. The injection lasts for 20 minutes, it is an amount of time long enough to achieve stationary state in case of presence of oil.

When the injection starts it is also started the recording of two cameras placed in front of the two sightglass on the vapor side of the circuit. Using these and visual observation it is possible to know the precise moment in which the oil reaches that point of the circuit, this information is very important for the calculation of the oil retention volume. At the end of the injection a sample of

the oil is taken from the oil loop. This is the actual procedure for the oil sampling:

- The sampling cylinder is cleaned from oil droplets by blowing air through it, vacuumed and weighted (M0).
- The sampling cylinder is connected to the oil loop and so filled with mixture. Then is weighted again (M1).
- The sampling cylinder is opened, the refrigerant boils and come out through an expansion valve so that only the oil remains in the sampling device. This is weighted again (M2).

This provide a precise measurement for the solubility of the refrigerant vapor in the oil injected and so calculate the exact oil mass fraction circulating in the system.

During the tests all the data about temperature, pressure and flow are recorded using the software Labview. In order to prove the test and to be able eventually to replicate the same conditions, a log sheet was filled before each test. The conditions of the room, of the chiller and of the heaters are written down so that they will always be available in a folder.

After the injection the recording goes on for 15 more minutes to provide information about the recovery of the system. At the end of this period in order to remove all the oil from the system liquid refrigerant is sent through the microchannel The microchannel blower speed is reduced and the refrigerant pump speed is increased so that there is still two phase at the outlet of the heat exchanger. In this way it is possible to remove all the oil droplets from the microchannel, the pipeline and the plate heat exchange placed before the oil separators. These are large enough to store the liquid refrigerant for a certain amount of time and let only vapor refrigerant passing through them.

Part of the oil retained measured during the injection test is retained in the suction line because it was not possible to place the sightglass exactly at heat exchanger outlet. To measure the amount of oil retained in the suction line before the sightglass outlet tests were performed. The oil was injected at a different port right after the coil. During an outlet test the conditions of flow, temperature and pressure at the end of the injection are reproduced in order to have the same behavior of the oil at the outlet of the microchannel. As it happens with the injection test the observed time at the two sightglasses is noted for the calculation of the oil retention volume. The test matrix of all the experiments taken is provided in Table 12

Table 12 Test matrix

Refrigerant	Evaporator	Temperature	Mass flux	Oil Mass Fraction	# Oil Test
R410A	A B	1°C 4.5°C 10°C	20 kg/m2 s 40 kg/m2 s	0% 0,5% 1% 3% 5%	48 test
R134a	A	1°C 4.5°C 10°C	20 kg/m2 s	0% 0,5% 1% 3% 5%	12 test
R1234yf	A	1°C 10°C	20 kg/m2 s	0% 0,5% 1% 3% 5%	8 test

5.8 Water test

Most of the pressure drop occurs in the distributor in the inlet header. For this reason a further test was carried out to have more information about it. A specific test section was built on the purpose. A second unit of the evaporator A was available. Water was made passing through the heat exchanger, using liquid water it was possible to avoid all the uncertainties caused by two phase flow. The inlet was connected to a gauge manometer and to a mass flow meter. At the outlet the water was drained to the atmosphere. The pressure measured by the manometer was equal to the pressure drop across the heat exchanger.

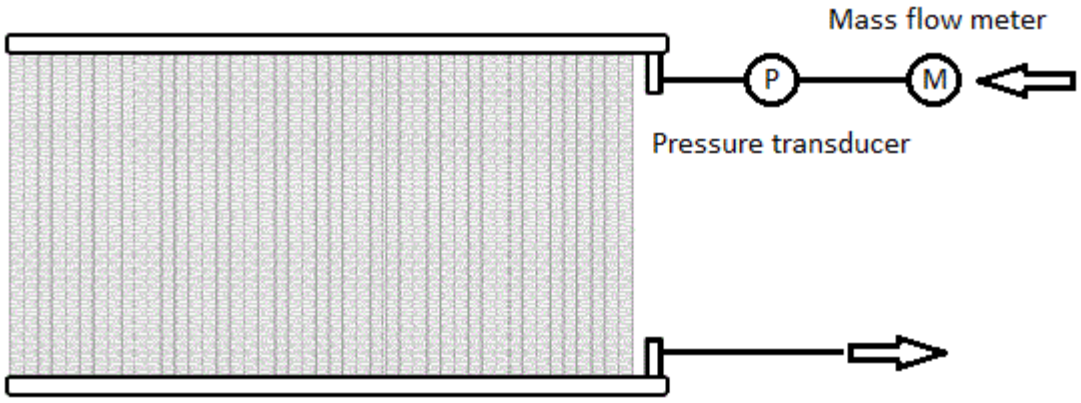

Figure 5.5 Schematic of the device used for the water test

The pressure drop was measured for a wide range of mass flow rates. A worksheet was generated to calculate the pressure drop using the same correlations of the model. The pressure drop for each part were calculated and the remaining pressure drop was addressed to the distributor.

5.9 Data reduction

During data reduction work some assumptions were made to make the analysis doable, a brief account of them is now reported.

The properties of the refrigerant, the oil and the mixture were considered constant for all the period of the test. This assumption is in particular valid for the solubility of the refrigerant in the oil injected in order to calculate the oil mass fraction. The assumption is based on the fact that the oil reservoir is large enough to have little variation in pressure and negligible variation in temperature. Above all the pressure of the tank was usually not that high (apart from R410A) so that the solubility was about very few percent.

The efficiency of the system of the two separators is assumed to be 100%. Under the condition the only oil present in the test section is the one injected since there is no recirculation. Thus the oil mass fraction can be easily calculated using the refrigerant and oil mass flow rate. The two separators works in ideal conditions since they deal with superheated vapor at low pressure. To be sure that there is no oil bypassing the oil separators one more sightglass is placed after them. Since dye is dissolved in the oil its presence would be immediately recognizable.

The oil retention reaches steady state in very little time. This assumption is very important for the calculation of oil retention volume. The calculation is based on the observed time at the sightglasses, assuming that the behavior of the oil is significant for the steady state one. Visual observation of the flow pattern at the two sightglasses shows as the oil flow pattern and amount of oil do not change after a few seconds after the first observed oil.

Using the first two assumption of constant solubility (S) and no recirculation, it is possible to calculate the effective OFM during a test:

$$\dot{m}_{oil+ref,inj} = \dot{m}_{ref,inj} + \dot{m}_{oil,inj} \qquad 5.1$$

$$S = \left(\frac{\dot{m}_{ref,inj}}{\dot{m}_{oil,inj}}\right) * 100 \qquad 5.2$$

$$\dot{m}_{oil,inj} = \dot{m}_{oil+ref,inj}/(1 + \frac{S}{100}) \qquad 5.3$$

$$OMF = \frac{\dot{m}_{oil,inj}}{(\dot{m}_{oil+ref,inj}+\dot{m}_{ref,main})} * 100 \qquad 5.4$$

These equations shows how it is possible to calculate the OMF using the flow measured by the oil and refrigerant mass flow meters and the solubility.

5.9.1 Heat transfer Calculation

To have a reliable calculation of the capacity of the heat exchanger during the test, the air side measurements were used. Thus because the variation in the composition of the mixture on refrigerant side made more difficult the calculation of the enthalpy. The volumetric air flow passing through the microchannel is calculated from the pressure drop on the nozzle placed in the air tunnel, the density was later calculated using the air properties and the ASHRAE Handbook. Since the tunnel is not long enough to fulfill the ANSI/ASHRAE standard to have a full developed flow the procedure for the air flow calculation was fixed with a correction factor. To find out the correction factor four tests having the refrigerant side always in the same conditions and changing the blower speed were carried out doing an inline calibration. The resolution of the following equation in order to grant the heat balance gave us the value of the correction factor.

$$\dot{m}_{ref}\left(h_{ref,MC\ out} - h_{ref,MC\ in}\right) = cf * \dot{m}_{air} * c_{p,air} * (T_{air,in} - T_{air,out}) \qquad 5.5$$

The actual value of cf was 1,48 resulting as the average of the four tests.

So it was possible to calculate the capacity of the heat exchanger on air side using the equation:

$$\boldsymbol{Q = cf * \dot{m}_{air} * (h_{air,in} - h_{air,out})} \qquad 5.6$$

The c_p was assumed as constant in the operating range. This equation is valid only under the assumption of dry surface for the heat exchanger otherwise is necessary to account for the heat of condensation. Since the transducer measuring the relative humidity of the air causes an increase in the uncertainty compared to the use of the only RTD, test were carried out avoiding condensation. Apart from the first series of tests with R410 and evaporator A all the test were carried out having the dew point lower than saturation temperature so that no condensation was expected. This results was achieved running the room in particular conditions:

- The cooling coil of the room was not bypassed and the temperature of the mixture of water and ethylene glycol was lowered as much as possible using a refrigerating cycle. A chiller connected to the water loop helped the mixture to reach very low temperature.
- Silica gel was put in the suction line of the blower so that air was forced to pass through it

For the series of tests with wet surface the capacity of the coil was calculated using this other formula:

$$\boldsymbol{Q = cf * \dot{m}_{air} * (h_{A,in} - h_{A,out})} \qquad 5.7$$

The air properties were calculated using the software EES. Some tests of this series were repeated in order to prove that the effects of oil on the heat exchanger are the same both in case of dry surface and wet surface.

5.9.2 HTPF and PDPF calculation

The heat transfer factor (HTF) is calculated by taking the ratio of heat transferred by the microchannel to the air in the presence of oil to the heat transferred in the absence of oil under the same operating conditions as shown in the equation:

$$HTF = Q_{air@OCR}/Q_{air@OCR=0} \qquad 5.8$$

The two tests were run having the same pressure, temperature and refrigerant mass flow rate both at the inlet and at the outlet of the microchannel.

Furthermore the temperature of the room and the blower speed were the same too.

The pressure drop factor (PDF) is calculated by taking the ratio of the pressure drop across the microchannel in the presence of oil to the pressure drop in the absence of oil under the same operating conditions, as shown in the following equation. The pressure drop values are measured using the most suitable differential pressure transducer placed between the inlet and the outlet lines of the microchannel heat exchanger.

$$PDF = \Delta P_{@OCR} / \Delta P_{@OCR=0} \qquad 5.9$$

When the oil injection test is performed, the pressure drop ($\Delta P_{@OCR}$) is measured and the heat transferred ($Q_{air@OCR}$) is calculated for every time step of two seconds. The HTF and the PDF are then calculated at every time step and averaged over the entire time period after steady state conditions.

The refrigerant mass flow rate was the same during all the experiments, but after the measurement of the refrigerant mass flow rate oil was injected. This way the total mass flow rate increased during the injection period. Two different procedures were used in order to analyze the data. The first one was used for the series with R134a and R1234yf. The value obtained during the injection was compared with the one right before the injection period. The two values shared the same mass of refrigerant but the total mass flow rate entering the coil was different. Part of the increase in pressure drop is caused by the increased total mass flow rate. For the series with R410A a different procedure was used. Baseline tests were run having refrigerant mass flow rate higher and lower than the nominal value. Using this information, it was possible to interpolate the values of capacity and pressure drop to have them as a function of the mass flow rate. As a consequence, the values measured during the injection were compared with equivalent experiments having the same total mass flow rate. When this procedure was used part of the decrease in the capacity was caused by the replacement of refrigerant with oil.

5.9.3 Oil retention volume calculation

The oil retention volume is calculated starting from the mass of oil in the heat exchanger and the density of refrigerant and oil. During the injection test the observed time for the oil to pass from the inlet port to the outlet sightglass is noted down. Using this and the data recorded from the Labview it is possible to integrate the oil flow during the injection time and obtain the mass of the

injected oil. The same procedure is repeated for the outlet test having the same thermodynamic conditions at the outlet of the microchannel as they were during the steady state of the injection test. The difference between the two values of mass is the oil retained in the heat exchanger. After the first series using R410A and evaporator A second sightglass was installed after the first one, an unused plate heat exchanger lies between them. The idea was to have two different values of oil retained that were supposed to be very similar. Actually was noticed that the delta time between the two observed time was not the same for injection and outlet test in case of same conditions and oil mass fraction. This showed that the behavior of the oil can be different whether it is dragged through the microchannel or injected at the outlet port. For this reason for the outlet was not used the mass of oil at the same oil mass fraction but at the oil mass fraction that is expected to have the same behavior. The following procedure was used

- The delta time between the two sightglasses is measured both for the injection and the outlet test, for the outlet test two more oil mass fraction were added to have more data, 0.8% and 2.5%
- The diagram oil mass fraction vs delta time measured during outlet tests is plotted and a power interpolation was made as shown in Figure 5.6.

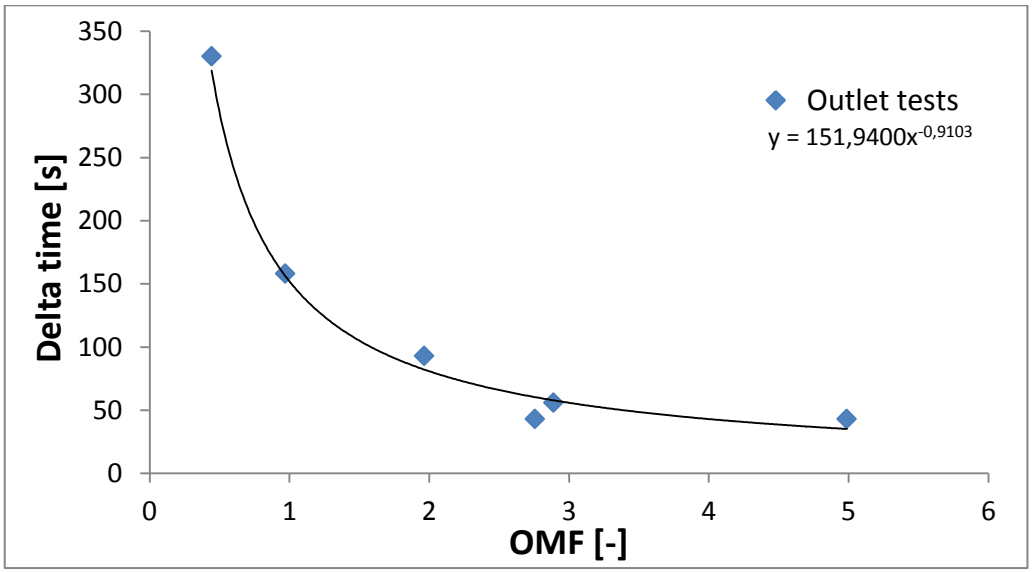

Figure 5.6 time occurring between observation time at sightglass 1 and sightglass 2

- A new OMF for the outlet is considered, the one which shows the same delta time as the inlet
- For this new equivalent OMF virtual values of oil injected are calculated interpolating the data from the others outlet tests as shown in Figure 5.7.

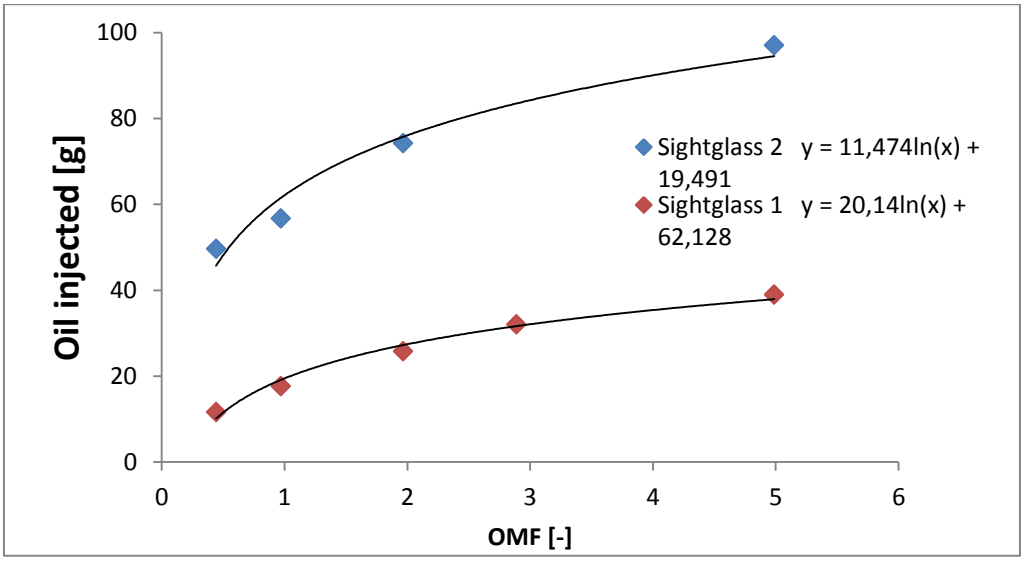

Figure 5.7 Mass of oil retained in the suction line

- The mass of oil retained in the microchannel is calculated as the difference between the mass measured in the inlet test and the virtual mass at the equivalent OMF

This procedure is supposed to be more accurate, it provide two values of oil retained, the one according to the first sightglass and the one according to the second one. The fact that the two values are always very similar showed that the procedure is working fine.The mass of oil retained in the microchannel heat exchanger is converted to the volume of oil retained using the density of the pure oil, as shown in the following equation. The density data for the pure POE are obtained from the available maps (Cavestri 1993, 1995, and Cavestri and Schafer 2000), and it is calculated as a function of the temperature (expressed in °C):

$$\boldsymbol{\rho_{oil}[g/cm^3] = -0,0005 * T + 1,0622} \qquad 5.10$$

$$\boldsymbol{ORV = ORM\ /\rho_{oil}} \qquad 5.11$$

The oil retention volume is further normalized by dividing it by the internal volume of the microchannel heat exchanger V_{mchx}; the microchannel heat exchanger used has an estimated internal volume of 1,526 dm^3. The normalized oil retention volume ORV_n is shown in Equation

$$\boldsymbol{ORV_n = ORV/V_{MC}.} \qquad 5.12$$

Taylor's expansion method was used for calculating the uncertainty of dependent variables using the following equation.

$$\boldsymbol{U_y = \sqrt{\sum_i (\frac{\partial y}{\partial x_i})^2 (U_{x_i})^2}}$$

Using this method of uncertainty for OMF, HTF, PDF and OMF was calculated. The results are reported in Table 13

Table 13 Uncertainty of the calculated parameters

	Uncertainty
OMF	0,3
ORV	0,02
HTF	0,045
PDF	0,04

6 Experimental results

The results of the experiments are discussed in this chapter. The data are divided in three main section. The first one includes the experiments using R410A and evaporator A, the second using R410A and evaporator B and the third shows data for R134a and R1234yf using evaporator A. In the legend of the figures, LMF stands for Low Mass Flux and HMF for High Mass Flux. The figures show the values for the Oil Retention Volume (ORV_N), the Heat Transfer Factor (HTF) and the Pressure Drop Factor (PDF), on the x-axis Oil Mass Fraction (OMF) is used.

6.1 R410A Evaporator A

Evaporator A was tested using two different mass fluxes and three different saturation temperatures: 1°C, 4.5°C and 10°C. The tests were run with constant refrigerant mass flow rate. During the injection the total mass flow rate increased because of the oil. Baselines were run at different total mass flow rate. Using interpolation, it was possible to generate baseline for the capacity of the coil and pressure drop for any mass flow rate within the range of the baselines. The injection tests were compared to tests with pure refrigerant having the same mass flow rate. This way the increase in pressure drop was caused only by the presence of the oil since the total mass flow rate was the same. On the other hand, part of the loss in capacity was caused by the oil replacing refrigerant.

6.1.1 Oil retention volume

The results of the tests for the measurement of the volume of oil retained in the system are shown in Figure 6.1

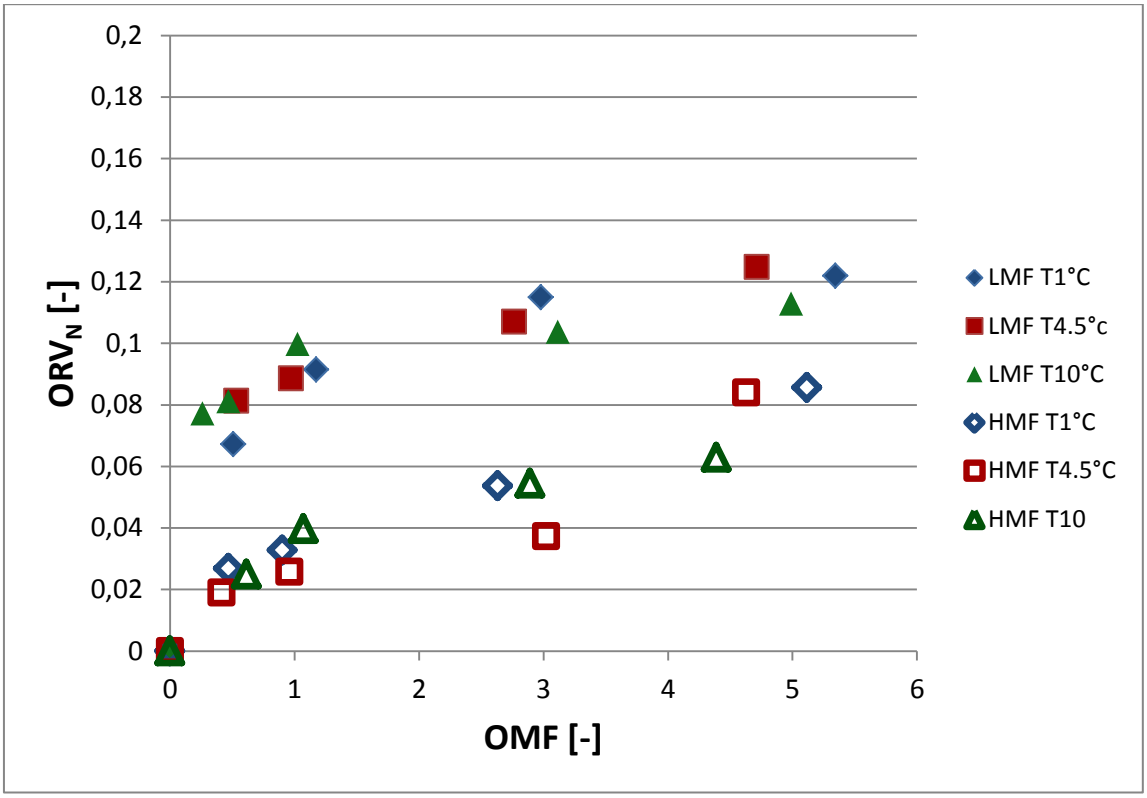

Figure 6.1 Normalized oil retention volume for evaporator A and R410A

The solid points represent the values measured at low mass flux, the hollow the points at high mass flux. The figure shows immediately the effect of mass flux on the oil retained in the system. Tests at low mass flux present a far larger amount of oil retained. The higher mass flux increases the shear stress and so the amount of oil retained decreases. The oil retention volume increases with the oil mass fraction. Considering the series at low mass flux is more evident that the trend line is not passing from the origin of the axis. It seems that there is a sort of filling process, it is likely to occur in the outlet header. The flow is going upward through the channels until it comes out in the header. The tubes enter in the header creating smaller volumes, they are in the bottom of the header. After the oil rich liquid mixture comes out from the channels in the outlet header, it fills part of the volumes before flowing to the outlet pipeline. One test at very oil mass fraction was taken and it confirmed this hypothesis since the amount of oil retained is still very high. The filling process is affected by the shear stress of the vapor refrigerant. The saturation temperature seems not to affect the amount of oil retained.

6.1.2 Heat transfer factor

The results of the experiments for heat transfer factor are presented in Figure 6.2

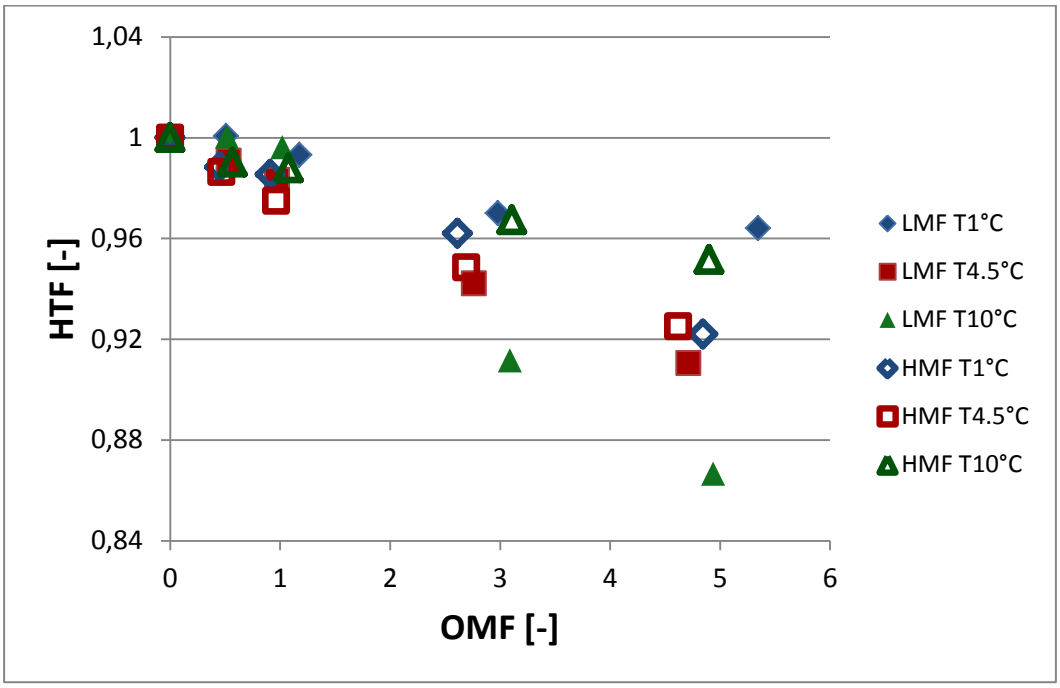

Figure 6.2 Heat transfer coefficient for evaporator A and R410A

The heat transfer factor shows a proportional decrease with the oil mass fraction. The magnitude of the loss of capacity is not affected by the change in the mass flux. Effect of saturation temperature is controversial. At high mass flux the series at saturation temperature of 10°C is the least affected by the presence of oil. On the other hand, at low mass flux the loss of capacity increases as the saturation temperature increases.

6.1.3 Pressure drop factor

The pressure drop factors are reported in Figure 6.3

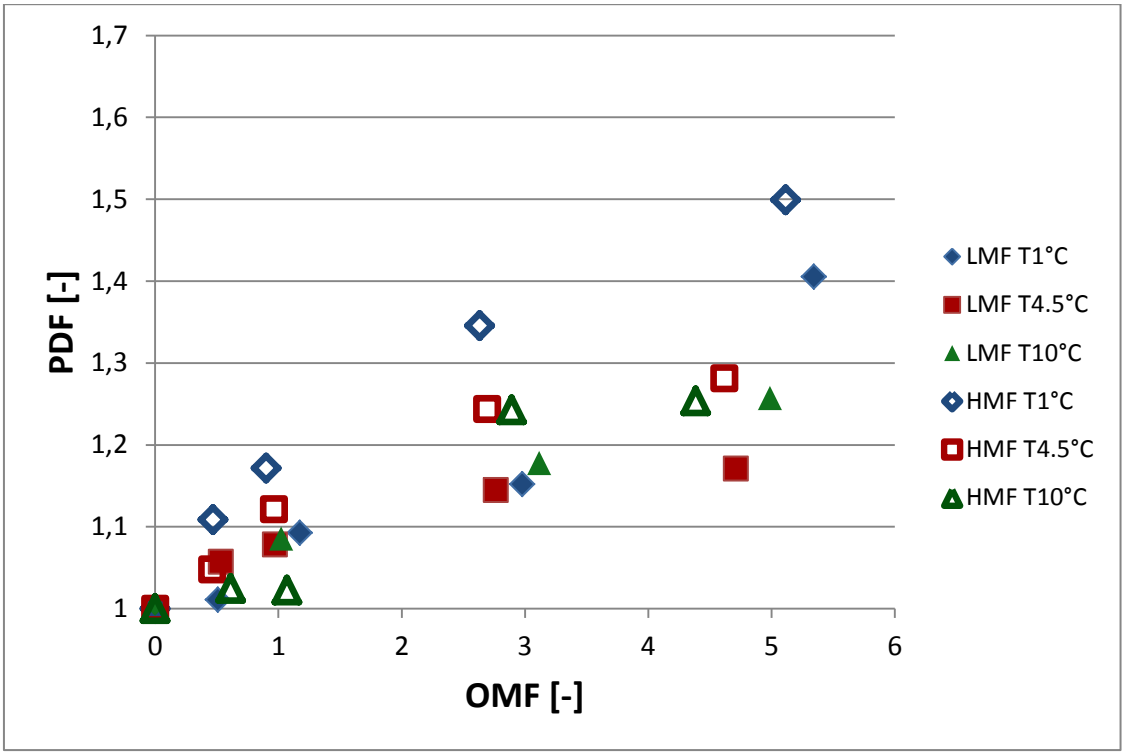

Figure 6.3 Pressure drop factor for evaporator A and R410A

The pressure drop factor shows an increase as the oil mass fraction increases. The pressure drop factor is always higher at high mass flow rate. At high mass flux it is more evident that the low saturation temperature causes a larger increase in the pressure drop since liquid density is higher.

6.2 R410A Evaporator B

6.2.1 Oil retention volume

The results of the tests for the measurement of the volume of oil retained in the system are shown in Figure 6.4

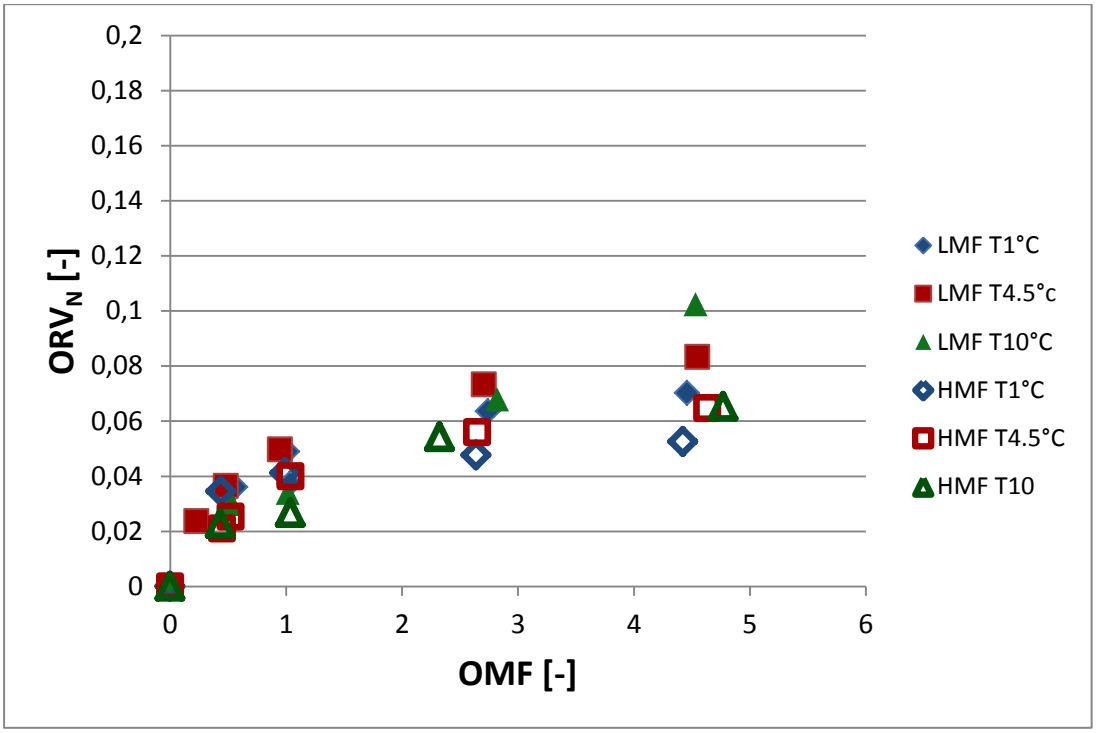

Figure 6.4 Normalized oil retention volume for evaporator B and R410A

The difference between high mass flow rate and low mass flow rate is less evident when evaporator B was used. The values at high and low mass flux present similar trend and magnitude, only the oil retention at low mass flux is a bit larger. The oil retained at low saturation temperature shows to be slightly smaller. Also with evaporator B was taken a test at very low mass flow rate. The result shows that there is still a filling mechanism in the outlet header but far more evident than it was in evaporator A.

6.2.2 Heat transfer factor

The results of the experiments for heat transfer factor are presented in Figure 6.5

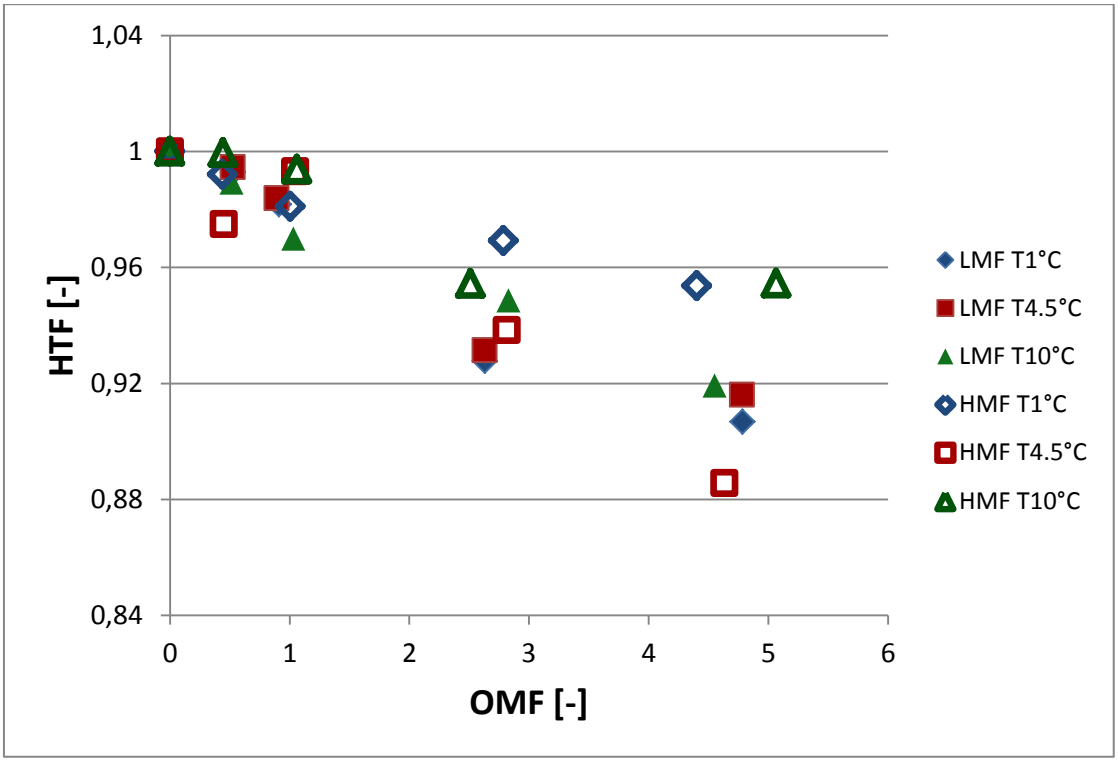

Figure 6.5 Heat transfer coefficient for evaporator B and R410A

The decrease in the capacity of the coil is almost linear with the oil mass fraction. The heat transfer factor is usually higher at high mass flow rate, only the series at saturation temperature of 4.5°C and high mass flux presents unusual low values. The heat transfer factor doesn't show to be affected by the change in the saturation temperature.

6.2.3 Pressure drop factor

The pressure drop factors are reported in Figure 6.6

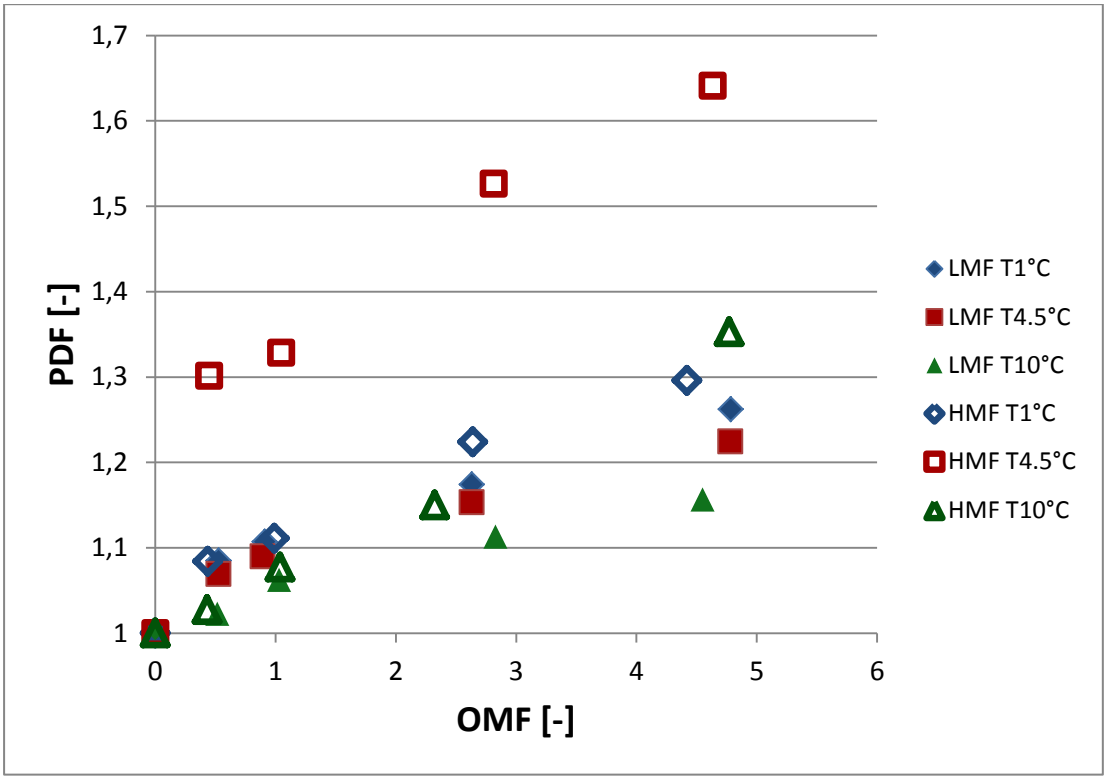

Figure 6.6 Pressure drop factor for evaporator B and R410A

At a first glance it is possible to recognize that the series at high mass flux and saturation temperature of 4.5°C shows values far higher than any other series. Nonetheless the increase in pressure drop caused by the presence of oil is always larger at high mass flow rate. At low mass flux it is possible to see that the effect of oil on pressure increases at low temperature, the magnitude of this change is very small.

6.3 R134a and R1234yf

R1234yf is supposed to replace R134a for the mobile air conditioning. Moreover the two refrigerants were used to perform tests in very similar conditions. They were tested at low mass flux and with temperature ranging from 1°C to 10°C. These tests were run having a constant mass flow rate of refrigerant, and more oil was injected during the tests. The results of the injected tests were compared to the values measured before the injection. Because of this reason a part of the increase in pressure drop is caused by the increased mass entering the coil. On the other hand, the decrease in capacity is only caused by the oil affecting the behavior of the same amount of refrigerant.

6.3.1 Oil Retention Volume

The results of the tests for the measurement of the volume of oil retained in the system are shown in Figure 6.7 where the solid points represent the values for R134a, the hollow point the one with R1234yf.

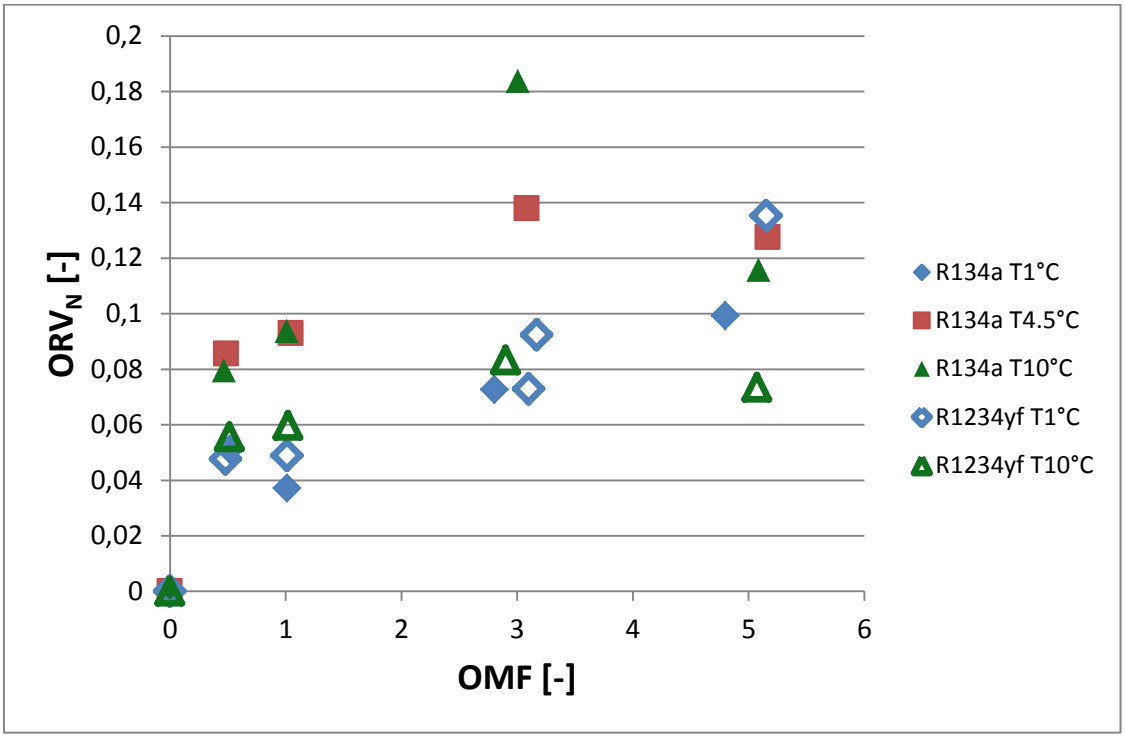

Figure 6.7 Normalized Oil Retention Volume for experiments using R134a and R1234yf

The amount of oil retained increases with the Oil Mass Fraction. At high saturation temperature it is reached a maximum around 3%. Probably the amount of oil retained is not affected only by the Oil Mass Fraction. It is likely that the increased OMF causes a loss of superheating at microchannel outlet. As a consequence a larger amount of refrigerant is present in the liquid mixture. The decrease in the viscosity of the liquid is a possible cause for the smaller oil retention at high mass flow rate.

An increase in the saturation temperature affected the amount of oil retained in the system. The values for the saturation temperatures of 4.5°C and 10°C is always higher. The high pressure makes the vapor more dense. As a consequence, the velocity of the vapor decreases and the shear stress on the liquid layer too.

R1234yf shows a more clear trend, the amount of oil retained in the system increases as the OMF increases. Only the value at 5% and T10°C is slightly smaller than the 3% one. The oil retention seems not to be affected by the saturation temperature, the two series always present very similar values except for very high oil mass fraction.

Comparing the two different refrigerants R1234yf seems to be more effective in preventing the oil retention. The difference is more evident at high saturation temperature when the difference is very significant. At low temperature the oil retained is about the same. This result is different from the findings of Sethi [41] in a suction line. Actually he pointed out that the oil retained was about the same for the two refrigerants in case of same system cooling capacity.

6.3.2 Heat Transfer Factor

The results of the experiments for pressure drop are presented in Figure 6.8

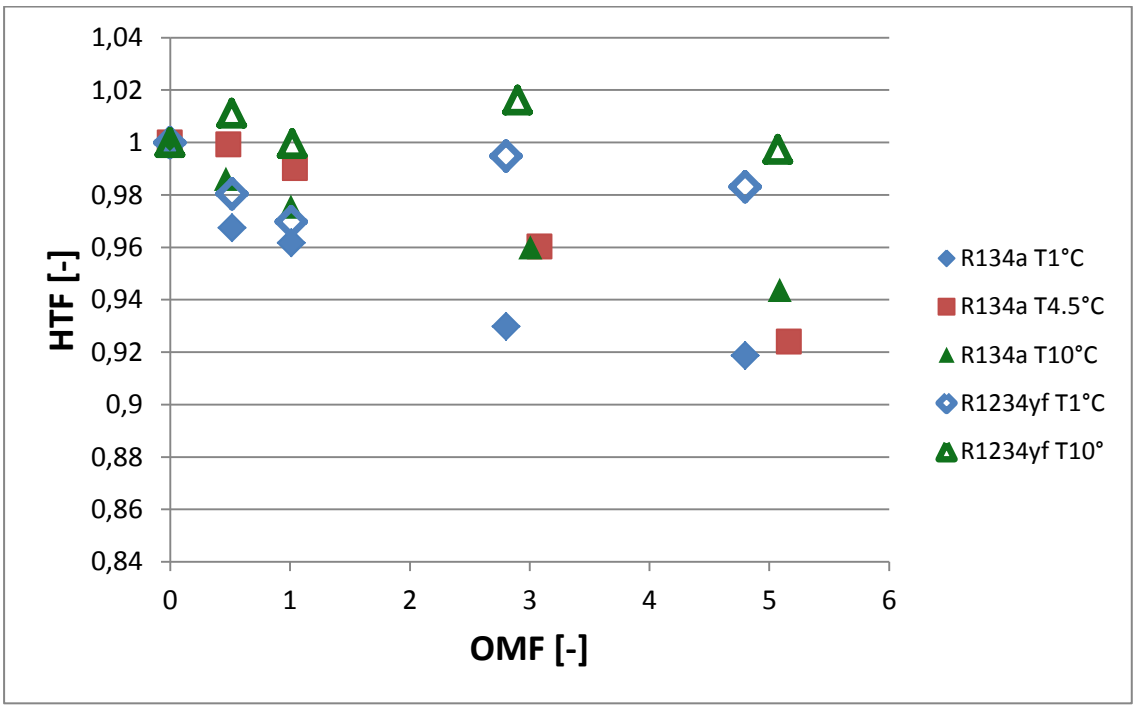

Figure 6.8 Heat transfer factor for experiments using R134a and R1234yf

Considering R134a, the decrease in the coil capacity results to be affected by an increase in the mass of circulating oil. Even if the amount of refrigerant

entering the coil during the experiments was always the same the cooling capacity decreased. Also the saturation temperature affects the impairment caused by the oil. The penalization at low saturation temperature is always larger than the one at high and medium temperature.

The same result is not showed in the results for R1234yf. The values of HTF are always higher at high saturation temperature. On the other hand, an increase in the oil fraction does not seem to affect the decrease in the coil capacity.

The two refrigerants show a very different behavior for the penalization in capacity due to the presence of oil. When R1234yf is circulating in the system it seems to be unaffected by the oil, it can even happen that the capacity of the coil slightly increases for the higher total mass flow rate. It is likely that the oil is not affecting the boiling refrigerant whereas R134a shows a reduction down to 92% at high mass flow rate.

6.3.3 Pressure Drop Factor

The pressure drop factors are reported in Figure 6.9

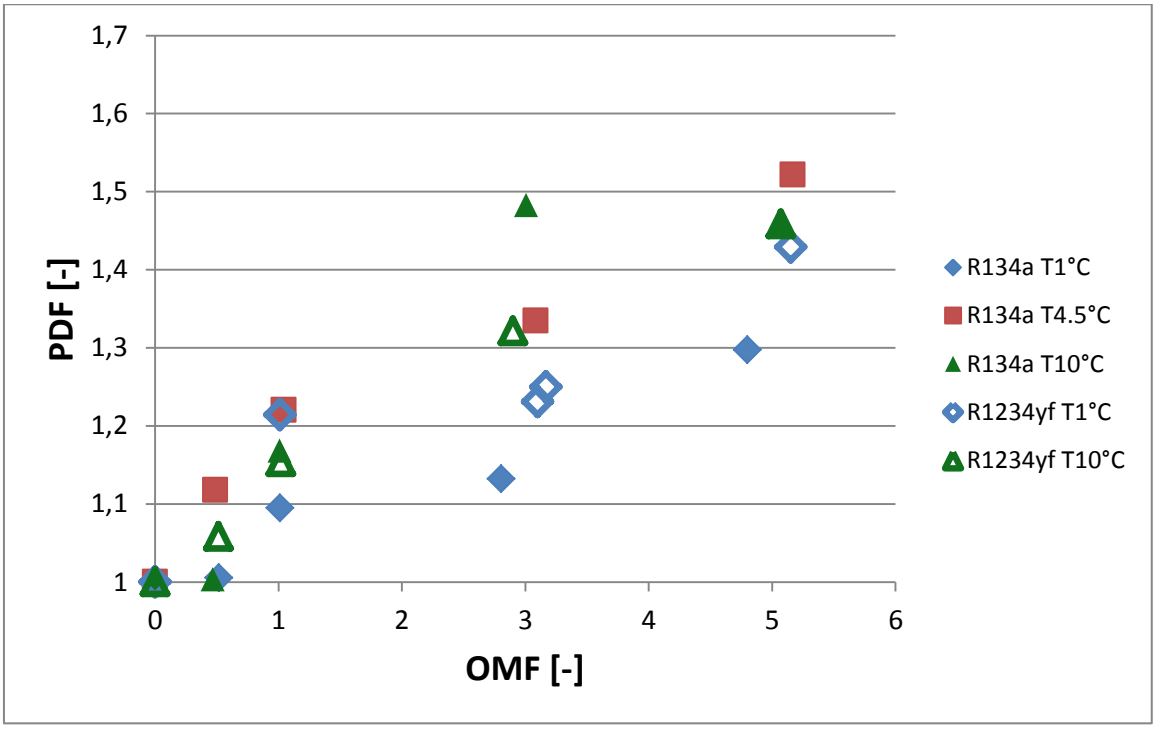

Figure 6.9 Pressure Drop Factor for experiments using R134a and R1234yf

The increase in pressure drop shows to be strongly dependent with the Oil Mass Fraction. Only one time the pressure drop decreases when the oil fraction increases.

Pressure drop seems to be unaffected by the saturation temperature when working with R1234yf. On the contrary the values of Pressure Drop Factor at low saturation temperature are always smaller for R134a.

Even if there is a certain scatter in the data the magnitude of the effect of oil on pressure drop on the two refrigerant is the same. The increase in pressure drop shows to be around 40% at high Oil Mass Fraction. Sethi [41] studies on a suction line found that with the same mass flux R134a had pressure drop 10-15% higher than R1234yf. This fact is not recognizable in the present work.

6.4 More observations

The effect of using different evaporators or refrigerants is investigated in this section.

Evaporator A has the microchannels entering in the header when the refrigerant is flowing upward. All the volumes created by the tubes entering the header tend to be filled of oil rich mixture because of the gravity force. This filling is observed mainly at low mass flux only in Evaporator A. In evaporator B the header is capsized, this effect is not observed. The presence of the filling phenomena stresses the difference between high and low mass flow rate when using evaporator A. A similar behavior was experienced by Jin ad Hrnjak [37] working with a microchannel condenser. They found that the amount of oil retained in the coil was very little sensitive to the input change of oil mass fraction. The heat exchanger they used had vertical header and horizontal channels. In the inlet header both gravity and refrigerant shear stress pointed downwards, so the header worked as an oil separator. The oil filled up the bottom of the header and the bottom channels too. Since the oil did not undergo phase change the surface temperature of the channels was cooled down faster than the rest of the two-phase tubes. The lower temperature of the bottom channels was verified by the infrared images taken.

The difference caused by the change in mass flux using evaporator B is far smaller than the change measured in evaporator A. In evaporator B the normalized oil retention volume is smaller, this is partially caused by the fact that the volume of the evaporator is bigger. Considering the mere mass of oil

retained in the microchannel evaporator, the values for evaporator A are still larger than the evaporator B ones.

The change of evaporator is not affecting that much the capacity of the heat exchanger. The heat transfer factor is slightly higher for evaporator A. To have the same conditions of refrigerant at the coil outlet when oil is not present in the system evaporator A needs a temperature about 2°C higher. It is possible that the lower temperature of the air affects the system when oil is injected in the system. The superheating at the outlet becomes smaller and there is a bigger amount of non-evaporating refrigerant in the oil rich mixture. This results in a larger penalization caused by the presence of oil.

The pressure drop factor presents similar trend for both the evaporators. Apart from some exceptions all the series have a pressure drop factor of about 1.3 at oil mass fraction of 5%.

The oil retention volume is about the same for all the refrigerants. The normalized value usually ranges between 0.08 and 0.13, the filling phenomena is recognizable using all the refrigerants. Only using R134a it is possible to recognize a clear trend caused by the change in saturation temperature. In the case of R410A the pressure was consistently higher, the increase in density of the vapor is balanced by the decrease in vapor speed.

R1234yf seems to be quiet unaffected by the presence of oil, the heat transfer factor is always around 1. R410A is the most affected considering the data presented. Is yet to be said that the procedure used for the normalization was different. Considering the different procedure is reasonable to assume that the impact of oil is more of less the same for R410A and R134a.

For the same reason the increase in pressure drop in the figures results to be higher. It is likely that, considering the different procedure, the magnitude of the effect of oil on pressure drop is similar for all the refrigerants.

All the parameters are proportional to the oil mass fraction. The presence of oil at low mass flow rate for evaporator A presents a sudden increase as soon as oil is injected. After this filling phenomena the oil retention volume increase in a linear way with the oil mass fraction. The increased oil mass fraction increases the amount of oil retained in the coil. More oil causes more refrigerant not to evaporate in the heat exchanger and the capacity decreases. Last the oil has larger viscosity causing the pressure drop to increase. Furthermore the oil retained decreases the flow cross sectional area for vapor.

The presence of oil makes the flow to turn to annular flow earlier, the annular flow presents higher pressure drop compared to churn flow.

The main issue related to saturation temperature is the appearance of immiscibility between oil and refrigerant. Since the effect of saturation temperature is almost negligible and often controversial, it is likely that cases of immiscibility never occur in the operating range of saturation temperatures.

6.5 Effect of superheating

During the experiments using R134a two more series were tested which were not reported in the test matrix. The two series were run having a different superheating compared to all the other experiments. The first series has a superheat around 3°C and the second a superheat of 15°C. The present work refers to them as Low SH and High SH.

The effect of superheating on oil retention volume is showed in Figure 6.10

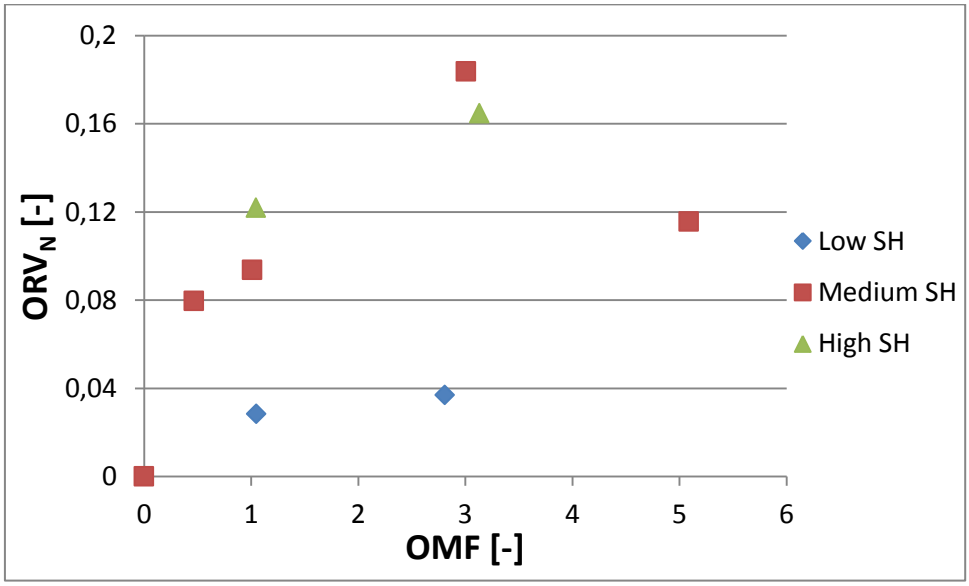

Figure 6.10 Effect of superheating on normalized oil retention volume

The superheating showed to have a big impact on the amount of oil retained in the system. A decrease of the superheating at the coil outlet increases the amount of refrigerant in the oil rich liquid mixture. The viscosity as a consequence has a drop. This makes the oil retention far smaller at low superheating.

The effect of superheating on the heat transfer factor is showed in Figure 6.11

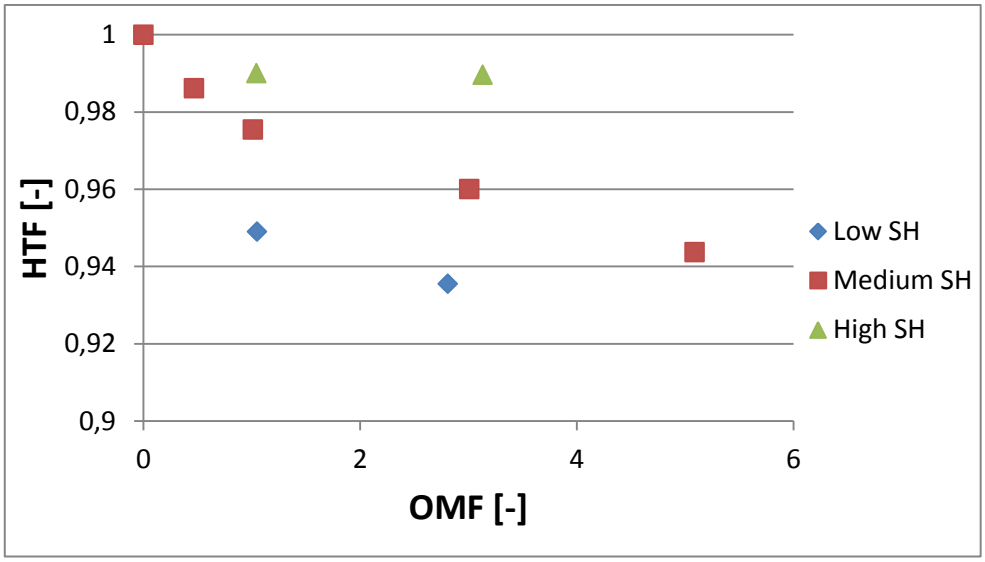

Figure 6.11 Effect of superheating on heat transfer factor

As stated before an increase in the superheating decrease the amount of liquid refrigerant at the coil outlet. As a consequence the impairment in the capacity is smaller. On the other hand, a decrease in the superheating results in a large reduction of the coil capacity. This experimental results confirmed had a good agreement with the results of the model from Youbi-Idrissi [30] about the effect of superheating on the enthalpy of the mixture.

The effect of superheating on the pressure drop factor is showed in Figure 6.12

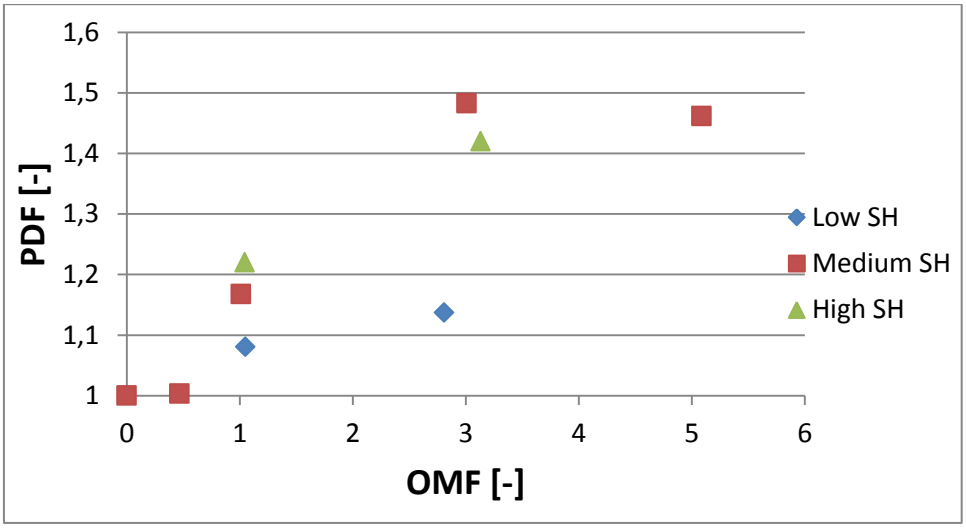

Figure 6.12 Effect of superheating on pressure drop factor

The pressure drop factor presents a trend which is very similar to the oil retention volume. The presence of a less viscous liquid mixture in case of low superheating results in smaller pressure drop.

7 Model Development

7.1 Assessment of previous work

The modeling of the microchannel evaporator started from the work from Ipseng Iu [42] who developed an air to air heat pump simulation program with the goal of designing an oriented tool filling the lack of product development experience with the new generation of HFC (i.e. R410A, R134a…). There are several remarkable point about this work:

- A great attention is paid to the heat exchanger circuiting. It is an important aspect in system design but is universally ignored in simple models. This is an important aspect for the optimization of systems.
- Refrigerant mixtures. The use of refrigerant mixtures is increasingly popular and simple models were not adequate to them. Instead of considering the mere average saturation temperature the model was able to account for the temperature change in the saturation region.
- Local air side heat transfer coefficient. The heat transfer coefficient varies from row to row. The model from Iu was able to account for this. He developed a row-by-row heat transfer coefficient correlation for this purpose.

Each heat pump component was developed as a stand-alone program, this to make possible to focus on a part at a time in case of further improvements. The models were also integrated into a single program to simulate overall system operations.

For the present work the Heat Pump Program was used in the Coil Only mode which allowed to solve just the evaporator regardless of all the other parts of the system.

7.2 Development of the model

To solve the problem, in order to solve the entire coil, only one tube was considered this requires to have uniform condition among all the tubes both on refrigerant and air side. On refrigerant side the manufacturer assured that the inlet header is able to provide a uniform distribution when the quality is below 10%. Great attention was paid when running tests to fulfill this requirement as previously stated in section 5.2 and 5.7 for the air side and the refrigerant side respectively. It is possible to obtain the whole capacity of the coil simply

considering the heat from a single tube times the number of channels. It is even easier for pressure drop since it is the same on all the channels

The tube was modeled using the discrete segment method dividing it into small elements. A schematic of the segmentation model is presented in Figure 7.1. The size of the segment is small enough to consider the properties of air and refrigerant constant within the segment with a little error. All the simulations presented in the current work were run having 100 segment, to check the sensitivity to the number of segment they were increased to 200 and no difference was observed. Each segment is resolved iteratively calculating the heat transferred and the pressure drop on both air and refrigerant side. The output properties of the refrigerant for a segment are used as input for the downstream one until the end of the coil is reached. For the element located at the coil inlet, the conditions are equal to the coil inlet conditions. Evaporator A has only one slab so the air at the inlet is always at the same condition of the room. Evaporator B has two slabs and it was installed in counter cross flow. This way the first slab refrigerantwise receives air coming from the other slab. Because of the fins the air mixing was considered negligible, so the inlet conditions of air are the same of the outlet of the corresponding segment in the front slab. Since to solve the first slab it was necessary to have the conditions of the air coming out from the second slab the coil was solved iteratively. For the first slab the conditions of the air at the inlet of the control volume were taken from the previous iteration, the iterations were stopped when the difference of capacity between two iterations were smaller than a threshold.

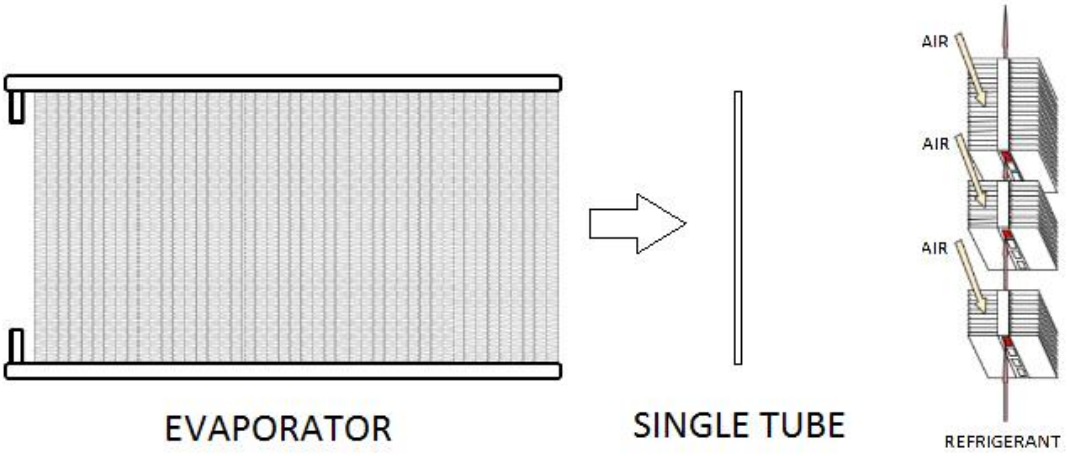

Figure 7.1 Graphic explanation of the model

For each segment the heat transfer capacity was calculated using the ε-NTU method:

$$\dot{\boldsymbol{Q}} = \boldsymbol{\varepsilon}\, \dot{\mathbf{C}}_{\boldsymbol{min}}(\boldsymbol{T_{air,in}} - \boldsymbol{T_{ref,in}}) \qquad 7.1$$

Where

$$\dot{\boldsymbol{C}}_{\boldsymbol{min}} = \boldsymbol{MIN}(\dot{\boldsymbol{m}}_{\boldsymbol{air}}\boldsymbol{c_{p,air}}, \dot{\boldsymbol{m}}_{\boldsymbol{ref}}\boldsymbol{c_{p,ref}}) \qquad 7.2$$

The coil effectiveness is calculated differently depending on the operating conditions using the following unmixed-mixed relations for crossflow.

For single-phase refrigerant if $\dot{C}_{min} = \dot{C}_{ref}$

$$\boldsymbol{\varepsilon} = \frac{\mathbf{1}}{\boldsymbol{C_r}}\left[\mathbf{1} - \boldsymbol{exp}\left(-\boldsymbol{C_r}(\mathbf{1} - \mathbf{exp}(-\boldsymbol{NTU}))\right)\right] \qquad 7.3$$

if $\dot{C}_{min} = \dot{C}_{air}$

$$\boldsymbol{\varepsilon} = \mathbf{1} - \mathbf{exp}\left[-\frac{\mathbf{1}}{\boldsymbol{C_r}}(\mathbf{1} - \mathbf{exp}(-\boldsymbol{C_r} * \boldsymbol{NTU}))\right] \qquad 7.4$$

Whereas for two phase refrigerant:

$$\boldsymbol{\varepsilon = 1 - \exp(-NTU)} \qquad 7.5$$

where

$$\boldsymbol{NTU = \frac{UA}{C_{min}}} \qquad 7.6$$

$$\boldsymbol{C_r = \frac{\dot{C}_{min}}{\dot{C}_{max}}} \qquad 7.7$$

Assuming negligible fouling resistances both inside and outside and no dew/frost on coil, the overall heat transfer coefficient is calculated in this way:

$$\boldsymbol{\frac{1}{UA} = \frac{1}{h_{ref}A_{in}} + \frac{Thk}{k_{tube}A_m} + \frac{1}{\eta_{surf}h_{air}A_{out}}} \qquad 7.8$$

Where the finned surface efficiency is

$$\boldsymbol{\eta_{surf} = 1 - \frac{A_{fin}}{A_{out}}(1 - \eta_{fin})} \qquad 7.9$$

The fin efficiency is calculated as a rectangular fin with height half of the distance between two tubes.

$$\boldsymbol{\eta_{fin} = \frac{\tanh(m_{fin} * L_{fin})}{m_{fin} * L_{fin}}} \qquad 7.10$$

Where

$$\boldsymbol{m_{fin} = \sqrt{\frac{h_{air} * 2p_{fin}}{k_{fin}A_{fin}}}} \qquad 7.11$$

7.3 Wet surface conditions

It may happen that the air coming across the heat exchanger is cooled below the dew point. Causing part of the moisture present in the air to condense. This case also occur just locally near to the cold tube surface even if the bulk temperature of the air is still above the dew point. For the calculation of the heat transfer in the segments where dehumidification occurs the procedure developed by Braun[43] was used. The capacity of the segment is calculated as

$$\boldsymbol{\dot{Q} = \varepsilon_w \dot{m}_{air}(h_{a,i} - h_{r,s})} \qquad 7.12$$

The equations for ε are the same as in dry condition but NTU_w is used instead of *NTU*. NTU_w is defined as:

$$NTU_w = \frac{UA_w}{\dot{m}_{air}} \qquad 7.13$$

Where

$$\frac{1}{UA_w} = \frac{c_s}{h_{ref}A_{in}} + \frac{c_s T_{hk}}{k_{tube}A_m} + \frac{c_{p,m}}{\eta_{surf}h_{air}A_{out}} \qquad 7.14$$

$C_{p,m}$ is the specific heat of the air-water mixture and *Cs* is the saturation specific heat defined as the derivative with respect to temperature of the saturated air enthalpy evaluated at the refrigerant temperature.

$$c_s = \frac{dh_{r,s}}{dT} \qquad 7.15$$

7.4 Air side heat transfer coefficient and pressure drop

For the calculation of the air side heat transfer coefficient, the most reliable correlation in the open literature are used. Published air side heat transfer correlations are usually presented in terms of the j-factor, as given by:

$$h_{air} = j * c_{p,air} * G_{air} * Pr_{air}^{-2/3} \qquad 7.16$$

Where G_{air} is the mass flux of the air based on the minimum free flow area of the heat exchanger. The j-factor is an empirical correlation that is derived from experimental data. Each fin pattern has its own j-factor correlation, for the louvered fin was used the correlation by Chang and Wang [44]. Their correlation is the following:

$$j = Re_{Lp}^{-0.49} \left(\frac{\theta}{90}\right)^{0.27} \left(\frac{F_p}{L_p}\right)^{-0.14} \left(\frac{F_l}{L_p}\right)^{-0.29} \left(\frac{T_d}{L_p}\right)^{-0.23} \left(\frac{L_l}{L_p}\right)^{0.68} \left(\frac{T_p}{L_p}\right)^{-0.28} \left(\frac{\delta_f}{L_p}\right)^{-0.05} \qquad 7.17$$

Valid for corrugated fin geometry and 100<Re_{Lp}<3000 The correlation was able to predict 89,3% of corrugated louver fin data from the database within ±15% and a mean deviation of 7,55%.

A further technical note always from Chang and Wang [45] provide the correlations to calculate the Fanning Friction Factor. The final equation form of the frictional factor is given as follows:

$$f = f1 * f2 * f3 \qquad 7.18$$

Where

$$f1 = 4,97 Re_{Lp}^{0,6049-\frac{1,064}{\theta^{0,2}}} (log_e((\frac{F_t}{F_p})^{0,5} + 0,9))^{-0,527} \qquad 7.19$$

$$f2 = \left(\left(\frac{D_h}{L_p}\right) log_e(0,3 Re_{Lp})\right)^{-2,966} (F_p/L_l)^{-0,7931(T_p/T_h)} \qquad 7.20$$

$$f3 = \left(\frac{T_p}{D_m}\right)^{-0,0446} log_e(1,2 + (L_p/F_p)^{1,4})^{-3,553} \theta^{-0,477} \qquad 7.21$$

Valid for Re_{Lp} between 150 and 5000

7.5 Refrigerant side correlations

7.5.1 Heat transfer coefficient

The two phase heat transfer coefficient is calculated using the correlation from Bertsch et al [46]. They developed a composite correlation which includes nucleate boiling and convective heat transfer terms while accounting for the effect of bubble confinement in small channels. The correlation was developed from a database of 3899 data points from 14 studies in literature. The range of hydraulic diameter was between 0.16 and 2.92 mm and the mass flux from 20 to 3000 kg/m^{2}s. This correlation was chosen because it was developed for microchannel and is able to account properly for the dryout. The two phase heat transfer coefficient is calculated as sum of weighted nucleate boiling and convective heat transfer. Two coefficient were added to have a proper description of flow boiling.

$$h_{FB} = S * h_{NB} + F * h_{conv,tp} \qquad 7.22$$

S is a suppression factor applied to the nucleate boiling term to account for dryout as the vapor quality increases, while *F* account for the enhanced convection due to higher flow velocity at increased vapor speed. For the nucleate boiling the Cooper [47]correlation was used:

$$\boldsymbol{h_{NB} = 55\, P_r^{0.12}\, (-log_{10} P_r)^{-0.55}\, M^{-0.5}\, (q")^{0.67}} \qquad 7.23$$

The convective heat transfer coefficient is calculated as the average of the convective heat transfer coefficients for pure liquid and pure vapor, with a linear dependence on the vapor quality *x*:

$$\boldsymbol{h_{conv,tp} = h_{conv,l}\,(1 - x) + h_{conv,v}\, x} \qquad 7.24$$

Due to the low Reynolds numbers usually encountered in microchannels, the correlation from Hausen [48] for developing laminar flow was used.

$$\boldsymbol{h_{conv} = \left(3.66 + \frac{0.0668 \frac{D_h}{L} Re\, Pr}{1 + 0.04 \left(\frac{D_h}{L} Re\, Pr\right)^{2/3}}\right) \frac{k}{D_h}} \qquad 7.25$$

The formulation chosen for the suppression factor assumed a linear decrease of the nucleate boiling heat transfer coefficient with increasing vapour quality.

$$\boldsymbol{S = 1 - x} \qquad 7.26$$

The enhancement factor is influenced by the confinement of bubbles in small channels. This is the primary reason for the observed differences in the heat transfer for conventional tubes and microchannels. The enhancement factor must reduce to 1 for pure liquid and pure vapour and be greater than within the two-phase regime. Therefore the following equations is adopted

$$\boldsymbol{F = 1 + 80\, e^{-0.6Co} (x^2 - x^6)} \qquad 7.27$$

Where Co is the Confinement number defined as:

$$\boldsymbol{Co = \left(\frac{\sigma}{g\,(\rho_l - \rho_v)\, D_h^2}\right)^{1/2}} \qquad 7.28$$

For the segment in which the refrigerant is single phase either the Gnielinski [49] correlation or a convenient Nusselt number was used to account for turbulent flow and laminar flow.

At very high quality the two phase heat transfer coefficient decreases to very small values. It may happen that the two phase heat transfer coefficient is

smaller than the single phase one for pure vapor. In this case the value for saturated single phase vapor is considered.

To account for the presence of the oil a correction was added to the model for pure refrigerant. The effect of liquid-phase mass transfer on the nucleate boiling contribution to flow boiling was included by introducing the Thome [50] mixture boiling equation into the Cooper correlation (7.23). The analytical mass transfer resistance factor Fc for nucleate boiling of mixtures is a function of the boiling range ΔT_{bp}. His factor Fc is:

$$\boldsymbol{Fc} = \left\{\mathbf{1} + (\boldsymbol{h_{id}}/\boldsymbol{q})\boldsymbol{\Delta T_{bp}}\left[\mathbf{1} - \boldsymbol{exp}\left(\frac{-\boldsymbol{q}}{\boldsymbol{\rho_l h_{LV} \beta_L}}\right)\right]\right\}^{-\mathbf{1}} \qquad 7.29$$

h_{id} is the ideal transfer coefficient calculated using the Cooper correlation and β_L is the mass transfer coefficient set to the fixed value of 0.0003 m/s based on numerous experimental pool boiling studies.

When oil is injected in the system liquid is still present in condition which would be impossible in case of pure refrigerant, so the flow is still two phase even if the vapor is in superheated condition. To account for this a single phase correlation for heat transfer coefficient is used in case the vapor is 1°C hotter than the saturation temperature of pure refrigerant at that pressure.

7.5.2 Pressure drop correlations

To predict the frictional pressure drop the Mishima and Hibiki [51] correlation was used. This correlation was chosen because it was developed specifically for microchannel heat exchanger. They ran their experiments with two phase flow in tubes diameter ranging between 1 and 4 mm. Their correlation is based on the Chisholm [52] equation:

$$\Delta \boldsymbol{P_{frict,tp}} = \boldsymbol{\phi_L^2 \Delta P_L} \qquad 7.30$$

$$\boldsymbol{\phi_L^2} = \mathbf{1} + \frac{\boldsymbol{C}}{\boldsymbol{X_{tt}}} + \frac{\mathbf{1}}{\boldsymbol{X_{tt}^2}} \qquad 7.31$$

$$\boldsymbol{X_{tt}} = \frac{\boldsymbol{\Delta P_L}}{\boldsymbol{\Delta P_V}} \qquad 7.32$$

The difference introduced was a new definition of the Chisholm's parameters developed in order to account for the size of the diameter. The hydraulic diameter for this correlation is expressed in mm.

$$\boldsymbol{C} = \mathbf{21}(\mathbf{1} - \boldsymbol{e^{-0.319 D_h}}) \qquad 7.33$$

In the database for the development of the correlation the diameter ranged from 1 mm to 4 mm and the Reynolds number ranged between 50 and 10000.

The momentum pressure drop were calculated according to Ragazzi [53]. The momentum is calculated at the inlet and at the outlet of the segment. The pressure drop is calculated considering the increase of the momentum of the flow

$$\Delta P_{mom} = G^2 \left\{ \left[\frac{x^2}{\rho_v \alpha} + \frac{(1-x^2)}{\rho_l (1-\alpha)} \right]_{out} - \left[\frac{x^2}{\rho_v \alpha} + \frac{(1-x^2)}{\rho_l (1-\alpha)} \right]_{in} \right\} \qquad 7.34$$

The correlation for the calculation of the void fraction is presented in chapter 6.8.

The gravitational pressure drop were calculated with the following equation:

$$\Delta P_{grav} = \rho \, g \, H_{mod} \qquad 7.35$$

where

$$\rho = \left(\frac{x}{\rho_v} + \frac{(1-x)}{\rho_l} \right)^{-1} \qquad 7.36$$

7.6 Pressure drop in the headers

Suitable correlations were used in order to calculate both the frictional and local pressure drop occurring in the pipeline, in the tube and in the contraction and expansion in the headers. Since vapor was present at the microchannel inlet, the correlation of Paliwoda [54] was used to properly account for the effects of two phase flow. Most of the pressure drop in the coil occurs in the distributor at the inlet. A picture of an inlet header is presented in Figure 7.2

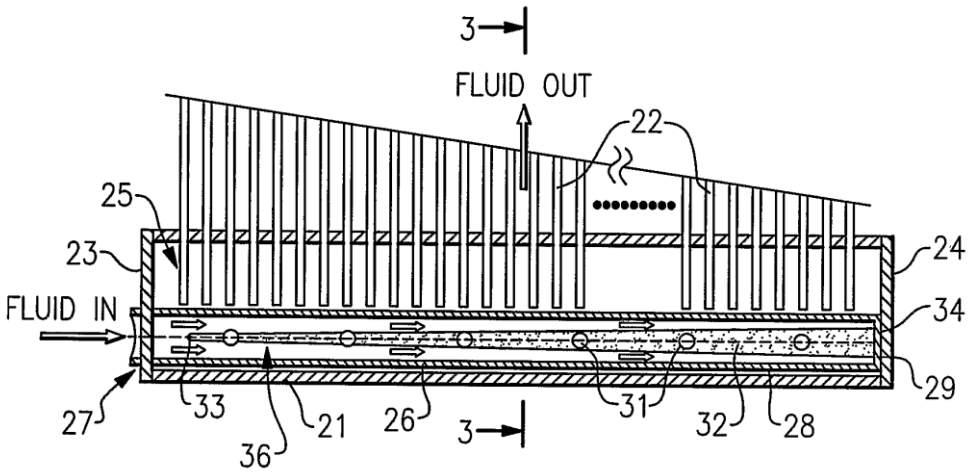

Figure 7.2 Schematic of an inlet header. The picture is taken by a patent from Johnson Control

It was assumed that the pressure drop occurred when the refrigerant came out from the distributor tube to the main volume of the header. All the holes in the tube were modeled as a single orifice and an equivalent diameter was assigned to it. To calculate the equivalent diameter the 1 D formula for pressure drop suggested in [55] was used:

$$\Delta \boldsymbol{P} = \frac{\boldsymbol{G^2}}{\boldsymbol{2\rho}}\left(\frac{\boldsymbol{1}}{\boldsymbol{Ar\ C_c}} - \boldsymbol{1}\right) \qquad 7.37$$

Where *Ar* is the area ratio between the tube entering the header and the equivalent valve and C_c is the contraction factor of the flow. The equivalent diameter of the orifice for evaporator A was found to be 3.1 mm, the equivalent diameter for evaporator B was found experimentally to be 2.4 mm

7.7 Calculation of refrigerant-oil mixture properties

The thermodynamic and transport properties of refrigerant-oil mixtures are very important for calculating heat transfer and pressure drop, so methods for calculating these properties were necessary. Shen and Groll [13] provided a comprehensive review of the literature regarding refrigerant-oil mixture property calculations. They suggested methods for calculating properties such

as density, viscosity, and specific heat of refrigerant-oil mixtures. These methods have been included in the present work to calculate mixture properties and are summarized below. The main reference for this method is from Thome [56]. Unless specified otherwise, the properties of oil used in the following equation were obtained from manufacturer data. The properties of liquid and vapor refrigerant were calculated by making function using table data generated from Refprop.

The local properties of the liquid refrigerant-oil mixture, including the mixture temperature, are highly dependent on the concentration of oil in the mixture. However, the concentration of oil in the liquid refrigerant-oil mixture actually changes throughout a heat exchanger. This is because the oil circulating through vapor compression systems does not evaporate, so the oil remains concentrated in the liquid phase refrigerant. Therefore, the concentration of oil in the liquid refrigerant is dependent on the quality of the refrigerant-oil mixture. As the mixture quality increases (i.e. more refrigerant evaporates) the concentration of oil in the remaining liquid refrigerant increases. In order to calculate the local oil concentration, a baseline oil concentration for a system must be defined at a point where the refrigerant-oil mixture is completely in the liquid phase. The absolute oil mass fraction for a system is defined at this location according to the following equation

$$\boldsymbol{\omega_0} = \frac{\dot{\boldsymbol{m}}_{\boldsymbol{oil}}}{\dot{\boldsymbol{m}}_{\boldsymbol{oil}}+\dot{\boldsymbol{m}}_{\boldsymbol{ref}}} \qquad 7.38$$

Analogous to the calculation of the quality of a refrigerant in the two-phase region, the local quality of the refrigerant-oil mixture can be calculated as follows

$$\boldsymbol{x_{mix}} = \frac{\dot{\boldsymbol{m}}_{\boldsymbol{ref,vap}}}{\dot{\boldsymbol{m}}_{\boldsymbol{ref,vap}}+\dot{\boldsymbol{m}}_{\boldsymbol{ref,liq}}+\dot{\boldsymbol{m}}_{\boldsymbol{oil}}} \qquad 7.39$$

Once the absolute oil mass fraction and the local mixture quality have been calculated, the local oil mass fraction can be calculated. Using the conservation of mass and assuming all of the oil remains in the liquid phase, the local oil mass fraction is given by the following equation

$$\boldsymbol{\omega_{local}} = \boldsymbol{\omega_0}/(\mathbf{1}-\boldsymbol{x_{mix}}) \qquad 7.40$$

Because it is assumed that the oil remains in the liquid phase, there exists a maximum possible quality for the refrigerant-oil mixture, which is less than 1

$$x_{mix,max} = \frac{\dot{m}_{ref,vap}}{\dot{m}_{ref,vap}+\dot{m}_{oil}} = 1 - \omega_0 \qquad 7.41$$

If during an evaporation process, the refrigerant-oil mixture reaches $x_{mix,max}$ the temperature of the mixture can increase without increasing the quality of the mixture. Thus, because the refrigerant has evaporated out of the liquid refrigerant-oil mixture, the refrigerant-oil mixture enters the so-called superheating region without all of the mixture being in the vapour phase. This affects the heat transfer, the pressure drop and the oil retention.

7.7.1 Bubble Point Temperature Calculation

In order to calculate the capacity of the coil, a method to calculate the temperature of the oil-refrigerant mixture is necessary. Oil refrigerant mixtures behave in a manner similar to zeotropic refrigerant mixtures because, at a constant saturation pressure, the temperature increases, resulting in a temperature glide during the evaporation process. In Thome's work [56] he included a method that can be used to calculate the bubble point temperature of different refrigerant-oil mixtures using an empirical equation which is proposed:

$$T_{bub} = \frac{A(\omega_{local})}{lnPsat - B(\omega_{local})} \qquad 7.42$$

Where *Psat* is the local saturation pressure expressed in MPa. The constants *A* and *B* can be calculated according to the following equations

$$A(\omega_{local}) = a_{0+}a_1\omega_{local} + a_2\omega_{local}^3 + a_3\omega_{local}^5 + a_4\omega_{local}^7 \qquad 7.43$$

$$B(\omega_{local}) = b_{0+}b_1\omega_{local} + b_2\omega_{local}^3 + b_3\omega_{local}^5 + b_4\omega_{local}^7 \qquad 7.44$$

The values of the constants a1-a4 and b1-b4 were found to be almost independent from the oil-refrigerant pair, probably because the vapor pressure of the oil is negligible. The values of these constants are provided in the following Table 14.

Table 14 Empirical constants used to calculate the bubble point temperature of refrigerant-oil mixture

a1	182,52	b1	-0,72212
a2	-724,21	b2	2,3914
a3	3868	b3	-13,779
a4	-5268,9	b4	17,066

Thome suggested that the values of the constants a0 and b0 can be correlated depending on the specific pure refrigerant and saturation pressure. They are calculated using the following procedure:

- Calculate the saturation temperatures for the pure refrigerant at two different pressures, one just below the local saturation pressure and one just above
- Set ω_{local} equal to zero and evaluate the previous equation with the two different pairs of *Tsat* and *Psat*
- Solve the resulting system of two equations for the two unknowns, a_0 and b_0

This method provides a relatively simple, yet accurate way to calculate the bubble point temperature of different oil-refrigerant mixtures during evaporation process

7.7.2 Enthalpy variation

The presence of oil in the system makes the system behave as a strongly zeotropic mixture. The increase of the bubble temperature decreases the amount of heat transferred making a clear understanding of the relationship between enthalpy of the mixture and bubble temperature crucial for a good prediction of the coil capacity. The rigorous procedure proposed by Thome [50] was used in the present work. The change in enthalpy in a segment consists of three components: latent heat due to evaporation, sensible heat due to the change in bubble point temperature of the liquid-phase refrigerant-oil mixture, and sensible heat due to the change in bubble point temperature of the vapor-phase refrigerant. The following equation allows one to generate the heat release curve:

$$\boldsymbol{dh = h_{LV}\, dx + (1 - x_{mix})\, c_{p,mix}\, dT_{bub} + x_{mix}\, c_{p,ref,v}\, dT_{bub}} \quad 7.45$$

Starting from the condition at the coil inlet the quality is increased of a definite amount, 0.5% for the present work, the specific heat and the bubble

temperature are calculated and then the increase in enthalpy. This way it is possible to obtain the relationship between enthalpy, quality, and temperature by using the local concentration of oil to calculate all the physical properties.

7.7.3 Liquid mixture density

The density of the oil can be lower than, higher than or equal to the density of the refrigerant. The oils used in the present study have densities that are lower than the density of the refrigerant. If the oil and the refrigerant are immiscible, this can lead to formation of an oil film, which floats on top of the liquid refrigerant. This can act as a barrier for the heat transfer. This model is assuming complete miscibility so this possibility is not considered. For lower oil concentrations, the density of the mixture can often be approximated to that of an ideal mixture. Thus the density of the mixture of liquid refrigerant and oil is calculated using the method given by Jensen and Jackman [57]:

$$\frac{1}{\rho_{mix}} = \frac{\omega_{local}}{\rho_{oil}} + \frac{1-\omega_{local}}{\rho_{ref,l}} \qquad 7.46$$

7.7.4 Miscibility

Miscibility is of importance for the effect of oil on the heat transfer. It is likely that an immiscible oil forms a film on the evaporator surface. This will then act as an insulation and lead to a decrease of the heat transfer. Several studies Shah [58] and Chaddock [59] investigated the behavior of immiscible oil refrigerant. They performed experiments with ammonia and mineral oil. The oil was in these cases seen to yield a decrease in the heat transfer. The fluid flow was visually observed and a tar like sludge was found flowing in the tube at high oil concentration. This would also deeply affects the calculation of the mass of oil retained in the system. Since POE proved to have good miscibility with the refrigerants used in the present work the assumption of perfect miscibility was done.

7.7.5 Liquid mixture viscosity

The viscosity of the oil is about one thousand larger than the viscosity of the refrigerant. Thus is very important to have a proper prediction of the mixture viscosity. It affects the heat transfer coefficient decreasing the convective boiling, and it increases the pressure drop and the volume occupied by liquid in two phase flow. The effect of the presence of the oil is more important at high

quality when the increase in local oil concentration makes the viscosity of the mixture strongly increasing. The viscosity of the mixture of liquid refrigerant and oil is calculated using the method provided by Yokozeki [60]

$$\ln \mu_{mix} = \zeta_{ref,liq} \ln \mu_{ref,liq} + \zeta_{oil} \ln \mu_{oil} \qquad 7.47$$

Where ζ_i is the Yokozeki factor:

$$\zeta_i = \frac{W_i^k \psi_i}{\sum_j W_j^k \psi_j} \qquad 7.48$$

And W_i and ψ_i are the molecular mass and mole fraction, respectively, of component i. The exponent *k* is an empirical constant that is specific to different refrigerant-oil pair. However, Yokozeki found that setting *k*=0,58 provided accurate results for most refrigerant-oil pairs. The mole fraction of the oil can be obtained from the equation

$$\psi_{oil} = \frac{\omega_{local}(W_{ref}/W_{oil})}{1-\omega_{local}+\omega_{local}(W_{ref}/W_{oil})} \qquad 7.49$$

7.7.6 Liquid mixture thermal conductivity

The oil thermal conductivity is usually higher than the one of the pure refrigerant affecting the heat transfer factor especially in the last part of the evaporator. Is yet to be said that the increase in thermal conductivity remains small in the experimental conditions. The thermal conductivity of the mixture of liquid refrigerant and oil is calculated according to the method produced by Filippov [61]

$$k_{mix} = k_{ref,liq}(1-\omega_{local}) + k_{oil}\omega_{local} - 0.72\left(k_{oil}-k_{ref,liq}\right)(1-\omega_{local})\omega_{local} \qquad 7.50$$

7.7.7 Liquid mixture surface tension

Oil has a surface tension bigger than the pure refrigerant. One of the effect of the surface tension is to increase the tube wetting. The consequence is a large transfer of heat since the liquid film covers more of the surface compared to the flow of pure refrigerant. The surface tension also affects the nucleation. An increase in the surface tension would presumably increase the resistance to forming bubbles. Nucleation plays a major role in many cases in microchannel

flow boiling. The surface tension of the mixture of liquid refrigerant and oil is calculated according to the method provided by Jensen and Jackman [57]:

$$\sigma_{mix} = \sigma_{ref,liq} + (\sigma_{oil} - \sigma_{ref,liq})\sqrt{\omega_{local}} \qquad 7.51$$

[56]

7.7.8 Liquid mixture specific heat

The specific heat of the mixture of liquid refrigerant and oil is calculated according to the linear method provided by Jensen and Jackman [57]:

$$c_{p,mix} = \omega_{local}\, c_{p,oil} + (1 - \omega_{local}) c_{p,ref,liq} \qquad 7.52$$

The specific heat of the oil is calculated according to the following equation recommended by Thome [56]

$$c_{p,oil} = 4.186\left(\frac{0.338+0.00045(1.8*T_{oil}+32)}{\sqrt{\rho_{oil}/\rho_{water}}}\right) \qquad \mathbf{7.53}$$

7.8 Void fraction and oil retention

To calculate the mass of oil retained in the heat exchanger a void fraction model is necessary. Once the volume of the segment occupied by the liquid is known, it is possible to calculate the amount of oil retained using the oil local concentration and its density. Most of the void fraction correlations were developed for water or pure refrigerants so the viscosity of the liquid was far smaller than the viscosity of oil. Thus it was necessary to find a correlation able to understand the effect of viscosity on void fraction. The correlation from Mandrusiak and Carey [62] was chosen since it provided good results in the work of Jin and Hrnjak [37]. This correlation is based on Lockhart-Martinelli parameter, which is able to account for the high viscosity in liquid phase and laminar flow.

$$\alpha = (1 + 0.025Xtt)^{-2} \qquad 7.54$$

Using the void fraction it is possible to calculate the liquid hold up and using the local concentration of oil the amount of oil retained in the heat exchanger. Suitable assumptions were made for the calculation of the oil retained in the headers. The inlet header is considered full of liquid, even if the quality at microchannel inlet is not zero the velocity in the header is so slow that gravity is supposed to make liquid occupy the whole volume. The homogeneous model applied to the suction line provided good results according to Cremaschi . The outlet header is divided in a number of segments equal to the number of tubes.

The void fraction is calculated for each volume, the mass flow is different for each segment increasing moving to the header outlet and so the void fraction is different for every segment.

8 Model results for pure refrigerant

The predictions from the model are compared to the experimental results. Unfortunately the table for the properties of R1234yf were not available in time for the present work. So the simulations presented have just only results for R410A and R134a.

8.1 Validation of the correlations used

Before simulating the entire heat exchanger, a check of the correlations was done. The algorithm for the solution of the whole heat pump was validated by Iu [42]. In order to decouple the heat transfer air and refrigerant side, to check if both the correlations were correctly implemented, data from literature was simulated and compared.

The refrigerant side correlations were compared with the data from Yun Heo Kim [63]. This paper was used because they worked with a microchannel heat exchanger and the hydraulic diameter of their experimental setup was similar to the values of the heat exchanger used in the present work. The result of the comparison is showed in Figure 8.1

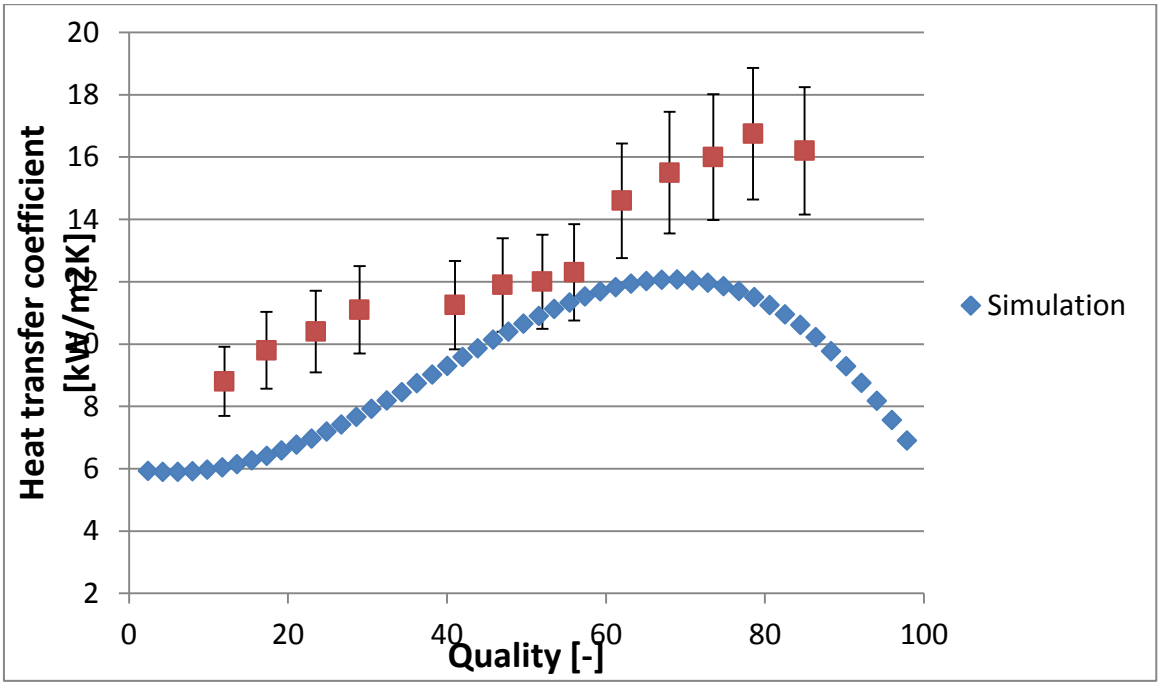

Figure 8.1 Comparison between experimental data from literature and the model

The simulation using the correlation from Bertsch [46] slightly under predicts the heat transfer coefficient, but it is always within the uncertainty of the correlation. The trend of Bertsch correlation was validated for a very wide range of conditions. The mean absolute error was found to be less than 30%. An increase of 30% of the simulation heat transfer coefficient would make them exactly of the same magnitude. The prediction of the heat transfer coefficient increases as the quality increases, as reported by the experimental data. The simulation curve shows the dryout occurring at slightly lower quality than it was measured.

Also the predicted pressure drop was compared to experimental data. The data were presented by the same paper from Yun Heo Kim. The model section developed to calculate the pressure drop shows a very good agreement with the experimental data. The prediction can capture both the magnitude and the trend of the pressure drop. The result of the comparison is showed in Figure 8.2

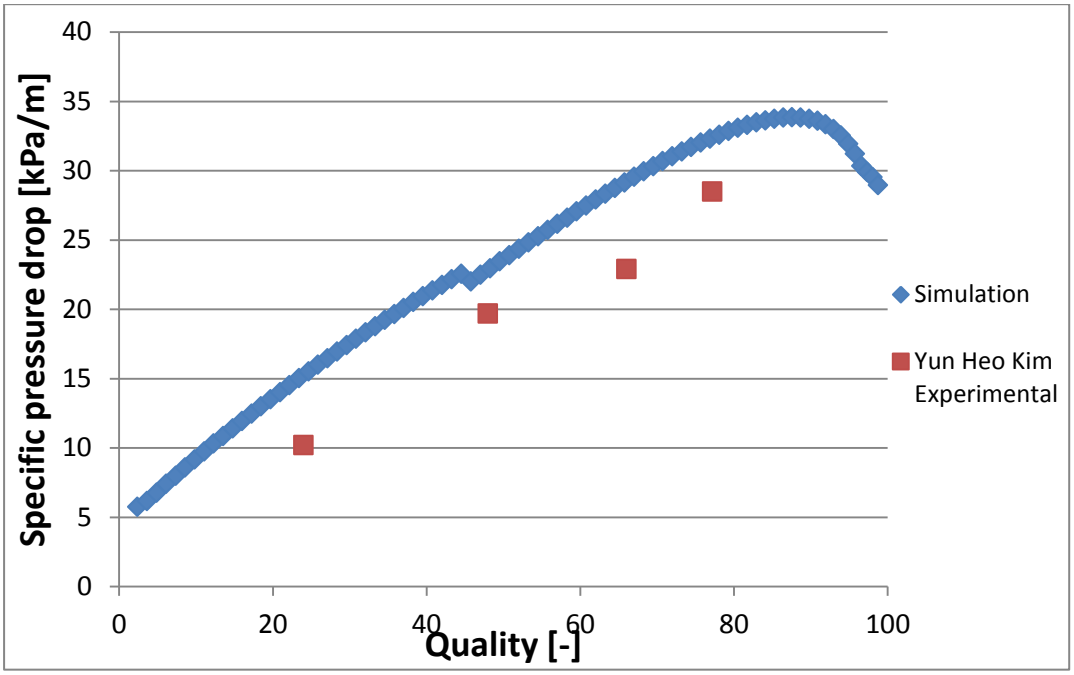

Figure 8.2 Comparison of the modelling results with experimental data from literature.

On the air side for the validation, data from Moallem [64] were used. While working on frost growing on louvered fins the heat transfer coefficient was measured for several fin geometry. All the data about the external geometry of the heat exchanger used are provided. He measured the dry heat transfer coefficient for six different louvered geometry. This make possible testing using the Chang and Wang [45] correlation in the same conditions and compare the results obtained. The results of the comparison are showed in Table 15

Table 15 Comparison of the modelling results with experimental data from literature

Geometry #	Experimental [kW/m^{2}K]	Model [kW/m^{2}K]
1	122	114,6
2	103	98,0
3	87	83,9
4	96	91,1
5	115	107,5
6	72	67,1

The predictions of the heat transfer coefficient are always lower than the measured ones but the error is always smaller than 10% which is the mean error for the Chang and Wang correlation

8.2 Validation of the heat exchanger

After the single parts were checked the whole heat exchanger was simulated. The capacity and the pressure drop both from experimental results and simulation are compared. The overall result of the predictions of the capacity using the proposed model is showed in Figure 8.3. The prediction of the capacity always showed a good agreement with the experimental data. The model tends to slightly underestimate the capacity at high mass flux. In 5% of the cases, the refrigerant is still in saturated conditions at the coil outlet. However all the results are within an error of ±5% and an average error of +1.4% considering both the evaporators and both the refrigerants.

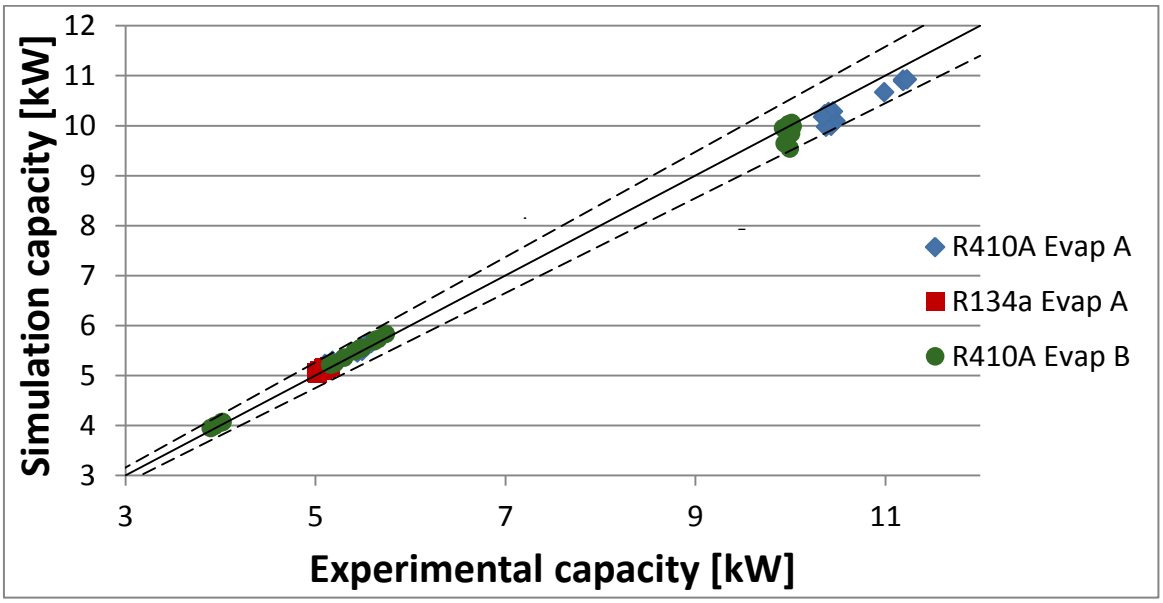

Figure 8.3 Comparison between the predicted capacity and the experimental ones

In the previous figure it is possible to see three different groups of point. Two main groups are located around 5 kW and 10 kW. They represent the capacity used for high mass flux and low mass flux. Furthermore a third series at very

low mass flux with a capacity around 4 kW was included to have a wider range of conditions.

The comparison on pressure drop shows a good agreement between predicted and experimental values. The average error is 14%, and 90% of the data are predicted with an error smaller than 30%. The results of the comparison are showed in Figure 8.4.

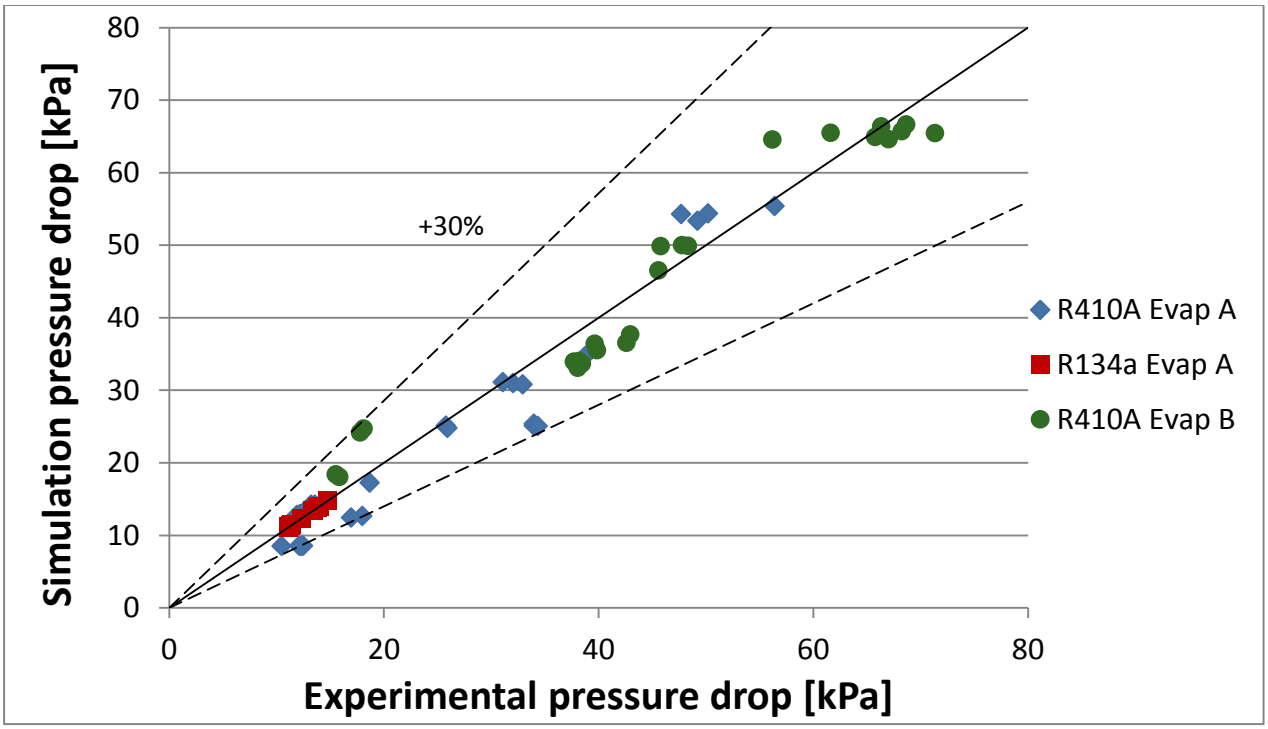

Figure 8.4 Comparison between the predicted pressure drop and the experimental one

The model is able to account properly for the trend in the case of different mass flow rates. Few data present large errors. A considerable part of the pressure drop is caused by the distributor in the inlet header. A small variation of the enthalpy at the inlet of the heat exchanger can cause the flow to change from two phase to sub cooled liquid. There is a sudden increase of the density and in the end a large decrease in the pressure drop. So the model presents a very high sensitivity to the inlet quality. Considering experiments which have the same flow rate, pressure drop having a quality of 5% at microchannel inlet are up to 35% higher than when the refrigerant enters in the coil sub cooled. The model with the orifice at microchannel inlet shows to be able to describe the physics of the problem.

A first verification of the thermal performance of the prediction of the heat exchanger was done comparing the temperature at the outlet of the microchannel in the simulation and using the thermocouple grid placed right after the heat exchanger. The predicted and measured temperatures are shown in Figure 8.5The simulation result is always within the uncertainty range of the measurement except from the first part of the heat exchanger. The most likely cause for this difference is probably that the heat transfer coefficient on the refrigerant side is underestimated.

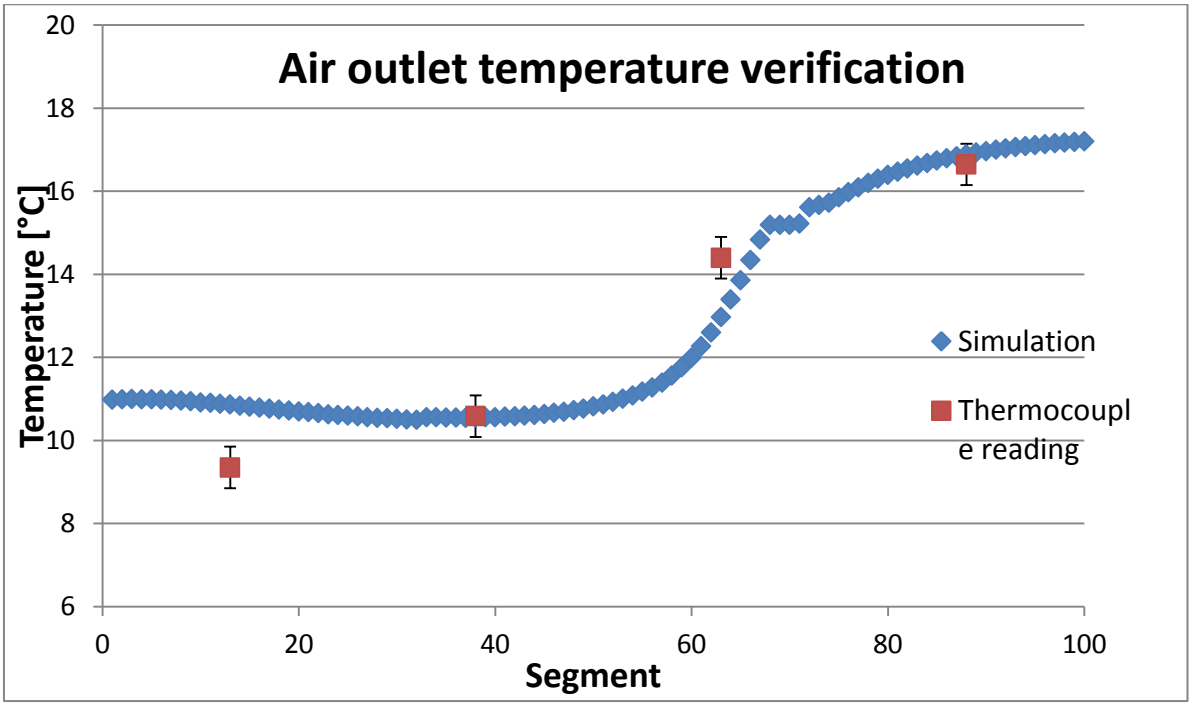

Figure 8.5 Comparison of the predicted temperature of the air at the outlet and the experimental one

A further verification was done comparing the surface temperature predicted by the model with the measurement taken using the thermocamera. Figure 8.6 shows an infrared picture of the coil.

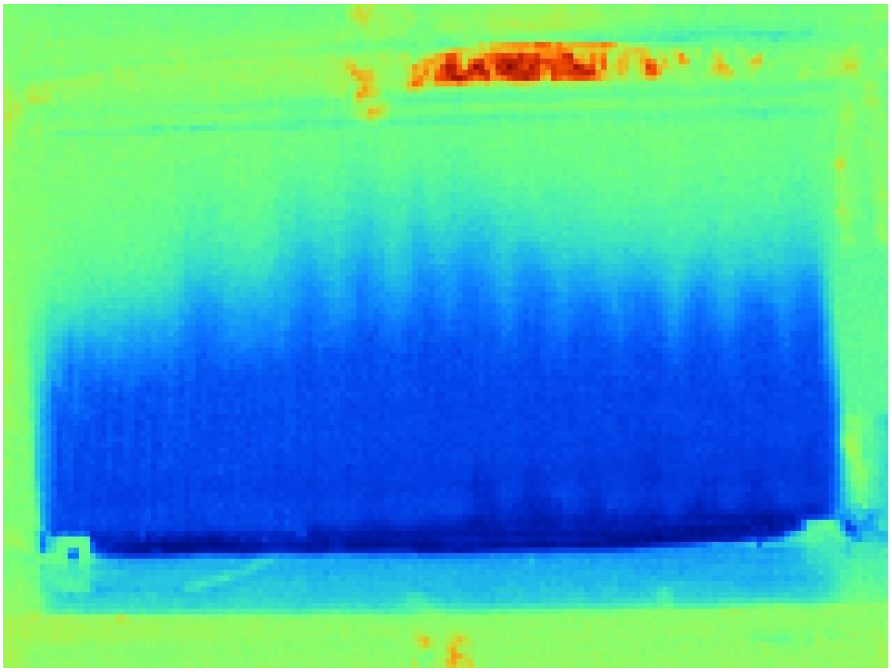

Figure 8.6 Infrared picture of the coil

The prediction is within the uncertainty error at the beginning and at the end of the evaporator, but the dryout occurs later in the simulation than in the experiment. Even considering the fact that the simulation is not able to account for conduction in the tube, it is clear that the dryout occurs earlier than it is expected. This observed result from the present work is in contrast with what was observed when the model was validated using the data from [63]. the difference in the behavior can be explained considering the average error of the correlation of Bertsch [46]. This seems to confirm the fact that the nucleate boiling at the beginning of the heat exchanger is underestimated as pointed before. Even if the local treatment could be improved, the overall prediction showed a good agreement with the experimental data.

The comparison between the predicted and the experimental temperatures is showed in Figure 8.7.

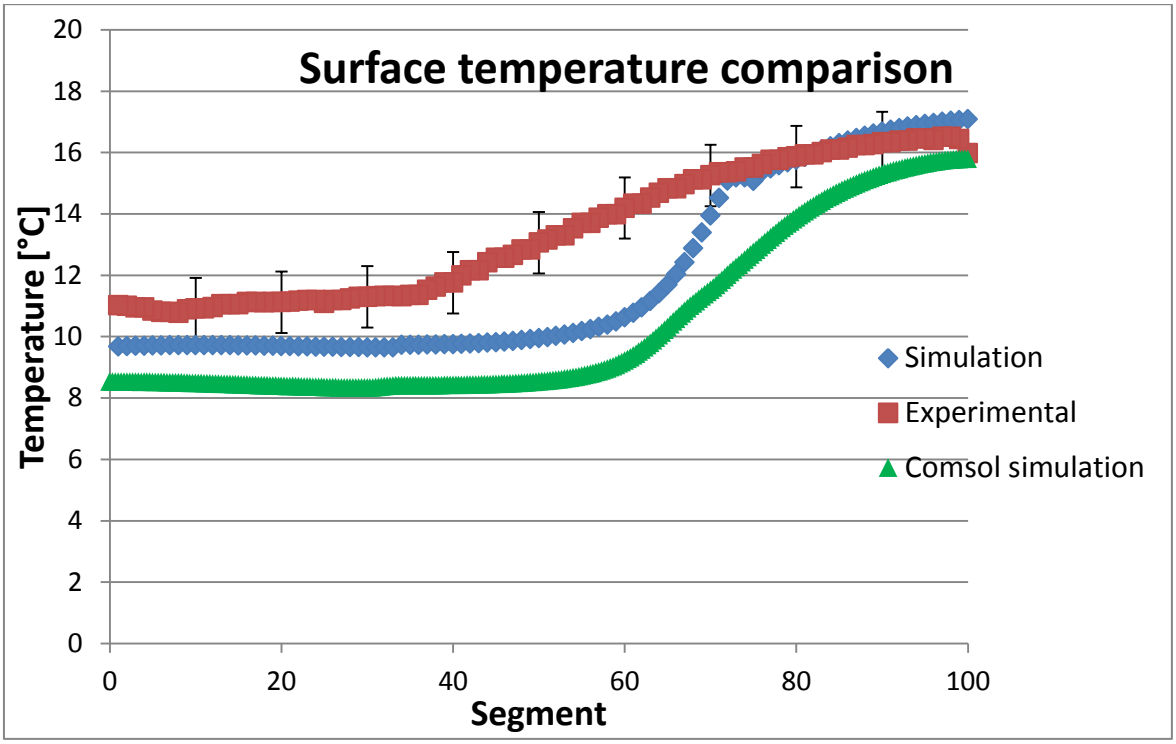

Figure 8.7 Comparison of the predicted surface temperature with the experimental one

The green triangle series was obtained using the software Comsol. It presents a trend which is very similar to the one obtained with the model but it is smoother since Comsol is able to account for the conduction within the tube.

8.3 More results

Using the model it is possible to go deeper into the analysis of the heat exchanger. The experimental measurements provide overall information, the model can give local information for each part of the coil.

It is possible to plot the temperatures of the air, the refrigerant and the surface along the coil, they are showed in Figure 8.8.

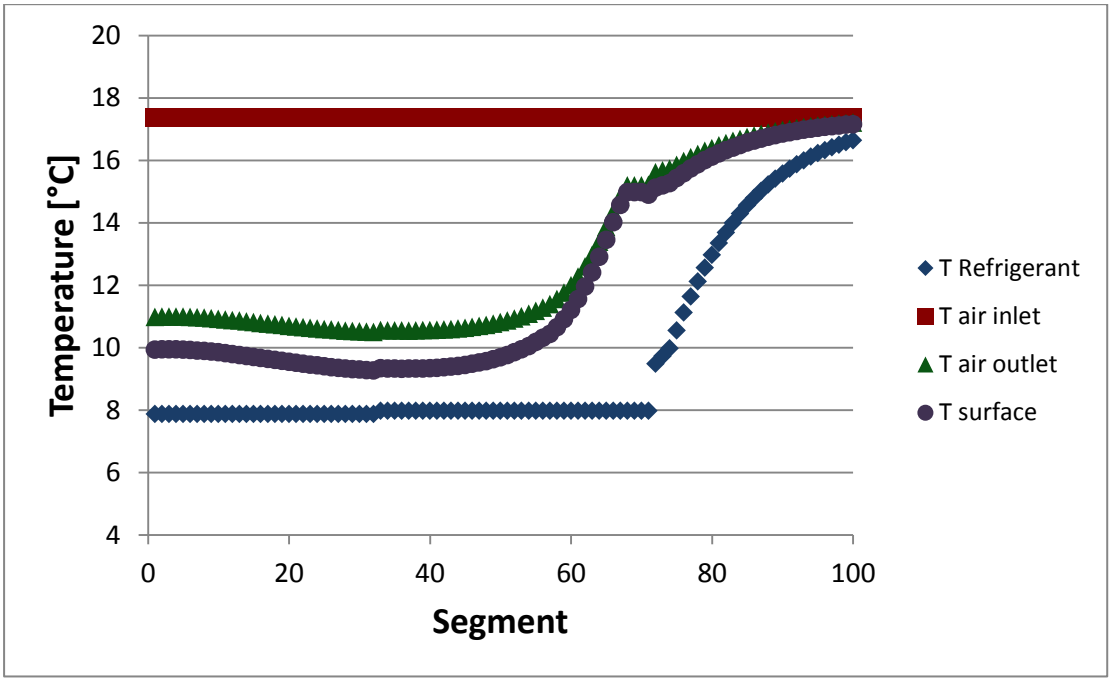

Figure 8.8 Predicted temperatures of the system

The refrigerant enters in the coil in two phase condition, the temperature is almost constant for most of the coil length because pressure drop in channels are negligible. When the quality reaches 1 the temperature of the refrigerant starts increasing and at the end is close to the temperature of the air. The temperature of the air at the inlet is always the same since it is uniform. The temperature at the outlet change along the coil. At the beginning of the coil the capacity of each segment is high and so the air at the outlet is cold. When the heat transfer coefficient on the refrigerant side starts decreasing the temperature of the air at the outlet becomes closer to the inlet. The surface temperature follows a trend which is similar to the temperature of the air at the outlet. At a certain point the two temperatures has a sudden change in the slope. This is caused by the change of heat transfer coefficient from two phase to single phase. The heat transfer coefficient for each segment is showed in Figure 8.9.

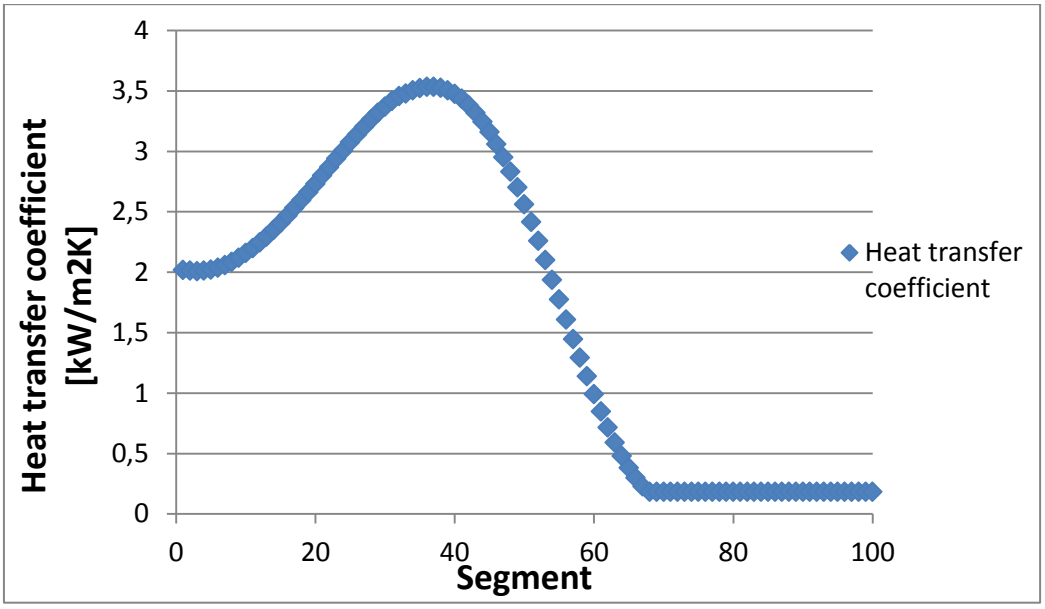

Figure 8.9 Heat transfer coefficient along the coil

At the coil inlet the quality is low and the nucleate boiling is predominant. When the quality increases the convective component makes the heat transfer coefficient to increase, it reaches a maximum and it decreases. At very high quality the Bertsch correlation provides a two phase heat transfer coefficient smaller than the single phase. In this case the higher between the single phase and the two phase is considered.

The model is able to address the pressure drop to each section of the heat exchanger. The results are reported in Table 16

Table 16 Pressure drop section by section

	Pressure drop [kPa]	Pressure drop [%]
Pressure drop liquid line	2,161	12,92
Pressure drop distributor	13,066	78,10
Pressure drop channels	0,87	5,20
Pressure drop outlet header	0,235	1,40
Pressure drop outlet pipeline	0,397	2,37
Total pressure drop	16,729	100

It is possible to see that most of the pressure drop occurs in the distributor. The pressure drop in the channels are only about 5% of the total.

9 Model results with oil

The overall results of the model are compared to the experimental results. To make the figure more clear only the data taken with oil mass fraction equal to 3% are shown. This value is big enough to capture the trend of the oil effects, but at the same time is small enough to be likely to occur in an air conditioning unit.

The experimental data were analyzed in two different ways. The procedure used to generate the simulation data tries to reproduce the one used for the experimental data. For tests with R410A it was possible to run baseline using pure refrigerant at different total mass flow rate entering the coil. Using an interpolation it is possible to obtain the pressure drop and the capacity as a function of the total mass flow rate entering the coil. This way the values measured during the oil injection are compared to baseline having the same total mass flow rate. For the simulation data the injection tests are ran having the same total mass flow rate of the corresponding experiment. After that, a baseline with the same total mass flow rate is generated and used for the normalization. For the tests using R134a it was not possible to run baseline at different total mass flow rate. The values measured during the injection are compared to the pre-injection ones. They have the same refrigerant mass flow rate but during injection the total mass flow rate is increased by the presence of the oil. In this case the simulation values are compared to a baseline generated with the same refrigerant mass flow rate.

9.1.1 Oil retention volume

The predicted normalized oil retention volume is plotted versus the experimental results in Figure 9.1

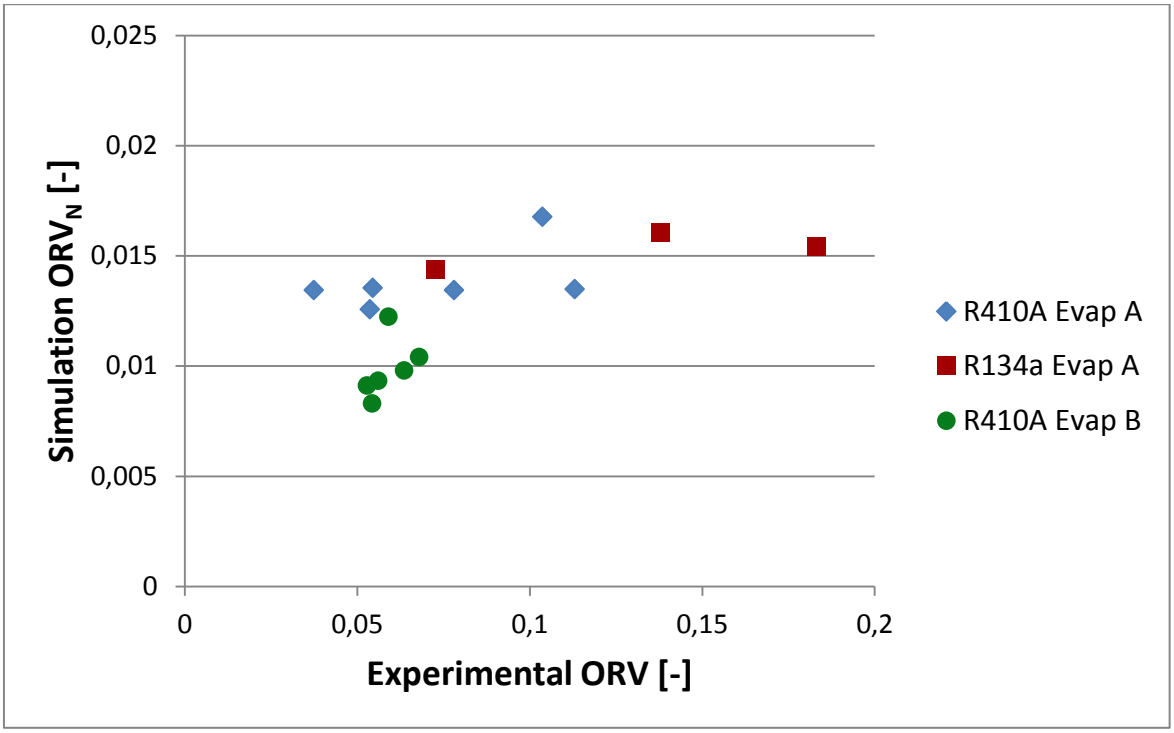

Figure 9.1 Comparison of the predicted oil retention volume with the experimental one

In the figure it is possible to see that the model under predicts the experimental results. The simulation values show a small scatter. The model is little affected by the change of saturation temperature, mass flux and refrigerant. The data for evaporator B show smaller values, this is because the volume is bigger. As a consequence the oil retention volume normalized results to be smaller. On the other hand the mass of oil retained is similar for both the evaporators.

9.1.2 Heat transfer factor

The predicted heat transfer factors are compared to the experimental values in Figure 9.2.

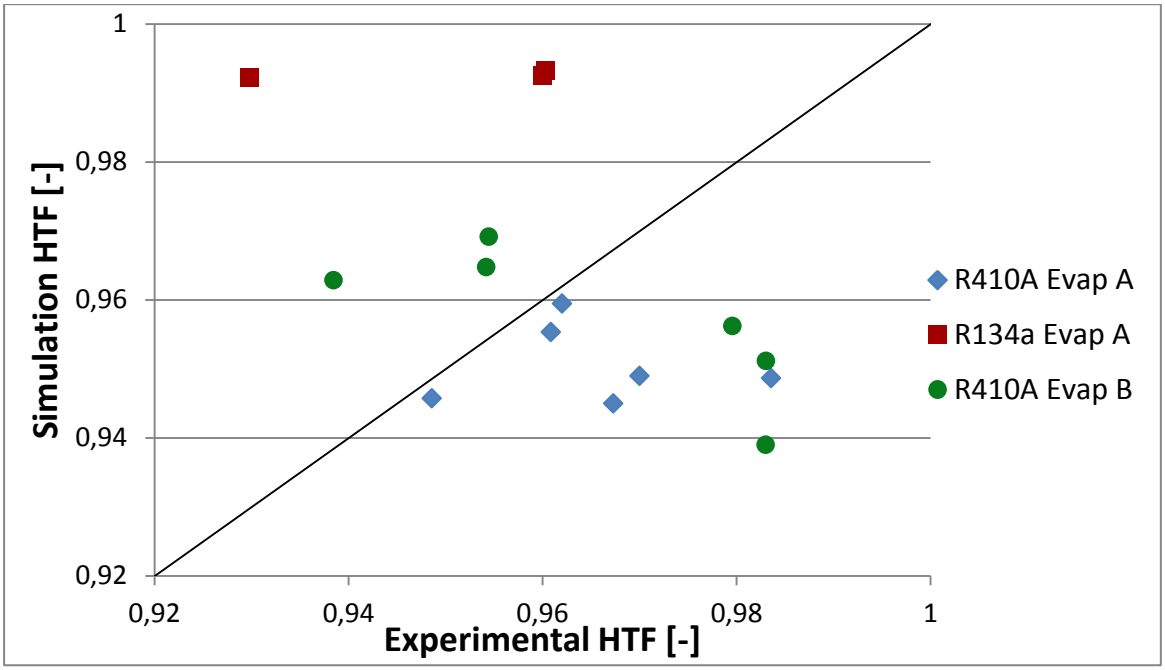

Figure 9.2 Comparison of the predicted heat transfer factor with the experimental one

The results with the two different refrigerants are significantly different. The predicted decrease of capacity for R410A data is of the same magnitude. The capacity reduction is both caused by the effects of oil and the replacement of refrigerant with oil. The scatter of the simulation results is small and it is not possible to recognize any trend due to change in mass flux, saturation temperature or different evaporator. The predicted decrease in the coil capacity for R134a is far smaller than the experimental one. The presence of oil in the heat exchanger seems to have little impact on the coil performance according to the model.

9.1.3 Pressure drop factor

The predicted pressure drop factors are compared to the experimental values in Figure 9.3.

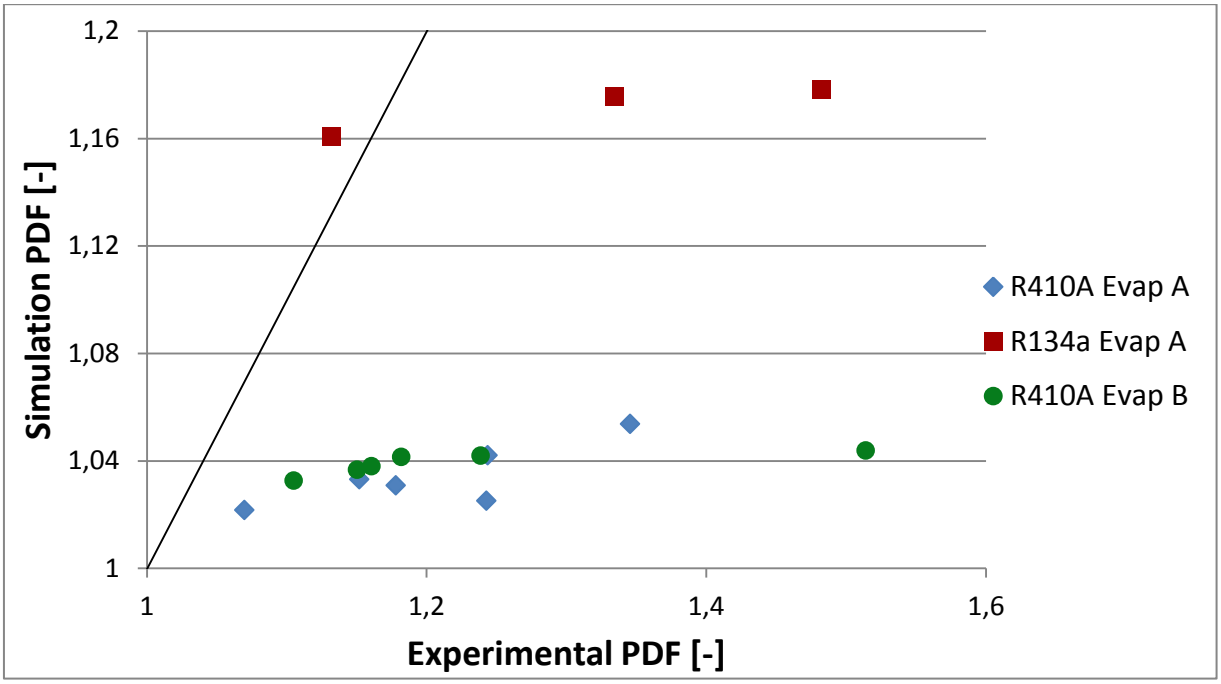

Figure 9.3Comparison of the predicted pressure drop factor with the experimental one

The increase in pressure drop caused by the presence of oil is small for R410A, all the results are in a narrow range and it is not possible to recognize any trend caused by the different conditions. The predictions with R134a show a relevant increase in the pressure drop, there is also one case in which the pressure drop effects of oil is over predicted. Is yet to be said that part of the increase in the pressure drop is caused by the larger total mass flow rate entering into the coil.

9.2 Results for R410A

After the overall results were presented one series of data is presented to go deeper into the model. Two series with two different refrigerants were chosen and are now presented to understand which are the limits of the model.

9.2.1 Oil retention volume

The first series is the one using R410A, evaporator A, low mass flux and saturation temperature of 4.5°C. The results of the changing in oil mass fraction are reported in the following figures. Figure 9.4 shows the effects of oil mass fraction on oil retention volume.

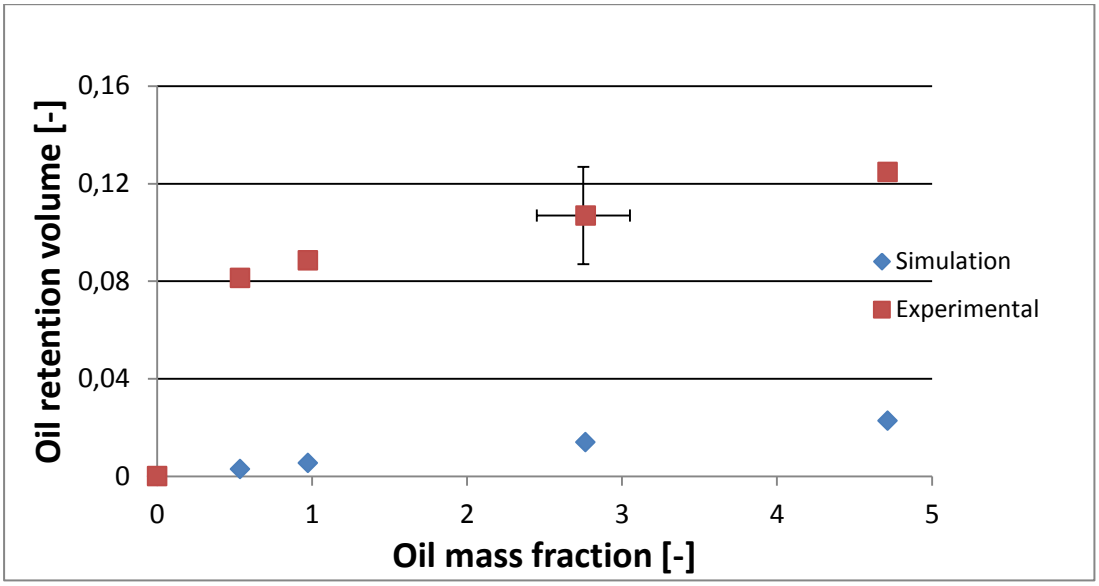

Figure 9.4 Comparison of the predicted oil retention volume with the experimental one

As pointed out previously the model under predicts the amount of oil retained. The predicted values show a trend similar to the experimental ones. The magnitude is completely different.

All the data about these series are provided in Table 17. To build this table a different procedure was used. The total mass flow rate entering the coil is always the same. This way it is possible to have only one baseline instead of four with slightly different mass flow rate.

Table 17 Results of the simulation with oil

Oil mass fraction [-]	0	0,535	0,974	2,765	4,715
Total mass flow rate [kg/s]	0,025578	0,025578	0,025578	0,025578	0,025578
Coil inlet pressure [kPa]	881,1	881,1	881,1	881,1	881,1
Coil inlet enthalpy [kJ/kg]	212,66	212,66	212,66	212,66	212,66
Coil inlet temperature [°C]	2,678	2,677	2,677	2,676	2,675
Coil inlet quality [%]	2,982	2,982	2,981	2,978	2,975
Coil outlet pressure [kPa]	868,249	867,992	867,878	867,527	867,307
Coil outlet enthalpy [kJ/kg]	433,275	431,747	430,557	424,644	417,64
Coil outlet temperature [°C]	11,376	11,265	11,19	10,669	10,062
Coil outlet quality [%]	100	99,056	98,526	95,983	93,028

Coil capacity [kW]	-5,643	-5,604	-5,574	-5,423	-5,243
Pressure drop [kPa]	12,851	13,108	13,222	13,573	13,793
Pressure drop distributor [kPa]	10,061	10,067	10,071	10,089	10,109
Pressure drop outlet pipeline [kPa]	0,366	0,487	0,523	0,598	0,632
Pressure drop outlet header [kPa]	0,215	0,25	0,256	0,266	0,267
Pressure drop channels [kPa]	0,774	0,867	0,932	1,172	1,326
Pressure drop liquid line [kPa]	1,435	1,437	1,44	1,448	1,459
Refrigerant inventory [g]	716,089	722,884	719,533	705,802	690,811
Oil retained [g]	0	4,466	8,234	21,394	34,736
Oil retained in the channels [g]	0	0,206	0,372	0,773	1,117
Oil retained in the inlet header [g]	0	3,279	5,972	16,959	28,919
Oil retained in the outlet header [g]	0	0,981	1,894	3,662	4,705

From the table is possible to address the oil retained to each section of the coil noting that most of the oil is retained in the inlet header. For the assumptions made, the amount of oil retained in the inlet header is directly proportional to the oil mass fraction. A small amount of oil Is retained in the channels compared to the amount in the inlet header. When oil mass fraction was low, the amount of refrigerant in the coil increased compared to the pure refrigerant case because of the amount of liquid refrigerant still present at the outlet. When the oil mass fraction increased the oil replaced part of the refrigerant and as a consequence the amount of refrigerant in the heat exchanger decreased.

The normalized amount of oil retained in the channels is showed in Figure 9.5. The oil retention is given in dimensionless form, it is the ratio between the local oil retention over the maximum oil retention in the circuitry. (Max OR_{segm}=0,026g).

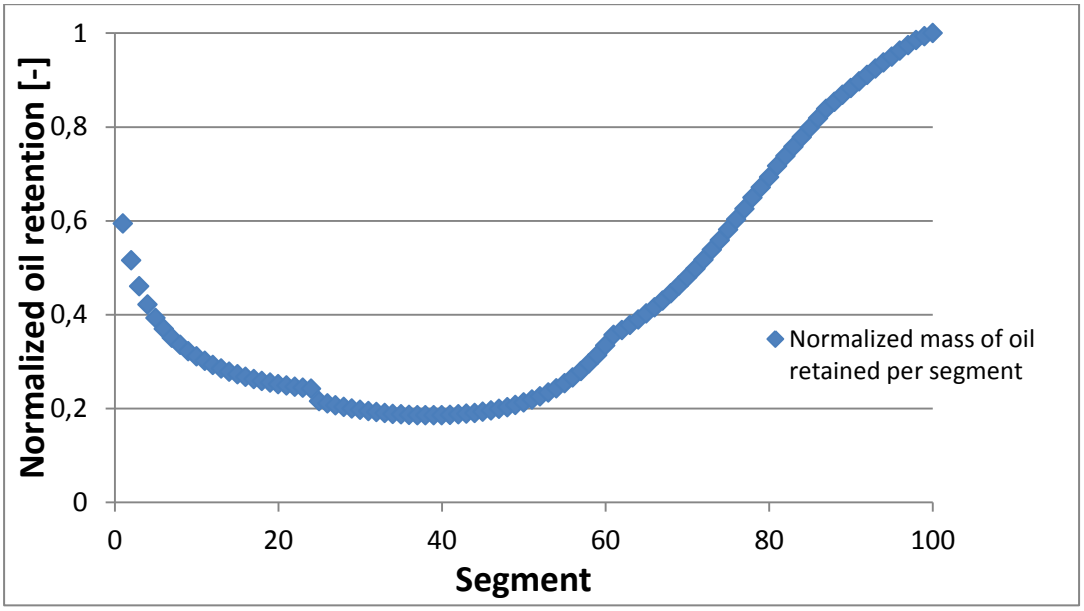

Figure 9.5 Normalized oil retention segment by segment

The dimensionless oil retention is about 0.6 at the inlet mixture quality of about x_{mix}=0.03.Almost all the refrigerant is in liquid phase. Along the heat exchanger the liquid refrigerant starts to evaporate, leaving higher percentage of oil in the liquid mixture. As the local oil concentration starts to rise in the second part of the coil, the dimensionless oil retention increases and reaches the maximum value at the evaporator outlet. Even if the amount of oil retained in the channels is small this trend is significant for the oil retention. It is likely that in the real heat exchanger most of the oil is retained at the end part of the evaporator where the liquid film viscosity reaches the highest value in the evaporator.

So it seems that the main difference between the experiment and the model is in the outlet header. The outlet header is considered as a smooth tube, the void fraction is calculated and thus the oil retained. Actually the geometry of the outlet header is not that simple. The tube of the microchannel enter in the header creating many small volumes which increase the oil retention. Moreover the mass flux of the flow in the header is very small. In the first part of the header the mass flux is out of the range used by Mandrusiak and Carey [62]. The range of the experiments they used was from 12 kg/m^{2}s to 120 kg/m^{2}s, the mass flux at the outlet of the header is around 40 kg/m^{2}s and it is assumed to linearly decrease along the header. This means that 30% of the length of the coil is not in the range of applicability of the correlation. Furthermore the correlation was developed for pure refrigerant. The viscosity

of the oil-refrigerant mixture is far larger than the pure refrigerant one. This can affect the void fraction.

9.2.2 Heat transfer factor

In Figure 9.6 the predictions and the experimental values for heat transfer factor are compared.

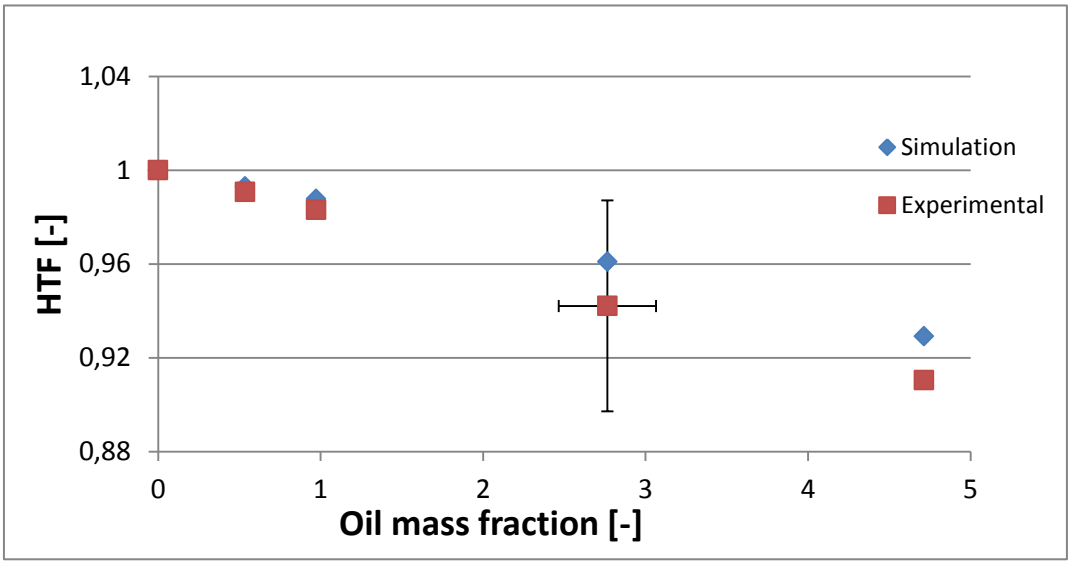

Figure 9.6 Comparison of the predicted heat transfer coefficient with the experimental one

The model is able to predict correctly both the trend and the magnitude of the penalization on capacity at different oil mass fraction. There are three possible cause for the reduction of the capacity of the coil. The total mass flow rate is constant, so the oil is replacing evaporating refrigerant. The lubricant is not boiling and so the average specific enthalpy difference decreases. The presence of oil makes the mixture behaving as zeotropic fluid. The temperature changes during the boiling process and at the end of the coil where a part of the refrigerant is still in liquid phase. Lastly the presence of the oil decreases the heat exchange and this results in a lower temperature at the coil outlet.

When the oil mass fraction is 4.7% the reduction of the temperature at the coil outlet is 1.37 °C. Considering the average specific heat of the flow this results in a loss of specific enthalpy difference equal to 1.65 kJ/kg on a total of 15.65 kJ/kg, which is the total decrease in specific enthalpy in the vapor phase. So the

loss of capacity due to sensible heat is about the 10% of the total. The latent heat of vaporization is around 210 kJ/kg, the replacement of 4.7% of refrigerant with oil causes a decrease of 9.87 kJ/kg. This represent 63% of the total. The remaining 27% is caused by the non-boiling liquid refrigerant at the end of the outlet.

Figure 9.7 shows the effects of the presence of oil on the heat transfer coefficient.

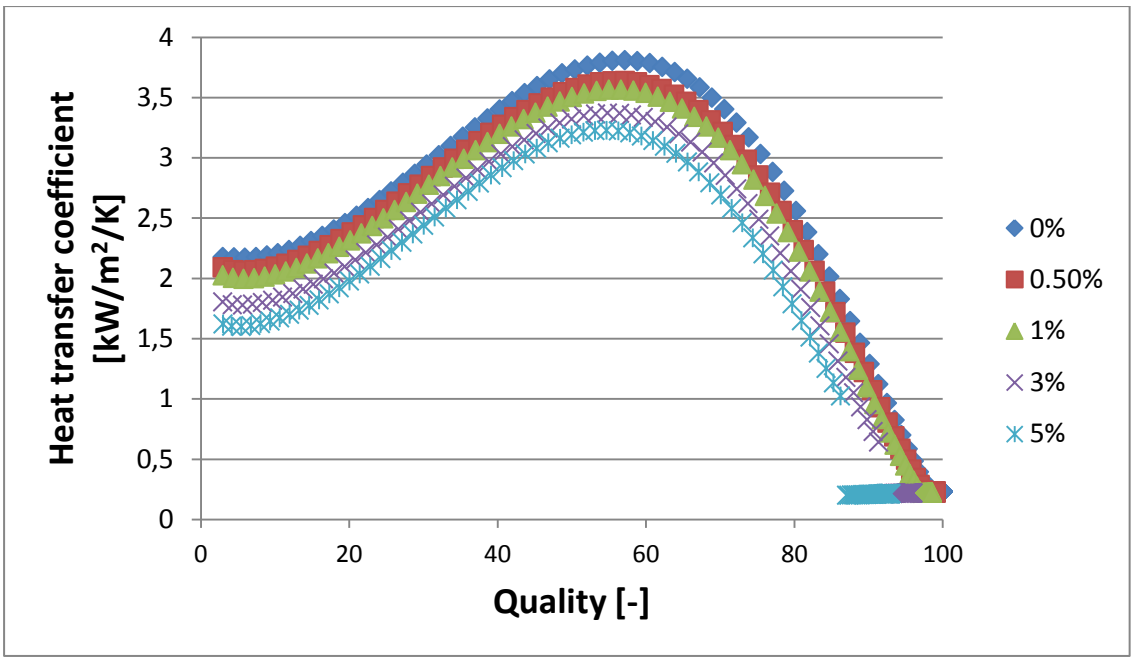

Figure 9.7 Effect of the oil on heat transfer coefficient

The correction from Thome [50]reduces the nucleate boiling considering the effect of mass transfer. As stated in Shen and Groll[13], in large tubes the oil at high quality causes an impairment of the convection boiling. This effect is not portrayed in the model since the Bertsch correlation was developed for laminar flow regime in the microchannel tested and so it is not affected by an increase of the viscosity.

The temperatures of the air, the refrigerant and the surface are showed in Figure 9.8

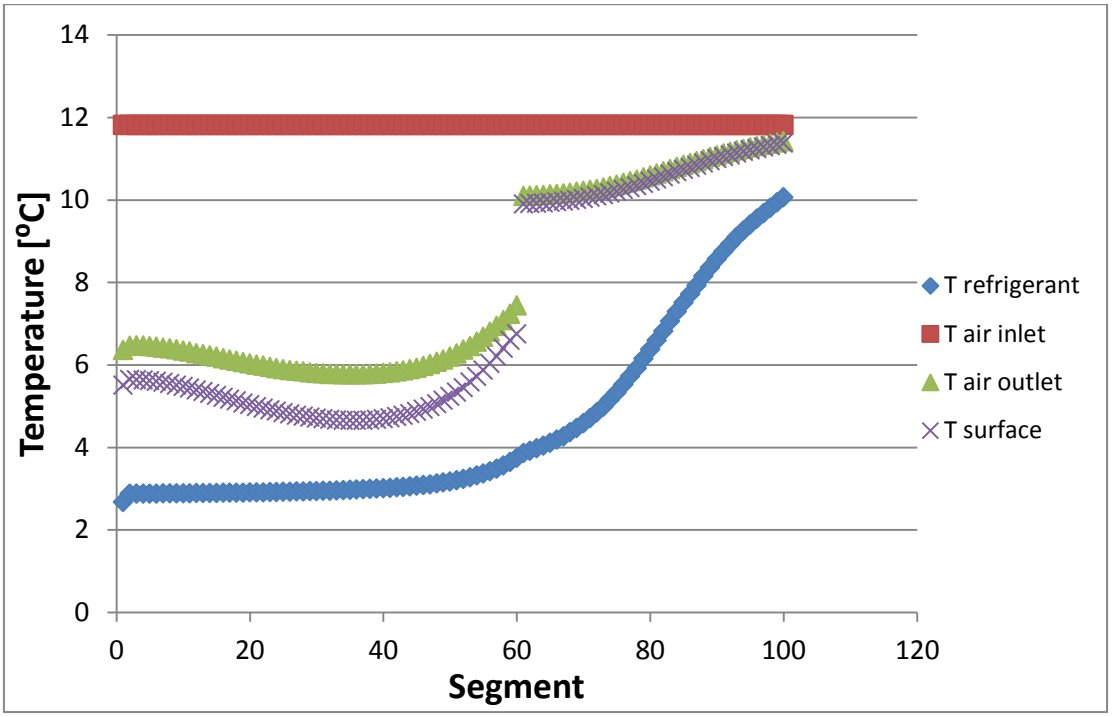

Figure 9.8 Predicted temperatures of the heat exchanger

The presence of oil makes the temperature on the refrigerant side continuously increasing (The bubble temperature is used which is a function of the local concentration of oil). The local oil concentration is affected by the quality which is a consequence of the enthalpy. So as heat is provided to the refrigerant its temperature increases. The temperatures of the surface and of the air at the outlet present a sudden change when the heat transfer coefficient is forced to the single phase. The difference between the air inlet temperature and refrigerant outlet temperature increases compared to the value for pure refrigerant. A decrease of the superheating at the coil outlet was observed during the experiments.

9.2.3 Pressure drop factor

In Figure 9.9 the predictions and the experimental values for pressure drop factor are compared.

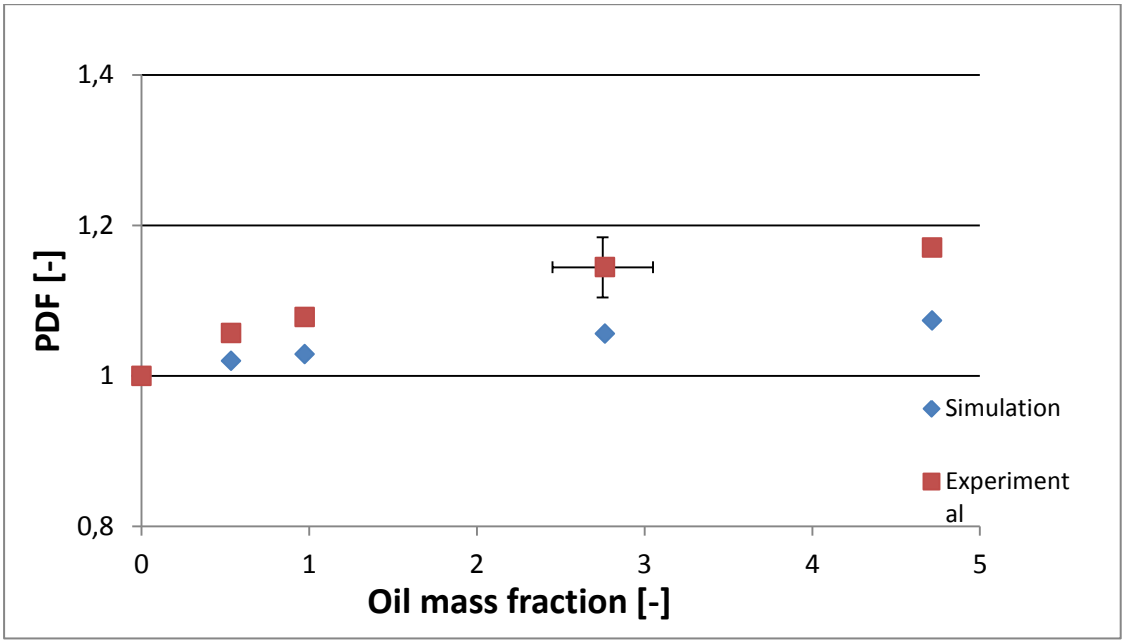

Figure 9.9 Comparison between the predicted pressure drop factor and the experimental one

The effect of oil on pressure drop is under predict compared to the experimental results. The predicted value for oil mass fraction equal to 5% is 43% of the value measured in the experimental test.

Table 18 shows the pressure drop calculated for each section of the heat exchanger. This way it is possible to see which parts are more affected by the presence of oil.

Table 18 Increase of pressure drop section by section

	ΔP no oil [kPa]	ΔP OMF=5% [kPa]	Increase [kPa]	Increase [%]
Pressure drop liquid line	1,44	1,46	0,02	1,67
Pressure drop distributor	10,061	10,109	0,05	0,48
Pressure drop channels	0,774	1,326	0,55	71,32
Pressure drop outlet header	0,215	0,267	0,05	24,19
Pressure drop outlet pipeline	0,366	0,632	0,27	72,68
Total pressure drop	12,851	13,793	0,94	7,33

The effect of oil is very different whether the quality is high or low. In the first part of the coil it is still present a big amount of liquid refrigerant. For this

reason the effect of oil on the physical properties of the liquid is small. Thus results in negligible increase of pressure drop. On the other hand, at the end of the coil the effect of the presence of oil is very relevant. The flow is no more single phase vapor but two phase, the pressure drop reaches a maximum for high quality. Furthermore the high local concentration of oil makes the liquid very viscous. The pressure drop in the final part of the heat exchanger increases dramatically, up to 70%. Since most of the pressure drop occurs in the inlet distributor the overall increase in the pressure drop is small.

9.3 Results for R134a

The detailed results for the simulation with R134a when oil is injected in the system are showed in this chapter. The saturation temperature for these tests was about 1°C. Only the results which differs from the ones using R410A are showed.

9.3.1 Oil retention volume

The comparison between the oil retention volume for experiments and simulation is presented in Figure 9.10

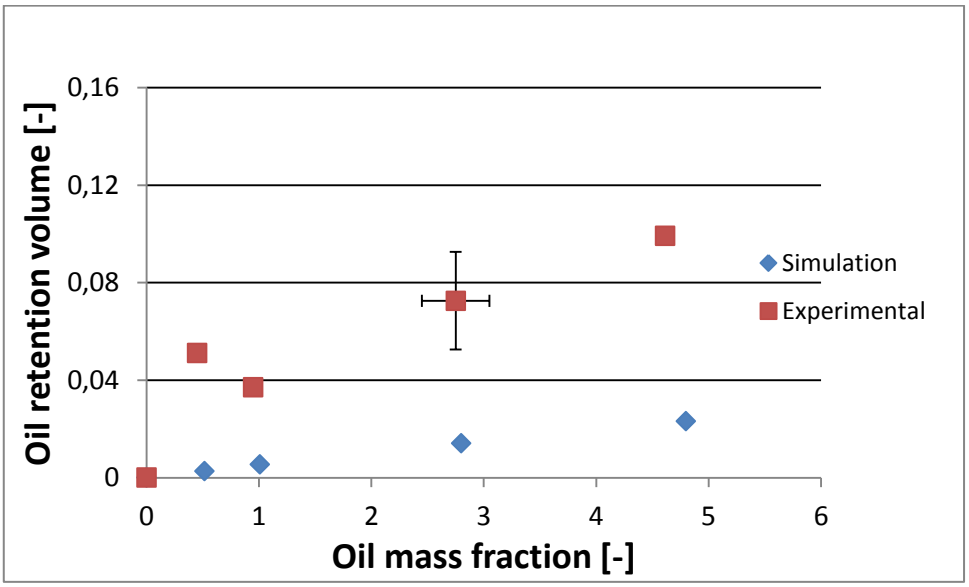

Figure 9.10 Comparison between the predicted and experimental normalized oil retention volume

The predicted amount of oil retained in the system is about the same as R410A and the trend is very similar too. There is a relevant difference between the two series even if the trend is not that different.

The noticeable results for this series are reported in Table 19

Table 19 Results of the simulations at different oil mass fraction

Oil mass fraction [-]	0	0,516	1,01	2,8	4,8
Total mass flow rate [kg/s]	0,025186	0,025382	0,02548	0,02597	0,02646
Coil inlet pressure [kPa]	294,6	294,6	294,6	294,6	294,6
Coil inlet enthalpy [kJ/kg]	203,48	203,48	203,48	203,48	203,48
Coil inlet temperature [°C]	-0,997	-1,01	-1,023	-1,071	-1,129
Coil inlet quality [%]	2,4	2,4	2,4	2,5	2,5
Coil outlet pressure [kPa]	279,58	278,886	278,465	277,165	275,66
Coil outlet enthalpy [kJ/kg]	407,267	405,627	404,545	400,009	394,574
Coil outlet temperature [°C]	9,353	9,355	9,33	9,115	8,679
Coil outlet quality [%]	100	99,105	98,535	96,222	93,565
Air inlet temperature [°C]	9,6	9,6	9,6	9,6	9,6
Coil capacity [kW]	-5,139	-5,125	-5,123	-5,099	-5,062
Pressure drop [kPa]	15,02	15,714	16,135	17,435	18,94
Pressure drop distributor [kPa]	10,609	10,728	10,844	11,278	11,793
Pressure drop outlet pipeline [kPa]	0,838	1,124	1,224	1,448	1,61
Pressure drop outlet header [kPa]	0,499	0,59	0,611	0,66	0,695
Pressure drop channels [kPa]	1,599	1,781	1,948	2,478	3,196
Pressure drop liquid line [kPa]	1,475	1,491	1,508	1,571	1,646
Refrigerant inventory [g]	782,718	782,541	777,791	760,579	741,448
Oil retained [g]	0	4,158	8,291	21,515	35,351
Oil retained in the channels [g]	0	0,182	0,377	0,812	1,16
Oil retained in the inlet header [g]	0	3,14	6,146	17,04	29,211
Oil retained in the outlet header [g]	0	0,836	1,768	3,664	4,98

The main part of oil is still in the inlet header and has a linear correlation with the oil mass fraction. The amount of oil retained in the channels and in the outlet header is the same as with R410A.

9.3.2 Heat transfer coefficient

In Figure 9.11 the predictions and the experimental values for heat transfer factor are compared

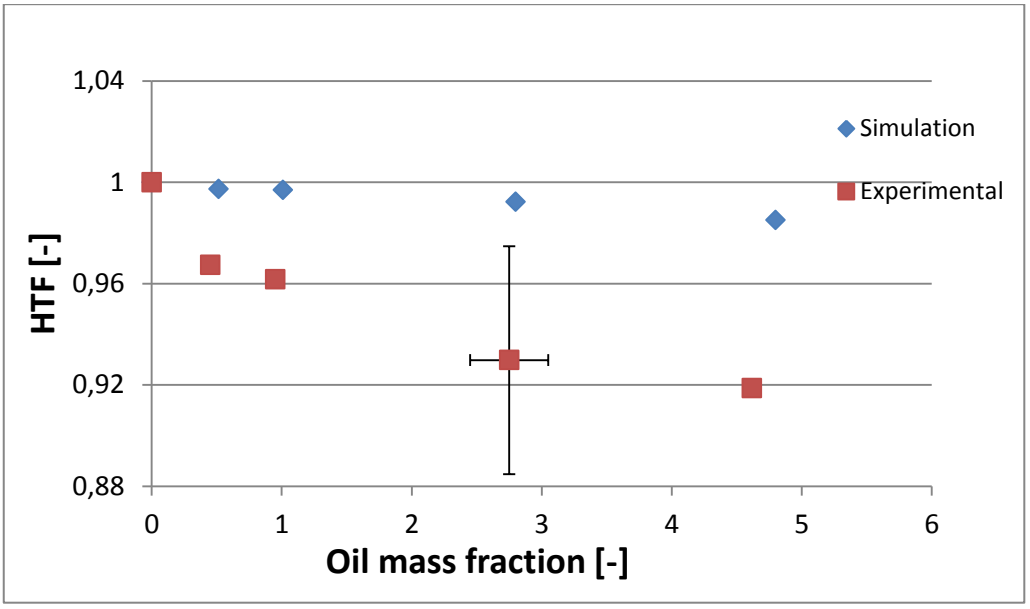

Figure 9.11 Comparison between the predicted and the experimental heat transfer factor

There is a large difference between the experimental values and the predicted ones. The experiments showed a relevant impairment in the capacity caused by the presence of oil. On the other hand, the simulation is quite unaffected. The refrigerant mass flow rate is always the same for all the simulations and more oil is injected. The effect of the replacement of refrigerant with oil is not present this time. It seems that the increased mass flow rate due to the presence of oil affects the capacity as much as the loss of latent heat for non-evaporating refrigerant. The Table 19 shows that the decrease of the temperature of the refrigerant when oil is injected is smaller for R134a compared to R410A. Looking at Figure 9.12, it is possible to see that even when the oil mass fraction is around 5% the temperature of the refrigerant at the coil outlet is still close to the inlet temperature of the air.

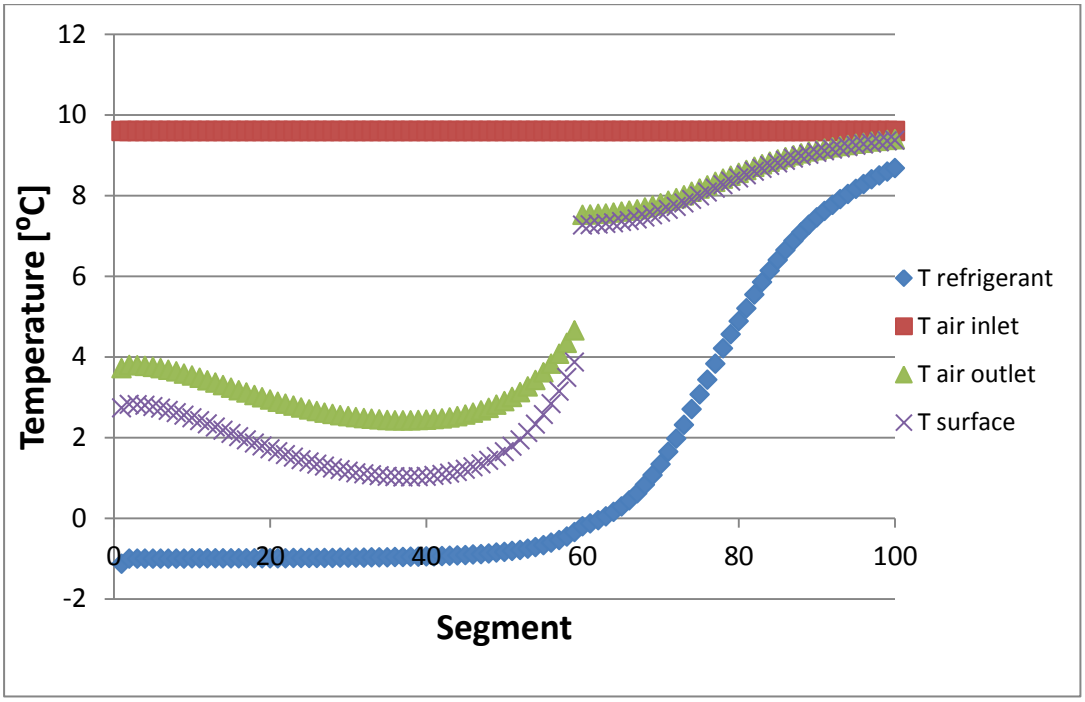

Figure 9.12 Predicted temperatures in case of oil injected in the coil

9.3.3 Pressure drop factor

In Figure 9.13 the predictions and the experimental values for pressure drop factor are compared.

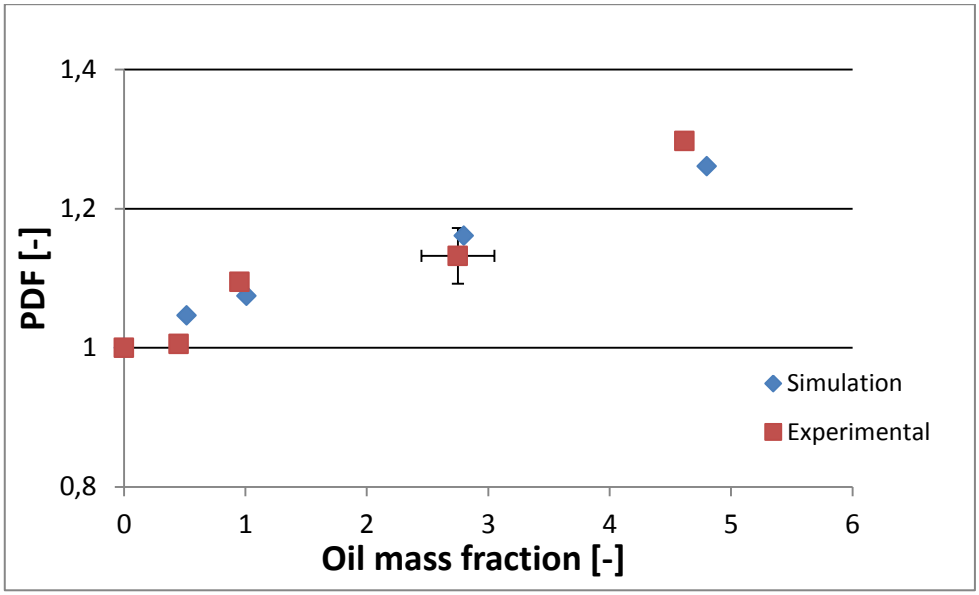

Figure 9.13 Comparison between the predicted and the experimental pressure drop factor

The predicted values and the experimental ones present similar magnitude and trend. The predicted value is always within the uncertainty range of the experimental result. Table 19 shows the effect of the presence of the oil on each section of the coil.

10 Conclusion

The objective of the present work was to investigate both experimentally and theoretically the oil effects in a microchannel evaporator. This was accomplished with extensive experiments and simulations

10.1 Conclusion from the experimental work

The experimental analysis proved that the presence of oil decreases the performances of a microchannel evaporator. A summary of the oil effect on the three main parameters chosen is reported below:

1. The presence of oil decreased the capacity of the coil. The oil made the mixture behave like a zeotropic fluid, the saturation temperature was a consequence of the composition of the flow and increased during the boiling process. As a consequence, a part of refrigerant was still liquid at microchannel outlet. This caused a decrease in enthalpy change and decreased the capacity of the coil. During the injection test the temperature on the refrigerant side decreased, also the sensible heat was reduced by the presence of oil. The change in evaporators or refrigerant did not seem to change the impairment of the performance caused by the oil apart from tests using R1234yf which was quiet unaffected by the presence of oil. The capacity decreased about 8% when the oil mas fraction was 5%.
2. The higher viscosity of the oil-refrigerant mixture and the non-evaporative nature of the oil caused the pressure drop to always increase when oil was present in the system. The pressure drop showed to increase as the oil mass fraction increased and usually experiments with high mass flux were more affected by the presence of oil. Pressure drop rose about 30% when the oil mass fraction was 5%.The main issue related to saturation temperature is the appearance of immiscibility between oil and refrigerant. Since the effect of saturation temperature is almost negligible on all the parameters and often controversial it is likely that cases of immiscibility never occur in the operating range of saturation temperatures.
3. The oil retention showed to be very sensitive to the oil mass fraction. An increase in oil mass fraction always results in a larger amount of oil retained. In evaporator A it was observed a filling phenomenon, even a very small oil mass fraction resulted in a large amount of oil retained.

This is likely to be caused by the geometry of the outlet header. The tubes entering in the header creates many small volumes which are filled of oil rich liquid by gravity force. This made the amount of oil retained in the system larger for evaporator A than it was for evaporator B. The filling phenomenon was magnified when the mass flux was low, whereas when the mass flux was high it can be barely seen. The increase of mass flux increases the shear stress, as a consequence the amount of oil retained at low mass flux was always larger. The oil occupied up to 15% of the internal volume of the coil when the oil mass fraction was 5%

10.2 Conclusion from the modeling work

A semi-empirical model of the heat exchanger is presented in the current work. The model was validated comparing the predicted values with the experimental ones.

1. The prediction of the capacity always showed a good agreement with the experimental data. The model tends to slightly underestimate the capacity at high mass flux. In 5% of the data, the refrigerant is still in saturated conditions at the coil outlet. However since most of the heat exchanged is latent heat, all the results are within an error of 5% and an average error of 1.4% considering both the evaporators and both the refrigerants. The comparison on pressure drop shows a good agreement between predicted and experimental values. The average error is 14%, and 90% of the data are predicted with an error smaller than 30%. The model is able to account properly for the trend in the case of different mass flow rates. Few data present large error. Most of the pressure drop is caused by the distributor in the inlet header, as a consequence the predicted pressure drop is very sensitive to the quality at the inlet of the coil.
2. The simulation of the effect of oil on the capacity of the coil provided good results compared to the experimental data. The capacity reduction had two different causes in the model. The first was that the oil reduced the heat transfer coefficient and as a consequence the superheat at the outlet decreased. The second one is that the presence of oil caused the temperature of the flow to increase even if there was still liquid refrigerant present. This way there was a loss of latent heat available since a part of the refrigerant was not boiling.

3. The model underestimated the increase in pressure drop caused by the oil. Most of the pressure drop of the heat exchanger is caused by the distributor. At the beginning of the coil the effect of oil on the properties of the mixture was negligible and so this pressure drop was unaffected by the presence of oil. On the contrary the oil strongly affected the final part of the channels and the suction line. The presence of a small amount of very viscous liquid made the pressure drop to increase up to 60% in the suction line. The increase in pressure drop in simulation was smaller than experienced in experiments. It is not clear whether the presence of oil is able to affect pressure drop at low local mass fraction or the effect of oil at high quality is underestimated.
4. The simulation underestimated the amount of oil retained in the system. The trend in simulation is linear because most of the oil is retained in the inlet header. The experimental results suggested that most of the oil is retained at the outlet header. The model failed when it tried to describe a complex geometry and very low mass flux

10.3 Future works

Maldistribution is a major issue for the performance of microchannel heat exchanger. During the experiments the focus was on the effect of oil on pressure drop and coil capacity, so maldistribution was not considered. In order to have an uniform distribution among the channels, as shown in Figure 8.6, the refrigerant entered the coil subcooled or at very low quality. This is not what usually happens in an air conditioning system. The presence of the expansion valve causes the quality to be sensibly higher than it was during the experiments for the present work and so the effect of maldistribution is not negligible.

In the work from Li and Hrnjak [5] the effect of oil on maldistribution was investigated. In their work they found that the presence of oil sensibly reduced the maldistribution in the coil. The system they used was a complete vapor compression cycle. The system kept the superheating constant at compressor inlet. Higher oil concentration caused higher bubble point temperature of the refrigerant-oil mixture and as a consequence higher superheat at a fixed pressure. So as oil mass fraction increased, in order to maintain the same superheat, a higher mass flow rate was required to achieve similar superheating at the compressor inlet compared with lower oil mass fraction cases. It is likely that the improved distribution is mainly affected by the increased mass flow rate. In a previous work from Zou et al [26] the distribution was found to decrease in case of increased mass flow rate. Test on

the effect of oil on maldistribution at constant mass flow rate would be beneficial to decouple the effect of change in mass flow rate from the effect of the oil.

The procedure to calculate the oil retained in the outlet header and in the suction line is a possible cause for the under prediction of the oil retention. The modeling of refrigerant and oil retention in heat exchanger is complicated because of changes in flow regimes and the energy transport. As a result, heat exchanger models rely heavily on correlation methods. The traditional way to calculate the inventory of refrigerant in the coil is based on the void fraction. This procedure was successfully used in Jin and Hrnjak [37] to calculate the amount of oil retained in a plate and fin heat exchanger.

Most of the void fraction correlations were developed for pure refrigerant, the viscosity of the liquid was far smaller than the viscosity of the oil rich mixture at the end of the evaporator. Instead of using this traditional approach it would be possible to use the correlation from previous studies on oil retention in suction line. The fact that that there is no heat exchanged should make this procedure easier. In Cremaschi [1] is described a procedure to calculate the oil retained in a suction line. Based on continuity equation and momentum balance, a set of equation was proposed to find the thickness of the oil rich mixture layer. For the solution of the problem an empirical correlation was necessary. It can be produced by experimental tests. A correlation was developed for the friction factor was proposed in that work and the .

11 Nomenclature

a	Coefficient for bubble temperature calculation [-]
A	Area [m2]
Ar	Area ratio [-]
b	Coefficient for bubble temperature calculation [-]
C	Chisholm parameter [-]
C	Capacity of the flow [W/K]
Cc	Contraction factor [-]
cf	Correction factor [-]
Co	Confinement number
C_p	Specific heat [J/Kg K]
*C*r	Capacity ratio [-]
Cs	Saturation specific heat [J/kgK]
D_h	Hydraulic diameter [m]
F	Two phase convective factor [-]
f	Friction factor [-]
FC	Correction factor for mixture pool boiling [-]
F_l	Fin Length [m]
F_p	Fin Pitch [m]
G	Mass flux [kg/m2 s]
h	Heat transfer coefficient [W/m2K]
h	Enthalpy [J/kg]
h_{id}	Ideal pool boiling heat transfer coefficient [W/m2K]
HTF	Heat Transfer Factor [-]
j	Colburn factor [-]
k	Thermal conductivity [W/m K]
k	Empirical coefficient for viscosity calculation [-]
L	Length [m]
L_l	Louver length [m]
L_p	Louver Pitch [m]

$\dot{m}$	Mass flow rate [kg/s]
M	Molecular weight [kg/kmol]
m	Fin parameter
NTU	Number of thermal unit [-]
OMF	Oil Mass Fraction [-]
ORM	Oil retention mass [-]
P	Pressure [-]
PDF	Pressure Drop Factor [-]
Pr	Prandtl number [-]
P_r	Reduced pressure [-]
q	Heat flux [W/m2]
Q	Heat exchanged [W]
Re	Reynolds number [-]
RH	Relative humidity [-]
S	Suppression factor [-]
T	Temperature [K]
T_d	Tube depth [m]
Thk	Thickness [m]
T_p	Tube pitch [m]
U	Overall heat transfer coefficient [W/m2K]
x	Quality [-]
X_{tt}	Lockhartt Martinelli Parameter [-]

Greek symbol

α	Void fraction [-]
β_L	Mass transfer coefficient [m/s]
δ_f	Fin thickness [m]
ΔT_{bp}	Boiling range [K]
ε	efficiency [-]
θ	Louver angle [°]
μ	Viscosity [Pa s]

ρ	Density [kg/m3]
σ	Surface tension [N/m]
ϕ_L	Two phase multiplier [-]
ψ	Mole fraction [-]
ζ	Yokozeki factor [-]
ω	Oil mass fraction [-]

Subscript

a,i	Air, inlet
bub	Bubble
conv	Convective
FB	Flow Boiling
frict	Frictional
grav	Gravity
inj	Injected
l	Liquid
LV	Liquid to Vapor
max	Maximum
MC	Microchannel
min	Minimum
mix	Mixture
mom	Momentum
n	Normalizes
NB	Nucleate Boiling
r,s	Saturation at Tref
ref	Refrigerant
sat	Saturation
tp	Two Phase
v	Vapor

12 References

1. Radermacher, R., Cremaschi, L.and Schwentker, R.A., *Modeling of oil retention in the suction line and evaporator of air-conditioning systems.* HVAC&R Research, 2006. **12**(1): p. 35-56.
2. Lee, J.-P., Hwang, Y.and Radermacher, R., *An Experimental Investigation Of Oil Retention Characteristics In CO2 Air-Conditioning Systems.* 2002.
3. Sundaresan, S.G. and Radermacher, R., *Oil return characteristics of refrigerant oils in split heat pump system.* ASHRAE journal, 1996. **38**(8): p. 57-61.
4. Schnur, N., *Effects of lubricant miscibility and viscosity on the performance of an R-134a refrigerating system/Discussion.* Transaction-ASHRAE, 2000.
5. Li, H. and Hrnjak, P., *Lubricant Effect on Performance of R134a MAC Microchannel Evaporators*. 2014, SAE Technical Paper.
6. Deokar, P., *Development of an experimental methodology for measurement of oil retention and its effect on the microchannel heat exchanger.* M.Sc. dissertation Oklahoma State University, 2013.
7. Ardiyansyah, Y., *Effect of lubricant on heat transfer and pressure drop in microchannel heat exchangers.* Phd Prelim, 2014.
8. Garimella, S., *Innovations in energy efficient and environmentally friendly space-conditioning systems.* Energy 28, 2003.
9. Jiang, Y. and Garimella, S. *Compact air-coupled and hydronically coupled microchannel heat pumps*. in *2001 ASME International Mechanical Engineering Congress and Exposition, Nov 11-16 2001*. 2001.
10. Bivens, D. and Yokozeki, A., *Composition Changes During Container Transfers for Multicomponent Refrigerants.* 1998.
11. Leck, T.J., *Evaluation of HFO-1234yf as a Potential Replacement for R-134a in Refrigeration Applications.* 3rd IIR Conference on Thermophysical Properties and Transfer Processes of Refrigerants, 2009.
12. Zürcher, O., Thome, J.R.and Favrat, D., *In-Tube Flow Boiling of R-407C and R-407C/Oil Mixtures Part II: Plain Tube Results and Predictions.* HVAC&R Research, 1998. **4**(4): p. 373-399.
13. Shen, B. and Groll, E.A., *Review Article: A Critical Review of the Influence of Lubricants on the Heat Transfer and Pressure Drop of Refrigerants, Part 1: Lubricant Influence on Pool and Flow Boiling.* HVAC&R Research, 2005. **11**(3): p. 341-359.
14. Manwell, S. and Bergles, A., *Gas-liquid flow patterns in refrigerant-oil mixtures.* ASHRAE Trans, 1990. **96**(2): p. 456-464.
15. Zürcher, O., Thome, J.R.and Favrat, D., *Flow boiling and pressure drop measurements for R-134a/oil mixtures Part 2: Evaporation in a plain tube.* HVAC&R Research, 1997. **3**(1): p. 54-64.

16. Kedzierski, M., *Simultaneous visual and calorimetric measurement of R11, R123, and R123/alkylbenzene nucleate flow boiling.* Heat transfer with Alternate Refrigerants, 1993. **Vol 243**: p. 27-33.
17. Hambraeus, K., *Heat transfer of oil-contaminated HFC134a in a horizontal evaporator.* International Journal of Refrigeration, 1995. **18**(2): p. 87-99.
18. Shen, B. and Groll, E.A., *Review Article: A Critical Review of The Influence of Lubricants on the Heat Transfer and Pressure Drop of Refrigerants—Part II: Lubricant Influence on Condensation and Pressure Drop.* HVAC&R Research, 2005. **11**(4): p. 511-526.
19. Schlager, L., Pate, M.and Bergles, A., *A survey of refrigerant heat transfer and pressure drop emphasizing oil effects and in-tube augmentation.* ASHRAE transactions, 1987. **93**: p. 392-416.
20. Kattan, N., Thome, J.and Favrat, D., *Flow boiling in horizontal tubes: Part 1—Development of a diabatic two-phase flow pattern map.* Journal of Heat Transfer, 1998. **120**(1): p. 140-147.
21. Steiner, D., *Heat transfer to boiling saturated liquids.* VDI Heat Atlas (Translator J. W. Fullarton), 1993.
22. Wojtan, L., Ursenbacher, T.and Thome, J.R., *Investigation of flow boiling in horizontal tubes: Part I—A new diabatic two-phase flow pattern map.* International Journal of Heat and Mass Transfer, 2005. **48**(14): p. 2955-2969.
23. Fukuta, M., Yanagisawa, T., Sawai, K.and Ogi, Y., *Flow characteristics of oil film in suction line of refrigeration cycle.* 2000.
24. Hwang, Y., Lee, J., Radermacher, R.and Pereira, R., *An Experimental Investigation on Flow Characteristics of Refrigeration/Oil Mixture in Vertical Upward Flow.* 2000.
25. DeAngelis, J. and Hrnjak, P., *Experimental Study of System Performance Improvements in Transcritical R744 Systems with Applications to Bottle Coolers.* Urbana, 2005. **51**: p. 61801.
26. Zou, Y., Tuo, H.and Hrnjak, P., *Modeling refrigerant maldistribution in microchannel heat exchangers with vertical headers based on experimentally developed distribution results.* Applied Thermal Engineering, 2014.
27. Tuo, H., Bielskus, A.and Hrnjak, P., *Experimentally validated model of refrigerant distribution in a parallel microchannel evaporator*. 2012, SAE Technical Paper.
28. Cremaschi, L., Hwang, Y.and Radermacher, R., *Experimental investigation of oil retention in air conditioning systems.* International Journal of Refrigeration, 2005. **28**(7): p. 1018-1028.
29. Jiang, H., *Development of a simulation and optimization tool for heat exchanger design.* Ph.D. Dissertation University of Maryland at College Park, 2003.
30. Youbi-Idrissi, M., Bonjour, J., Meunier, F.and Marvillet, C. *Enthalpy calculation for a refrigerant/oil mixture: consequences on the evaporator performance working with R407C and POE oil*. in *Proceedings of the IIR/IIF conference*. 2001.

31. Youbi-Idrissi, M., Bonjour, J., Terrier, M.-F., Marvillet, C.and Meunier, F., *Oil presence in an evaporator: experimental validation of a refrigerant/oil mixture enthalpy calculation model.* International Journal of refrigeration, 2004. **27**(3): p. 215-224.
32. Schwentker, R.A., *Advances to a computer model used in the simulation and optimization of heat exchangers.* M.Sc. Dissertation University of Maryland at College Park, 2005.
33. Lottin, O., Guillemet, P.and Lebreton, J.-M., *Effects of synthetic oil in a compression refrigeration system using R410A. Part I: modelling of the whole system and analysis of its response to an increase in the amount of circulating oil.* International Journal of Refrigeration, 2003. **26**(7): p. 772-782.
34. Lottin, O., Guillemet, P.and Lebreton, J.-M., *Effects of synthetic oil in a compression refrigeration system using R410A. Part II: quality of heat transfer and pressure losses within the heat exchangers.* International journal of refrigeration, 2003. **26**(7): p. 783-794.
35. Talik, A.C., *Heat transfer and pressure drop characteristics of a plate heat exchanger*. 1995, Texas A&M University.
36. Premoli, A., DiFrancesco, D.and Prina, A., *A dimensionless correlation for the determination of the density of two-phase mixtures.* Termotecnica,(Milan), 1971. **25**(1): p. 17-26.
37. Jin, S. and Hrnjak, P., *An Experimentally Validated Model for Predicting Refrigerant and Lubricant Inventory in MAC Heat Exchangers*. 2014, SAE Technical Paper.
38. Li, H. and Hrnjak, P., *Effect of lubricant on two-phase refrigerant distribution in microchannel evaporator*. 2013, SAE Technical Paper.
39. Li, H. and Hrnjak, P., *A possible cause for the under prediction of the amount of oil retained in the system of the modeling* 15th International Refrigeration and Air conditioning COnference at Purdue, 2014.
40. Cremaschi, L. and Lee, E., *Design and heat transfer analysis of a new psychrometric environmental chamber for heat pump and refrigeration systems testing.* ASHRAE Transactions, 2008. **114**(2): p. 619-631.
41. Sethi, A., *Oil retention and pressure drop of R1234yf and R134a with POE ISO 32 in suction lines.* M.Sc. Dissertation at University of Illinois at Urbana-Champaign, 2011.
42. Iu, I.S., *Development of air to air heat pump simulation program with advanced heat exchanger circuitry algorithm.* M.Sc. Dissertation at Oklahoma State University, 2007.
43. Harms, T.M., Groll, E.A.and Braun, J.E., *Accurate charge inventory modeling for unitary air conditioners.* HVAC&R Research, 2003. **9**(1): p. 55-78.
44. Chang, Y.-J. and Wang, C.-C., *A generalized heat transfer correlation for Iouver fin geometry.* International Journal of heat and mass transfer, 1997. **40**(3): p. 533-544.

45. Chang, Y.-J., Hsu, K.-C., Lin, Y.-T.and Wang, C.-C., *A generalized friction correlation for louver fin geometry.* International Journal of Heat and Mass Transfer, 2000. **43**(12): p. 2237-2243.
46. Bertsch, S.S., Groll, E.A.and Garimella, S.V., *A composite heat transfer correlation for saturated flow boiling in small channels.* International Journal of Heat and Mass Transfer, 2009. **52**(7): p. 2110-2118.
47. Cooper, M., *Heat flow rates in saturated nucleate pool boiling, a wide-ranging examination using reduced properties.* Advanced heat transfer, 1984: p. 157-239.
48. Hausen, H., *Darstellung des Warmeuberganges in Rohren durch verallgemeinerte Potenzbeziehungen.* Z. VDI Beih. Verfahrenstech, 1943. **4**: p. 91-98.
49. Gnielinski, V., *New equations for heat and mass transfer in turbulent pipe achannel flow.* International Chemical Engineering, 1976. **16**(2): p. 359-368.
50. Thome, J., *Engineering data book III.* 2007: p. 10-1 10-29.
51. Mishima, K. and Hibiki, T., *Some characteristics of air-water two-phase flow in small diameter vertical tubes.* International Journal of Multiphase Flow, 1996. **22**(4): p. 703-712.
52. Chisholm, D., *A theoretical basis for the Lockhart-Martinelli correlation for two-phase flow.* International Journal of Heat and Mass Transfer, 1967. **Vol 10**: p. Pag 1767-1778.
53. Ragazzi, F., *Modular-based computer simulation of an air-cooled condenser*. 1991, Air Conditioning and Refrigeration Center. College of Engineering. University of Illinois at Urbana-Champaign.
54. Paliwoda, A., *Generalized method of pressure drop calculation across pipe components containing two-phase flow of refrigerants.* International Journal of Refrigeration, 1992.
55. Citrini, D. and Noseda, G., *Idraulica*. 2009: Casa Ed. Ambrosiana.
56. Thome, J., *Comprehensive thermodynamic approach to modelling refrigerant-lubricant oil mixtures.* HVAC&R Research, 1995.
57. Jensen, M. and Jackman, D., *Prediction of nucleate pool boiling heat transfer coefficients of refrigerant-oil mixtures.* Journal of heat transfer, 1984. **106**(1): p. 184-190.
58. Shah, M., *Visual observations in an ammonia evaporator.* ASHRAE Transactions, 1975. **81**(1): p. 295-306.
59. Chaddock, J., *Film coefficients for in-tube evaporation of ammonia and R-502 with and without small percentages of mineral oil.* ASHRAE Trans., 1986. **92**: p. part A.
60. Yokozeki, M., *Solubility and viscosity of refrigerant-oil mixtures.* Proceedings of the 1994 International Refrigeration Conference at Purdue, 1994: p. 335-340.
61. Filippov, L., *Liquid thermal conductivity research at Moscow University.* International Journal of Heat and Mass Transfer, 1968. **11**(2): p. 331-345.

62. Mandrusiak, G. and Carey, V., *Pressure drop characteristics of two-phase flow in a vertical channel with offset strip fins.* Experimental Thermal and Fluid Science, 1988. **1**(1): p. 41-50.
63. Yun, R., Hyeok Heo, J.and Kim, Y., *Evaporative heat transfer and pressure drop of R410A in microchannels.* International journal of refrigeration, 2006. **29**(1): p. 92-100.
64. Moallem, E., *Experimental and Theoretical investigation of effect of fin geometry on frost formation on Microchannel Heat Exchangers.* Ph.D. dissertation Oklahoma State University, 2012.